The Thesis Committee for Kate Christina McCaul
Certifies that this is the approved version of the following thesis:

Cloning, Expression, and Purification of *Burkholderia* Protein Targets for Diagnostic and Vaccine Development

APPROVED BY
SUPERVISING COMMITTEE:

Supervisor:

G. Barrie Kitto

Co-Supervisor:

Katherine A. Brown

Cloning, Expression, and Purification of *Burkholderia* Protein Targets for Diagnostic and Vaccine Development

by

Kate Christina McCaul, B.S.

Thesis

Presented to the Faculty of the Graduate School of

The University of Texas at Austin

in Partial Fulfillment

of the Requirements

for the Degree of

Master of Arts

The University of Texas at Austin

May 2012

Dedication

This thesis is dedicated to my loving husband, Ward McCaul. You are my balance and my better half. And you bring me ice cream! I love you more.

This thesis is also dedicated to my wonderful mom, Lori Strauss. You have always believed in me, and helped me believe in myself. I wouldn't be where I am today without you, or, seriously, I wouldn't be here at all!

Acknowledgements

Several people have given me advice and assistance during my graduate career. I'd especially like to thank Drs. Annie Gnanam and Omar Qazi for all their instruction and support in the laboratory. Drs. Katy Brown and Barrie Kitto have helped me immensely along the way. My wonderful family and friends have been available for a good laugh or cry, and that was indispensable. And lastly, I would like to thank my adorable dogs, Sadie and Max, for making me smile even on the most difficult days.

Abstract

Cloning, Expression, and Purification of *Burkholderia* Protein Targets for Diagnostic and Vaccine Development

Kate Christina McCaul, MA

The University of Texas at Austin, 2012

Supervisor: G. Barrie Kitto

Co-Supervisor: Katherine A. Brown

Burkholderia pseudomallei and *Burkholderia mallei* cause the diseases melioidosis and glanders, respectively. These diseases are endemic mainly in southeastern Asia and northern Australia, but they also pose a bioterrorism threat in the developed world. These diseases have high mortality, partially due to the lack of vaccines and rapid, accurate diagnostic assays. The work discussed here represents a part of a larger project to develop a dependable diagnostic assay for use in both developing endemic areas and the developed world, as well as a subunit vaccine to protect against disease. In this study, several proteins from *B. pseudomallei*, *B. mallei*, and the closely related but less virulent *B. thailandensis* have been cloned, expressed and purified in order to develop highly sensitive and specific diagnostic reagents for the detection of *B. pseudomallei* and *B. mallei* in infected patient samples. Protein targets expressed in this study were also used in subunit vaccine development for melioidosis and glanders.

Table of Contents

List of Tables

List of Figures

Chapter 1: Introduction

SECTION 1.1 *BURKHOLDERIA* SPECIES STUDIED

Section 1.1a Genus *Burkholderia*

The genus *Burkholderia* consists of more than 40 species of Gram-negative, non spore-forming, oxidase positive bacteria. With the exception of *Burkholderia mallei*, they are all motile soil saprophytes (Vial et al. 2007) The genus is diverse, containing animal and plant pathogens as well as non-infectious organisms. For this study, the focus is on the major animal pathogens *Burkholderia pseudomallei* and *B. mallei*, with *Burkholderia thailandensis* being used as a model organism to develop methods for use on the above pathogenic species.

Section 1.1b *Burkholderia pseudomallei*

B. pseudomallei is a saprophytic Gram-negative bacillus that is found in soil and surface water between latitudes 20 ˚N and 20 ˚S (reviewed in Cheng and Currie 2005). *B. pseudomallei* causes the often fatal disease melioidosis in humans, and can also cause lethal infections in several other species including large primates, birds, rodents, ungulates, and even sea mammals (reviewed in Cheng and Currie 2005). Melioidosis is primarily endemic in Southeast Asia and Northern Australia, but has also been found in the Middle East, China and South America (reviewed in Galyov et al. 2010). *B. pseudomallei* is extremely prevalent in Thailand, where it is estimated to be found in 50%

of all rice paddies (White 2003). The Centers for Disease Control (CDC) has classified *B. pseudomallei* as a biosafety level 3 agent and category B biothreat agent, because it could be easily disseminated, results in high mortality rates, and would require special action for public health preparedness (www.bt.cdc.gov/agent/agentlist-category.asp, (Dance 2002). It has been investigated for potential bioweapon use by both the former USSR and the United States, and while *B. pseudomallei* has not been weaponized in the past, it has the potential to be an extremely lethal bioweapon (Peacock et al. 2012). *B. pseudomallei* does not form spores, but it does have a polysaccharide capsule which produces a slime that makes it resistant to external factors including many antibiotics (White 2003). The capsule is a major virulence factor: mutants that have lost capsule production are greatly attenuated in virulence (Atkins et al. 2002). The bacterium needs water to survive environmentally, and does not tolerate cold or high or low pH conditions (Tong et al. 1996). *B. pseudomallei* is motile by means of a polar tuft of 2-4 flagella. The flagella are a major antigenic component during infection, and they may be involved in attachment to the host cells (reviewed in Dance 2005). Other virulence factors of *B. pseudomallei* include lipopolysaccharide (LPS), capsule, quorum sensing molecules, and the Types III and VI Secretion System components (reviewed by Galyov et al. 2010 and references therein).

B. pseudomallei strain K96243 was the first strain to be fully sequenced and its genome consists of two circular chromosomes (Holden et al. 2004). Chromosome one is 4.07 Mb and encodes 3,460 coding sequences, with a large proportion of these coding for

core functions of the bacteria including amino acid metabolism and protein biosynthesis. Chromosome two is 3.17 Mb and encodes 2,395 coding sequences, a higher proportion of which code for accessory functions such as osmotic protection and iron acquisition (Holden et al. 2004). In addition, *B. pseudomallei* has many insertion sequences, transposable islands, and horizontally-acquired genomic islands (Woods 2002; Holden et al. 2004). Presently, there are 4 strains that have been completely sequenced, *B. pseudomallei* 1106b, 1710b, 668 and K96243, and several more have been partially sequenced (ncbi.nlm.nih.gov/genome/genomes/476?subset=).

Bp82, an avirulent mutant of *B. pseudomallei* strain 1026b (Brett et al. 1997), has been recently generated for research in biosafety level 2 settings (Propst et al. 2010). This strain is a **Δ***purM* mutant, and is avirulent even at high doses. The *purM* gene encodes phosphoribosylformylglycinamide cycloligase, an enzyme upstream from the adenine and thiamine *de novo* synthesis pathway in the bacterium (Holden et al. 2004). The **Δ***purM* mutant Bp82 has been engineered with a deletion that removes residues 95-132, leaving a markerless space and predicted expression of a truncated and nonfunctioning, 99 residue protein (Propst et al. 2010). As a result, the mutant is an adenine auxotroph, however, repair of the mutation to the *purM* gene restores full virulence to the organism (Propst et al. 2010). Purine biosynthesis mutants have also been successfully generated for attenuation of other pathogens including: *Francisella tularensis* (Pechous et al. 2008), *Brucella abortus* (Alcantara et al. 2004), *Shigella flexneri* (Cersini et al. 2003), *Mycobacterium tuberculosis* (Jackson et al. 1996) and *Pseudomonas aeruginosa* (Lehoux

et al. 2002).

Section 1.1c *Burkholderia mallei*

B. mallei is a Gram-negative obligate intracellular pathogen that is the causative agent of glanders, a disease that is endemic in domestic animals in Asia, Africa, the Middle East, and South America (Elschner et al. 2011). Its natural reservoir is solipeds (e.g. horses and mules), where it causes a chronic form of the disease glanders, but the organism can also infect humans who are in close contact with infected animals. In animals other than horses and in humans the bacillus causes an acute form of glanders (Whitlock et al. 2007). *B. mallei* cannot persist in the environment outside of its natural host (Galyov et al. 2010).

The CDC has classified *B. mallei* as a biosafety level 3 agent and category B biothreat agent, because it could be easily disseminated, results in high mortality rates, and would require special action for public health preparedness (www.bt.cdc.gov/agent/agentlist-category.asp, (Dance 2002). *B. mallei* has been used against horses in biowarfare throughout history, including the American Civil War, World Wars I and II, and in the Russian invasion of Afghanistan between 1979-1988. Glanders was believed to have been spread deliberately by German agents to infect large numbers of Russian horses and mules on the Eastern Front. *B. mallei* has also been used against prisoners of war by the Japanese in WWII (Lehavi et al. 2002; Rotz et al. 2002; Horn 2003; Woods 2005).

B. mallei does not form spores, but it does have a polysaccharide capsule which produces a slime that makes it resistant to external factors including many antibiotics (DeShazer et al. 2001). The capsule is a major virulence factor: mutants that have lost capsule production are avirulent in hamsters, mice and horses (DeShazer et al. 2001; Lopez et al. 2003). *B. mallei* is the only member of the genus *Burkholderia* that is non-motile due to being non-flagellated. This is because of three major mutations in the flagellar synthesis pathway. There is a frameshift mutation in a methyl-accepting chemotaxis gene, a 65-kb sequence inserted into the *fliP* gene, which is essential for flagellum biosynthesis, and a second frameshift mutation in the *motB* gene, which codes for the flagellar motor protein (Nierman et al. 2004). Major virulence factors of *B. mallei* include lipopolysaccharide (LPS), capsule, quorum sensing proteins, and Types III and VI Secretion system components (reviewed by Galyov et al. 2010).

B. mallei strain ATCC 23344 was the first strain reported to be fully sequenced and its genome consists of two circular chromosomes (Nierman et al. 2004). Chromosome one is 3.5 Mb and encodes 3,344 coding sequences, with a large proportion of these coding for core functions of the bacteria including amino acid metabolism and protein biosynthesis. Chromosome two is 2.3 Mb and encodes 2,091 coding sequences, a higher proportion of which code for accessory functions such as virulence factors (Nierman et al. 2004; Whitlock et al. 2007). In addition, *B. mallei* has many insertion sequences, transposable inserts, horizontally-acquired genomic islands, and extensive, genome-wide rearrangements (Dance 2005; Galyov et al. 2010). Despite *B. mallei* having

greater than 1000 predicted genes less than *B. pseudomallei*, the two organisms have 99% sequence identity in the genes that that they share (Galyov et al. 2010). It is widely believed that *B. mallei* recently evolved from a single clone of *B. pseudomallei* through genome downsizing by gene loss and insertion sequences (Godoy et al. 2003; Losada et al. 2010). Ten different strains of *B. mallei* have been either partially or fully sequenced and sequence data is available online (ncbi.nlm.nih.gov/genome/genomes/477?subset=).

Section 1.1d *Burkholderia thailandensis*

Burkholderia thailandensis is a Gram-negative soil saprophyte closely related to *B. pseudomallei*. It is found endemically near *B. pseudomallei* in Southeast Asia, and was first isolated in Thailand (Brett et al. 1998). Originally it was considered to be a nonpathogenic subtype of *B. pseudomallei* that could not assimilate arabinose, but in 1998 (Brett et al. 1998) it was recognized as its own species.

B. thailandensis has two chromosomes, 3.8 Mb and 2.9 Mb, with a total of 5,645 predicted protein-coding ORFs (Yu et al. 2006). Five strains of *B. thailandensis* have been sequenced, including strain E264 used in this study (http://www.ncbi.nlm.nih.gov/genome/genomes/721?subset=) *B. thailandensis* and *B. pseudomallei* are broadly similar at many genomic levels, and they share many genes responsible for functions such as core metabolism and accessory pathways. Even bacterial virulence factors are conserved between the two species, although there is evidence that the virulence genes in *B. pseudomallei* have undergone accelerated

evolution in comparison to *B. thailandensis* (Yu et al. 2006). Because of this, *B. thailandensis* has been used as a model organism for the study of *B. pseudomallei*. (reviewed in Galyov et al., 2010). Genome comparison between the two organisms has helped to identify major *B. pseudomallei* virulence factors based on their absence or differences in *B. thailandensis* (Haraga et al. 2008; Galyov et al. 2010 and references therein).

Human cases of infection from *B. thailandensis* or *B. thailandensis*-related organisms are extremely rare and the clinical view is that this organism poses little danger to humans. It has, however, been shown that high intranasal inoculating doses ($1x10^6$ cfu, as compared to $1x10^3$ cfu of *B. pseudomallei)* of *B. thailandensis* can cause fulminant, lethal infections in a mouse model of infection (Wiersinga et al. 2008). In fact, there are case studies that have found *B. thailandensis* infection in humans, including in an amputated knee in Thailand (Lertpatanasuwan et al. 1999), and a potential case of pneumonia and septicemia caused by *B. thailandensis* was reported in northeastern Texas (Glass et al. 2006). *B. thailandensis* infection is dependent on shared virulence factors with closely related species *B. pseudomallei* and *B. mallei* (West et al. 2008). There is evidence that these shared virulence factors, including LPS, Types III and VI Secretion systems, and quorum sensing molecules (reviewed by Galyov et al. 2010), contribute to intracellular spread in eukaryotic cells (Harley et al. 1998). After intranasal infection in a mouse model, the lungs are most commonly affected and the bacterium can spread to the spleen and other organs (Wiersinga et al. 2008).

SECTION 1.2 MELIOIDOSIS

Section 1.2a Melioidosis Disease History, Transmission, Clinical Presentation and Progression

The disease melioidosis, previously known as Whitmore's disease, was first discovered in Burma by Captain Alfred Whitmore, a British pathologist, and his assistant C.S. Krishnaswami in 1912 (Whitmore 1913). Independently, at the Institute for Medical Research in Malaysia, bacteriologist Ambrose Thomas Stanton and pathologist William Fletcher began to study an outbreak of "distemper-like" disease in animals. In 1917 (Stanton and Fletcher 1932), the two scientists identified *Bacillus pseudomallei* as the causative agent of the disease. Stanton and Fletcher named the disease 'melioidosis' from the Greek, *melis,* which translates to 'distemper of asses,' and *eidos,* which translates to 'resemblance' because of the strong resemblance of the disease to glanders (Stanton and Fletcher 1932).

There is a high prevalence of melioidosis in northeastern Thailand and northern Australia. In Thailand, there are an estimated 2,000-5,000 cases of melioidosis per year, though the number of cases is likely underreported (Dance 1991). Melioidosis is the most common cause of community-acquired septicemia in Thailand, accounting for 20% of all septicemias. In parts of northern Australia melioidosis is the most common cause of community-acquired bacteraemic pneumonia (Cheng and Currie 2005; Limmathurotsakul

et al. 2010).

Several predisposing conditions have been linked to melioidosis infection, and between 66-80% of melioidosis cases have underlying predisposing conditions (Suputtamongkol et al. 1999; Currie et al. 2000). The most common predisposing condition, diabetes mellitus with poor sugar control, is present in 37-60% of melioidosis cases in Australia and Thailand (Sarkar-Tyson and Titball 2010). Other predisposing conditions include chronic renal failure, immunosuppressive treatments, including steroids, thalassemia, chronic liver disease, chronic lung disease (including cystic fibrosis) and kava consumption (reviewed by Limmathurotsakul and Peacock 2011). Surprisingly, although HIV is also prevalent in Thailand, no link has been identified between melioidosis and HIV infection, and melioidosis patients who are HIV+ have similar outcomes to patients who are HIV- (Chierakul et al. 2004).

There are three generally accepted routes of melioidosis infection: inhalation, inoculation, and ingestion (Cheng and Currie 2005). While percutaneous inoculation following exposure to muddy soils or surface water is considered to be the natural infection route, it is thought that under certain environmental conditions, such as tropical storms, cyclones, and typhoons, inhalation is the main mode of infection (reviewed in Patel et al. 2011 and references therein). The inhalational route is also supported by observations during the Vietnam War that helicopter crews were frequently infected with *B. pseudomallei* due to the aerosols generated by the helicopter blades (Howe et al. 1971). Increases in melioidosis cases have also been documented during the rainy season,

after monsoons, and after the tsunami in 2004 (Chierakul et al. 2005). In fact, rainfall fourteen days before hospital presentation with melioidosis is a strong indicator of disease severity (Cheng and Currie 2005). Person-person or animal-animal spread through the respiratory route is very rare and not considered to be a mode of transmission (Limmathurotsakul and Peacock 2011).

From a well-defined exposure to *B. pseudomallei*, the incubation period for acute melioidosis is between 1-21 days, with a mean incubation time of 9 days (Currie et al. 2000). Melioidosis is a febrile illness, and the most common presentation is pneumonia, with or without septicemia (Currie et al. 2000). Other common symptoms include superficial pustules and subcutaneous abscesses (Limmathurotsakul and Peacock 2011). The lungs are most commonly affected, and from the lungs the organism is spread throughout the body via macrophages (White 2003). The most common secondary sites of *B. pseudomallei* colonization include the liver, spleen, skin and soft tissues (Limmathurotsakul and Peacock 2011). Clinical patterns of the disease differ in Thailand and Australia. In Thailand, 30-40% of children who acquire melioidosis infections present with suppurative parotitis, which is not seen in Australia. In Australia, melioidosis can cause encephalomyelitis and, in 18% of infected males, can also cause genitourinary infection with prostatic abscesses. These manifestations have not been reported in Thailand (Cheng and Currie 2005; Limmathurotsakul and Peacock 2011).

Treatment of melioidosis is difficult. *B. pseudomallei* is intrinsically resistant to many antibiotics, including the drugs that are customarily given to patients with

pneumonia and septicemia (Cheng 2010). In addition, *B. pseudomallei* has many mechanisms that it uses to exploit the host cells' defenses and evade the immune system. The organism has the ability to overcome innate, cell-mediated, and antibody-mediated immunities, as well as the ability to invade and replicate inside both epithelial and phagocytic cells (reviewed by Galyov et al. 2010). The mortality rate for melioidosis infection in Thailand is 40-50%, and it is the third most common cause of death from infectious disease there after HIV/AIDS and tuberculosis (Limmathurotsakul et al. 2010). In Australia the mortality rate is 15-19% (Cheng et al. 2008; Limmathurotsakul et al. 2010). The difference in mortality is largely due to the inequality of intensive care facilities between the two areas (Limmathurotsakul et al. 2010).

Chronic infections are also seen in melioidosis. Chronic melioidosis has similar manifestations to disseminated fungal infection or tuberculosis (Weber et al. 1969). Not much is understood about the location or activities of the bacteria during latent infections, but it has been observed that in animal models, the bacteria are located in the lungs, liver and spleen (Dance 2005). Latent infection can reemerge after stresses such as illness or aging (Sanford 1978). The longest recorded latency of melioidosis infection was in a WWII veteran, where the infection recurred after a latent period of 62 years (Ngauy et al. 2005). Many Vietnam War veterans who had contracted melioidosis during the war had recurrence of illness between 1-5 years after the initial event, mostly after a precipitating event such as an unrelated illness (Sanford 1978). Because of this, melioidosis has been nicknamed "the Vietnamese Time Bomb." One Vietnam War veteran had recurrence of

melioidosis after a 36 year latency (Wells et al. 2011), and it is possible that there are veterans who yet have latent *B. pseudomallei* infections.

Section 1.2b Melioidosis Treatment and Antibiotic Resistance

As previously noted, treatment of melioidosis is challenging. *B. pseudomallei* is intrinsically resistant to penicillins, cephalosporins, macrolides, rifamycins, colistin, aminoglycosides, quinolones, beta lactams, and polymixins (Wuthiekanun et al. 2011). The current protocol for antibiotic treatment of melioidosis includes an initial intensive intravenous phase followed by a prolonged oral eradication phase. The initial phase consists of either ceftazimide or carbapenem for 10-14 days, followed by 3-6 months of eradication with trimethoprim-sulfamethoxazole with or without doxycycline. Even with 20 weeks of treatment the disease can still relapse in 5-25% of cases (Limmathurotsakul and Peacock 2011).

B. pseudomallei is also susceptible to silver carbene complexes *in vitro*, and could be used to treat infection (Panzner et al. 2009). Cationic liposome DNA (CLDC) has also been studied as a potent activator of innate immunity in a mouse model. It has been demonstrated that CLDC can provide nearly complete protection if it is administered via an intranasal route shortly after bacterial challenge (Goodyear et al. 2009). Interferon-γ (IFN-γ) has also been used for the treatment of melioidosis. Previous reports indicate that IFN-γ plays an important role in the host's defenses against *B. pseudomallei* infection. Combination treatment with ceftazimide and IFN-γ has shown a strong synergistic

inhibition of *B. pseudomallei* growth in macrophages (Propst et al. 2010).

Section 1.2c Melioidosis Current Diagnostics

Culture of *B. pseudomallei* is the gold standard of melioidosis diagnostics (White 2003). Isolation of even a single colony from a low quality sample may be enough to diagnose melioidosis, as any *B. pseudomallei* colonization is extremely rare (Walsh and Wuthiekanun 1996; Peacock 2006; Cheng 2010). Isolated growth of *B. pseudomallei* is ideally performed on Ashdown's media (Ashdown 1979), which contains glycerol and gentamicin. Glycerol enhances the wrinkled appearance of the colonies, and gentamicin selects against many normal bacterial species. Ashdown's media also contains a dye that is taken up into the colonies, and this facilitates presumptive identification of *B. pseudomallei* (Dance et al. 1989). Positive blood cultures take 48 h, but it can take up to 5-7 days for culture confirmation (Weber et al. 1969; Cheng 2010). As acute melioidosis infection can be fatal within this time period, improved sensitive and specific diagnostic tests are necessary.

Many diagnostic tests exist for melioidosis, including latex agglutination, indirect hemagglutination (IHA), polymerase chain reaction (PCR), and immunofluorescence; as well as several commercially available kits. Each of these diagnostic tests has its own strengths and shortcomings.

Latex agglutination, an assay where monoclonal or polyclonal antibodies are attached to latex beads are combined with culture to detect surface epitopes, has been

shown to be highly sensitive and specific when used with a monoclonal antibody against *B. pseudomallei* polysaccharide capsule (Wuthiekanun et al. 2002). Although this assay is able to differentiate between *B. pseudomallei* and *B. thailandensis* (which lacks a capsule), the assay does not differentiate between *B. pseudomallei* and *B. mallei*, and it requires a bacterial culture to be performed, which does not increase the speed of diagnosis (Amornchai et al. 2007). However the test is inexpensive and technically simple, thus making it very amenable for use in developing countries where melioidosis is endemic (Amornchai et al. 2007).

IHA is the only widely used serological test for melioidosis, despite many reports of low sensitivity and specificity (Cheng et al. 2006). It is a simple and inexpensive test to perform, and it tests for antibodies against *B. pseudomallei* antigens in the blood. However, it has a high rate of false positives in endemic areas because many people are seropositive to *B. pseudomallei* as a result of environmental exposure (Cheng and Currie 2005). In Thailand, 60-70% of children are seropositive according to IHA testing (Wuthiekanun et al. 2006)

There have been several reports of PCR assays for the detection of *B. pseudomallei*. The evidence for success of these assays is difficult to deduce because of many conflicting reports and difficulty of reproduction. PCR is an ideal medium for differentiating between *B. pseudomallei* and *B. mallei*, which is useful in the case of a bioterrorism event (Peacock 2006). A few genes that have been used in PCR diagnostic assays include: 16S rRNA gene, *rpsU*, *fliC*, genes encoding the Type III Secretion

System, and *recA* (Suppiah et al. 2010). However, due to the high cost, PCR assays are not suitable for use in rural endemic areas, where Gram stains and immunofluorescence are much cheaper. PCR assays also have relatively low sensitivity from direct blood specimens because of the low bacterial load found in the blood (Cheng 2010).

Immunofluorescence is a very promising diagnostic assay for endemic areas. A one-step, rapid immunofluorescence assay has been developed that can detect *B. pseudomallei* in sputum, pus, or urine in under 30 min using fluorescence-labeled monoclonal antibodies raised against *B. pseudomallei* (Wuthiekanun et al. 2005). This assay is highly specific and fairly sensitive. Unfortunately, the monoclonal antibody used for this assay was produced in-house at the clinic where it was used, and the animal that provided the antibody is now dead. This assay could easily be recreated with other monoclonal antibodies against *B. pseudomallei*, and with high quality antibodies the sensitivity and specificity would be greatly increased. This has been demonstrated on *B. thailandensis* using a commercially available *B. mallei* anti-LPS monoclonal antibody (Qazi et al. 2011).

Several commercial kits have been tested for their ability to diagnose *B. pseudomallei*. The API20NE test, a biochemical panel that relies on culture, has widely varying reports of sensitivity and specificity, but may be suitable for detection of certain strains of *B. pseudomallei*. The Vitek 1 and 2 automated identification systems have reliability issues in *B. pseudomallei* detection, and are therefore not ideal for diagnosis (Dance 2005; Peacock 2006). The Rapid Immunochromogenic Cassette test (ICT) has

been found to be less specific and sensitive than culture, and the RapID NF Plus test, a culture-based biochemical panel, has been found to be ineffective (Peacock 2006). It has been surmised that the most cost effective and sensitive diagnostic tests for acute infections will involve direct detection of bacterial antigens or whole organisms (Qazi et al. 2011).

Section 1.2d Melioidosis Vaccine Status

There is currently no vaccine available for melioidosis, though many strategies for vaccination have been investigated. Various levels of protection from *B. pseudomallei* infection have been observed for several of these strategies, but sterile immunity is rarely reported (Sarkar-Tyson and Titball 2010). One of the hurdles to an effective vaccine is an unresolved understanding of the protective innate and adaptive immune responses of the host (Whitlock et al. 2007). It has been speculated that a multicomponent vaccine will have the best protection against *B. pseudomallei* due to our current understanding of protective responses (Sarkar-Tyson and Titball 2010). Humeral and cell-mediated immunity, both intrinsic and acquired, are essential for protection (Whitlock et al. 2010).

As previously mentioned, several strategies for protection against *B. pseudomallei* infection have been investigated in mice, including passive transfer, heat-killed and attenuated vaccination, and subunit vaccination. Passive transfer is a protection strategy that uses antibodies as protective agents. There has been some success in passive transfer vaccination using antibodies raised against LPS, flagellin, and capsule. Passive transfer of

anti-capsule and anti-LPS antibodies has been shown to double survival time post challenge with *B. pseudomallei* (Nelson et al. 2004). Data on immunizations with heat-killed *B. pseudomallei* are conflicting, but one study has found some sterilizing immunity using a heat-killed vaccination strategy (Sarkar-Tyson et al. 2009). Live, attenuated auxotrophic *B. pseudomallei* mutants have shown protection against challenge in mice, however, it seems unlikely that an attenuated mutant would be approved for use in human vaccines (reviewed in (Sarkar-Tyson and Titball 2010). Subunit vaccine development has identified several *B. pseudomallei* antigens that offer some level of protection. Capsule and LPS polysaccharides provide protection (Nelson et al. 2004) as well as recombinant *B. pseudomallei* proteins including LolC (Harland et al., 2007), and BimA, HcpI, and BopA (Whitlock et al. 2010). These five recombinant proteins all had 80% protection after 14 days, which is comparable to other studies (reviewed by (Patel et al. 2011). However, 60% of mice immunized with BopA survived 55 days post-infection, which makes BopA extremely promising for future vaccine work (Whitlock et al. 2010). Nieves *et al*. have reported a promising immunization approach against *B. pseudomallei* that utilizes bacterial derived outer membrane vesicles (OMVs). They have demonstrated that immunization with naturally shed *B. pseudomallei* OMVs provide significant protection against lethal aerosol challenge in a murine model of melioidosis (Nieves et al. 2011).

SECTION 1.3 GLANDERS

Section 1.3a Glanders Disease History, Transmission, Clinical Presentation and Progression

Glanders was first described by early Greek and Roman writers Aristotle, Apsyrtus, and Vegetius around BC 350, and Aristotle called the disease of horses mellis, or distemper of asses (Derbyshire 2002; Whitlock et al. 2007). The contagious nature of glanders was first described by the French veterinarian Solleysel in 1664, and by the early 19th century transmission of glanders from horse to human was well described in Europe (Derbyshire 2002). In 1882 *B. mallei* was identified as the causative agent of glanders from horse sputum by two independent groups; Loeffler and Shutz in Germany, followed by the French microbiologists Bouchard, Charrin, and Capitan (Derbyshire 2002). Shortly afterwards, three groups independently developed the mallein skin test (described in section 1.3c) for specific diagnosis of glanders (reviewed by Derbyshire 2002; Whitlock et al. 2007 and references therein).

Glanders was successfully eradicated from Great Britain, the United States, Canada, and all of Europe between 1928 to 1938 (reviewed by Derbyshire 2002). Eradication was tedious, as every animal was tested with the mallein skin test before entry to the country and infected animals were culled. In Canada alone, eradication took 34 years, during which over 13,000 horses were killed and $1 million was spent in compensation for infected animals (Derbyshire 2002). While lower dependence on horses as a mode of transportation has decreased the incidence of glanders, recent outbreaks in the last two decades have occurred in Turkey, the United Arab Emirates, Iraq, Iran, India,

Pakistan, Mongolia, China, Brazil and Bahrain (reviewed in Elschner et al. 2011).

Horses are the primary carriers of glanders, but donkeys and mules can also become infected when they come into contact with *B. mallei* in food and water that has been contaminated with infected sputum. In endemic regions, *B. mallei* infections have also been known to occur in other mammals including cats, dogs, bears, wolves and camels (Wernery et al. 2011 and references therein). Direct animal-animal transmission in horses is facilitated by crowding and by sharing food and water sources with glanderous animals (Galyov et al. 2010). Humans can become infected either by close interaction with infected animals or by laboratory exposure, but human glanders is extremely rare and human-human transmission has not been documented (Whitlock et al. 2007). Glanders has not historically linked to predisposing conditions like melioidosis has, but the most recent case of laboratory-acquired glanders occurred in a diabetic man (Srinivasan et al. 2001). Laboratory-acquired glanders is more common than laboratory-acquired melioidosis, leading to the suspicion that *B. mallei* is more infective than *B. pseudomallei* in the laboratory setting (Howe and Miller 1947).

Glanders is a febrile illness, and it can be either a chronic or acute disease. The chronic form is seen in horses, where it causes mucopurulent nasal discharge, lesions on the lungs, nodules in the liver and spleen, enlargement of lymph nodes, and pustules on the flanks and extremities (Whitlock et al. 2007; Galyov et al. 2010 and references therein). Discharge from the nose and pustules is infectious. Acute glanders is seen primarily in donkeys and mules and causes high fever, emaciation, ulceration of the nasal

septum, and nasal discharge that is mucopurulent and sometimes hemorrhagic. Symptoms of human glanders have been reported as left axillary adenopathy, fever, fatigue, night sweats, malaise, rigors, and weight loss (Srinivasan et al. 2001).

Glanders was deadly before the invention of antibiotics, and it is extremely antibiotic resistant (Dance 2005). Treatment of glanders requires a prolonged course of antibiotics for eradication of the organism. Septicemic glanders has a 95% fatality rate in untreated cases, but for infections treated with antibiotics the fatality rate is still 50% (Whitlock et al. 2008).

Section 1.3b Glanders Treatment and Antibiotic Resistance

B. mallei is intrinsically resistant to many antibiotics including penicillins, cephalosporins, macrolides, rifamycins, colistin, quinolones, beta lactams, and polymixins (Kenny et al. 1999; Thibault et al. 2004). Ceftazimide and levofloxacin are effective *in vitro* and *in vivo* against *B. mallei* for acute infection in a mouse model, but they fail to completely eradicate the bacterium, leading to a chronic, non-lethal form of glanders (Judy et al. 2009). Granulysin, a lytic peptide component found naturally in cytotoxic lymphocytes, may have potent lytic effects on *B. mallei*. Granulysin works by directly disrupting the microbial membrane by electrostatic charge disruption (Endsley et al. 2009). Silver carbene complexes are also effective *in vitro* against *B. mallei* and could be tested *in vivo* for activity during experimental glanders infections, which has not yet been done (Panzner et al. 2009). Treatment immediately before or after intranasal

bacterial challenge with cationic liposome DNA (CLDC) has also been shown to protect from *B. mallei* infection by activating the innate immune system (Goodyear et al. 2009).

Section 1.3c Glanders Current Diagnostics

Definitive diagnosis of glanders is made from isolation and identification of *B. mallei* from culture. *B. mallei* does not grow as well in culture as *B. pseudomallei*, and produces smooth, grey, translucent colonies. Most of the diagnostic tests for glanders are for use in horses and other equids, and there are not many diagnostic tests for glanders in humans (Dance 2005).

Historically the mallein test has been used to diagnose glanders in horses. The mallein test is similar to the tuberculin skin test, where mallein, a crude *B. mallei* cell extract, is injected subcutaneously or intradermally. Delayed hypersensitivity at the injection site is indicative of a positive mallein test (Derbyshire 2002). Mallein test sensitivity and specificity can vary depending on the type of mallein preparation.

The Complement Fixation Test (CFT) is the most valuable screening tool available for glanders in horses (Elschner et al. 2011), as it can detect carriers of the disease (Sprague et al. 2009). The assay is based on crude whole-cell preparations of *B. mallei*, which are used to detect anti-*B. mallei* antibodies in the horse's serum. CFT has 97% sensitivity compared to culture (Neubauer et al. 2005). False positive results occur in about 1% of tests, and could be due to cross reactivity with strangles, equine influenza, or petechial fever. False negatives can occur in animals that are old, pregnant, or worn

out (Sprague et al. 2009).

Section 1.3d Glanders Vaccine Status

There is no animal or human vaccine for glanders, however studies to develop vaccines are ongoing (Peacock et al. 2012). One of the hurdles to an effective vaccine is an unresolved understanding of the protective innate and adaptive immune responses of the host (Whitlock et al. 2007). It is understood that both humoral and cell-mediated immune responses are essential for protection against *B. mallei* infection (Whitlock et al. 2008). Live attenuated strains of *B. mallei* as well as heat killed cells may be good vaccines (Whitlock et al. 2007), and several proteins have been investigated for use in a subunit vaccine. Among the proteins that have been shown to be protective are LolC, BimA, HcpI, and BopA, with BopA demonstrating the best protection (Whitlock et al. 2010). Because of its nature as an intracellular pathogen, sterilizing immunity is difficult to achieve.

SECTION 1.4 PROTEIN TARGETS

Section 1.4a FliC, BPSL_3319

Flagella are long, hair-like structures that extend from the surface of many bacterial species. They are mainly used for swimming motility, but they can also be used in other functions, such as attachment to host cells during infection. FliC is the protein

subunit that makes up the flagellar structure, and there are thousands of copies of the FliC protein present in bacterial flagella (Aldridge and Hughes 2002).

Within the pathogenic *Burkholderia* species, *B. pseudomallei* is motile via a polar tuft of flagella, and *B. mallei* is non motile and non-flagellated. While *B. mallei* do have an intact copy of the *fliC* gene, a gene upstream in the flagellar biosynthesis pathway, *fliP*, is disrupted, leading to no flagella being made (Nierman et al. 2004). This makes FliC an ideal diagnostic target, as reagents recognizing the bacterial flagella would be able to differentiate between *B. pseudomallei* and *B. mallei*. While this differentiation is less important in natural cases because of the low rate of human glanders, it could be very important in the event of an intentional bioterrorism release.

B. pseudomallei FliC is well-known to be immunogenic during melioidosis infection, with anti-flagellin antibodies present during infection (Felgner et al. 2009). It has also been indicated as a virulence factor, and mutant strains of *B. pseudomallei* that do not produce flagella are attenuated in virulence (Chua et al. 2003; Wikraiphat et al. 2009). It has been suggested that flagella are involved in macrophage invasion (Chuaygud et al. 2008). In diagnostics, a recombinant, truncated FliC was successfully used as a probe against sera from melioidosis infection in ELISA, detecting anti-flagellin antibodies produced during active disease (Chen et al. 2003). The *fliC* gene has also been used in PCR-based diagnostic assays, which have their own drawbacks (Section 1.2c) (Sonthayanon et al. 2002; Tomaso et al. 2004; Tomaso et al. 2005). Because of its immunogenicity, FliC has also been tested in vaccines, most notably, a DNA vaccine

which showed protection against infection (Chen et al. 2006). Additionally, glycoconjucates of FliC with the O-polysaccharide moiety from *B. pseudomallei* have been shown to be protective in the diabetic rat model of disease (Brett and Woods 1996)

Section 1.4b PilA, BPSL_0782 and FimA, BPSL_1801

Type IV Pili (TFP) are surface structures found on a large variety of Gram-negative bacteria as well as a couple of Gram-positive species. They are thin, flexible fibers that are 6-8 nm wide and several micrometers long, and they often aggregate into bundles. Because of their location and structure, TFP are involved in a number of functions including host-cell adhesion, biofilm formation, and twitching motility (Proft and Baker 2009). TFP are homopolymers composed of thousands of copies of the pilin subunit PilA, a small 17 kDa protein (Craig et al. 2004).

It has been demonstrated that TFP are expressed during infection with *B. mallei* (Fernandes et al. 2007) and that they are highly immunogenic, but immunization with PilA is not protective. TFP are involved in adherence of *B. pseudomallei* to host cells, and are therefore a potent virulence factor in infection (Essex-Lopresti et al. 2005; Boddey et al. 2006).

Fimbrae are much like pili. They are long, proteinaceous structures that extend from the surface of the bacterium (Dodd et al. 1984). Fimbrae are comprised of many helically-arranged identical subunits of the FimA protein (Brinton 1965) It has been shown that both fimbrae and pili may be up-regulated during melioidosis infection

(Nandi et al. 2010)

Section 1.4c LolC, BPSL_2277

The LolABCDE complex is responsible for the transport of lipoproteins from the cytoplasm to the outer membrane in Gram-negative bacterial species. The LolCDE complex is an ATP-Binding Cassette (ABC) transporter that is responsible for moving lipoproteins from the cytoplasm, across the inner membrane, and into the periplasmic space using energy from ATP (Narita 2011). From there the hydrophobic lipoprotein is shuttled through the hydrophilic periplasm via LolA and passed to LolB in the outer membrane, where it is flipped to the outer leaflet of the membrane (Narita 2011). The Lol system is well conserved in Gram-negative bacteria, and disruption of this system is lethal in *Escherichia coli* (Harland et al. 2007).

The LolCDE complex is generally composed of four parts: one copy of the LolC protein, one copy of the LolE protein, and two copies of the LolD protein. LolCDE is directly involved with ATP hydrolysis necessary to transfer the lipoprotein to LolA as well as the recognition of sorting signals on peptides (Narita 2011). LolC is an integral membrane protein, spanning the inner bacterial membrane 4 times. In addition, it has a large periplasmic domain between the first and second transmembrane helices, composed of amino acid residues 44-266 (Harland et al. 2007; Narita 2011). In the LolCDE complex, LolC is responsible for the direct transfer of the lipoprotein to LolA.

LolC is considered an excellent protective antigen for use in a melioidosis vaccine

(Harland et al. 2007). It has repeatedly been shown to have protective qualities against multiple strains of *B. pseudomallei* as well as against *B. mallei* (Harland et al. 2007; Whitlock et al. 2010). The protective qualities of LolC are due to its ability to initiate a cell-mediated immune response in the host (Tippayawat et al. 2009) through the activation of T cells, and they are conserved across many *Burkholderia* species including *B. pseudomallei, B. mallei, B. thailandensis,* and *Burkholderia cepacia* (Tippayawat et al. 2011).

Section 1.4d BopA, BMA_1521

The type-three secretion system (T3SS) of *B. mallei* is involved in the translocation of effector proteins into the host-cell cytoplasm (Ulrich and DeShazer 2004). The genome of *B. mallei* contains two T3SS and the genome of *B.* pseudomallei contains three T3SS (reviewed in Galyov et al. 2010). This assists the bacterium in invading the host defenses and also allows it to survive in the intracellular environment. Many of the intracellular virulence functions of *B. mallei*, including replication, are dependent on a functional T3SS. BopA is one of these T3SS effector proteins, and it is likely involved in replication inside the host cell (Whitlock et al. 2009).

Mutant strains of *B. pseudomallei* deficient in BopA have demonstrated an increased time to death in infection (Whitlock et al. 2009). Immunization with BopA protein from *B. mallei*, has demonstrated protective properties during experimental glanders, as well as cross protective during experimental melioidosis, in the mouse model

of infection (Whitlock et al. 2010).

Section 1.4e SodC, BMA_0713

SodC is an outer-membrane superoxide dismutase enzyme that has been reported to act on exogenous, host-generated reactive oxygen species in a Cu^{2+} and Zn^{2+} dependent manner (Vanaporn et al. 2011). Because of this, SodC has been linked to virulence in many species of bacteria including *M. tuberculosis, Neisseria meningitidis, Vibrio vulnificus,* and *B. cepacia* (Vanaporn et al. 2011). In addition, SodC mutants of *Salmonella enterica* serovars Typhimurium, Cholerasuis and Dublin, have demonstrated attenuation in mice. SodC has recently been shown to be a key virulence factor in *B. pseudomallei*, where it is important for survival in host macrophages (Vanaporn et al. 2011).

Section 1.4f pIII Protein

Phage M13K07 is a derivative of the M13 filamentous phage that is generally used for phage display during selection of fragment antibodies (fABs). The pIII protein, the product of the g3p gene of the phage, is essential for propagation of the phage by being directly involved in the infection of the host bacteria (Holliger et al. 1999). There are 3-5 copes of the pIII protein located at one end of the virion. In phage display, these are engineered to also express fAB sequences, and these fABs interact with the target protein (Schmitz et al. 2000). It was during phage display against LolC-t protein that a

strong affinity of the naked phage (with no fABs present) to the LolC-t protein was noticed (M. Rani, unpublished data). It was then hypothesized that the pIII protein was responsible for the affinity, and this work attempts to characterize this high affinity binding.

Section 1.5 Project Aims

The aims of this project are to clone, express, and purify target proteins that have been identified as surface located or immunogenic by bioinformatic or experimental means. Specifically for this work, these protein targets include FliC, PilA, FimA, LolC, and BopA. Protein targets that have potential as diagnostic targets will be used for the selection of highly selective and specific diagnostic reagents: RNA aptamers, fragment antibodies (fABs), or commercially-produced monoclonal antibodies. High specificity and selectivity is important for rapid and accurate diagnosis of melioidosis and glanders without cross-reactivity to other organisms that could cause similar diseases in the endemic areas. These reagents will also then be used in the development of a novel diagnostic assay for melioidosis and glanders infections. Protein targets will also be tested in a subunit vaccine against melioidosis and glanders.

Chapter 2: Materials and Methods

SECTION 2.1 CHEMICAL REAGENTS

Chemicals were purchased from Fisher Scientific (Fair Lawn, NJ) and Sigma-Aldrich (St. Louis, MO). Kanamycin, ampicillin, and chloramphenicol were from Sigma-Aldrich (St. Louis, MO) and carbenicillin was from Carbenicillin Direct (United Kingdom). IPTG was from Gold Biotechnology (St. Louis, MO). Oligonucleotides were synthesized by Integrated DNA Technologies (IDT) (Coralville, Iowa). Expand Long Template High Fidelity Taq/Tgo polymerase mixture and Complete EDTA-Free protease inhibitor were from Roche (Indianapolis, IN), Taq polymerases were from Qiagen (Maryland) and NEB (Ipswich, MA), and Q-buffer and Ni^{2+}-NTA were from Qiagen (Maryland). Restriction enzymes and T4 DNA ligase were from NEB (Ipswich, MA). DNA molecular weight standards were from Bioline (Tauton, MA) and NEB (Ipswich, MA). Magnetic beads were from Millipore (Temecula, CA) and Bangs Laboratories (Fishers, IN). pEXP5/TOPO TA expression kit was from Invitrogen (Carlsbad, CA). Protein molecular weight markers, Sodium Dodecyl Sulfate (SDS), molecular grade agarose, tetraethylmethyldiamide (TEMED), nitrocellulose membrane, were from BioRad (Hercules, CA). 30% Bis-Acrylamide mixture, Nunc Maxisorp microtiter plates, and Coomassie Brilliant Blue stain were from Sigma Aldrich (St. Louis, MO). Dry skimmed milk powder was from SACO foods (Middleton, WI). Amicon Ultra centrifugal

filters were from Millipore (Temecula, CA). Mouse monoclonal Anti-polyhistidine peroxidase antibody, Streptavidin-Peroxidase Polymer- Ultrasensitive, and 4-chloro-1-naphthol were from Sigma (St. Louis, MO). 1-Step Ultra TMB ELISA reagent and biotinylation reagents were from Thermo Scientific (Rockford, IL). Dialysis tubing and dialysis clamps were from Spectrum Laboratories (Rancho Dominguez, CA).

SECTION 2.2 MEDIA

Luria-Bertani Broth (LB broth) was made with reagents from Fisher Scientific (Fair Lawn, NJ) according to published protocols (Sambrook et al. 1989). LB media is composed of 1% (w/v) tryptone, 0.5% (w/v) yeast extract, and 0.5% (w/v) NaCl and media was sterilized by autoclaving (15 min at 120 ˚C, 1.5 Bar pressure) and stored at room temperature.

Luria-Bertani agar (L-agar) consisted of LB supplemented with 2% (w/v) agar. Appropriate antibiotics were added as needed: 100 µg/mL carbenicillin and 50 µg/mL kanamycin.

Overnight Express Instant TB Medium (OE), an autoinduction medium, was purchased from Novagen (Darmstad, Germany). This medium contains components that automatically induce protein expression from *lac*-based promoters in a time-released manner. The OE was prepared according to manufacturer's specifications, sterilized by microwaving, and stored at 4 ˚C in the dark.

SECTION 2.3 BACTERIAL STRAINS

Five *Escherichia coli* strains were used in this study (Table 2.1). All strains were grown in either LB or OE. In addition, three *Burkholderia* strains were also used in this study (Table 2.1). All *Burkholderia* strains used in this study have been fully sequenced and the sequence data is available through online databases at www.burkholderia.com (Winsor et al. 2008).

E. coli strain DH5α allows excellent propagation of plasmid vectors. The *endA*$^-$ mutation knocks out the EndA endonuclease allowing for preparation of high quality plasmid DNA with lower levels of plasmid degradation.

E. coli BL21 (*DE3)* strains are deficient in proteases and designed for high level protein production from T7 RNA polymerase-based expression systems. These strains are naturally deficient in the Lon protease and are engineered to be deficient in the OmpT protease, both of which may cause degradation of recombinant proteins if present. The IPTG-induced expression of T7 RNA polymerase gene, which was integrated into the bacterial chromosome by *DE3* λ phage, allows expression of the plasmid-encoded gene to be tightly regulated. BL21_Star™ (*DE3*) has a mutation in the RNaseE gene, *rne*131, which is responsible for most mRNA degradation. BL21_Star™ (*DE3*) pLysS is designed to have low basal levels of heterologous gene expression and is designed for the expression of proteins that may be toxic to the *E. coli* host. Codon bias between recombinant genes and *E. coli* hosts can leave the tRNA pools depleted in the host leading to translational stalling, premature translation termination, translation frameshifting and amino acid misincorporation (Novagen). However, the Rosetta strain

of BL21 provides additional copies of rare tRNA genes on the pRARE plasmid that contains the *argU, ileX, leuW, proL,* and *glyT* genes that code for tRNAs that recognize the codons AGG/AGA, AUA, CUA, CCC, and GGA, respectively.

The bacterial strain OQ-Rosetta-BopA114, a modified form of BL21_Rosetta (*DE3*) containing the pET-28a(+)-OQBOPA114 construct, was obtained as a gift from Dr. Omar Qazi. This strain was used to express and purify BopA-t protein.

B. pseudomallei strain K96243 and *B. mallei* strain ATCC 23344 were not directly used, but genomic DNA from these strains was obtained as a gift from Dr. Alfredo Torres at the University of Texas Medical Branch in Galveston, Texas. *B. thailandensis* strain E264 was used for genomic DNA extraction by Dr. Annie Gnanam at The University of Texas at Austin, Austin Texas, and the obtained genomic DNA was used as template for PCR. Heat-killed *B. pseudomallei* K96243 and *B. thailandensis* E264 as well as live *B. thailandensis* E264 were also used in ELISAs.

B. pseudomallei strain Bp82, a gift from Dr. Herbert Schweizer is an attenuated derivative of *B. pseudomallei* 1026b (Section 1.1b). This strain was used in ELISA.

Escherichia coli strain	Genotype	Provider
DH5α	F^- Φ80*lacZ*ΔM15 Δ(*lacZYA-argF*) U169 *recA1 endA1 hsdR17* (rK^-, mK^+) *phoA supE44* λ– *thi-1 gyrA96 relA1*	Invitrogen
BL21 (*DE3*)	F^- *ompT hsdS*$_B$(r_B–, m_B–) *gal dcm* (DE3)	Invitrogen
BL21_Star™ (*DE3*)	F^- *ompT hsdS*$_B$(r_B–, m_B–) *gal dcm rne131* (DE3)	Invitrogen
BL21_Star™ (*DE3*) pLysS	F^- *ompT hsdS*$_B$(r_B^-, m_B^-) *gal dcm rne131* (DE3) pLysS (Cam^R)	Invitrogen
BL21_Rosetta (*DE3*)	F^- *ompT hsdS*$_B$(r_B^- m_B^-) *gal dcm* pRARE (Cam^R)	Novagen

Table 2.1 *E. coli* Strains used in this study

SECTION 2.4 PLASMIDS

All plasmids in this study have a T7 promoter and are IPTG inducible.

The pET-28a(+) plasmid (Novagen; Figure 2.1a) is an expression vector that confers kanamycin resistance and allows for expression of recombinant protein with either an N-terminal or C-terminal polyhistidine affinity tag.

The pET-15b plasmid (Novagen; Figure 2.1b) and the pEXP5-NT/TOPO plasmid (Invitrogen; Figure 2.1c) are expression vectors that confer carbenicillin resistance and incorporate an N-terminal 6x polyhistidine onto recombinant proteins expressed using it.

Plasmid pET-15b-OQFLICR containing a truncated portion of the FliC gene from *B. pseudomallei* strain K96243 (BPSL_3319) was obtained as a gift from Dr. Omar Qazi (UT Austin). This construct was designed based on the crystal structure of the *S. typhimurium* flagellin structure (1UCU). The FliC construct Qazi5-6 was designed to remove the oligimerization domains comprised of both the C- and N-termini. This plasmid has a pET-15b backbone with DNA sequence corresponding to amino acid residues 175-297 cloned between the *NdeI* and *BamHI* sites in the multiple cloning region of the plasmid (Figure 2.2a).

Plasmid pET-15b-OQFIMA containing a truncated portion of the FimA gene (BPSL_1801) from *B. pseudomallei* strain K96243 was obtained as a gift from Dr. Omar Qazi (UT Austin). This construct, Qazi7-8, is in the pET-15b plasmid with the DNA sequence corresponding to residues 21-170 of the FimA protein inserted between the *NdeI* and *BamHI* sites in the multiple cloning region of the plasmid (Figure 2.2b).

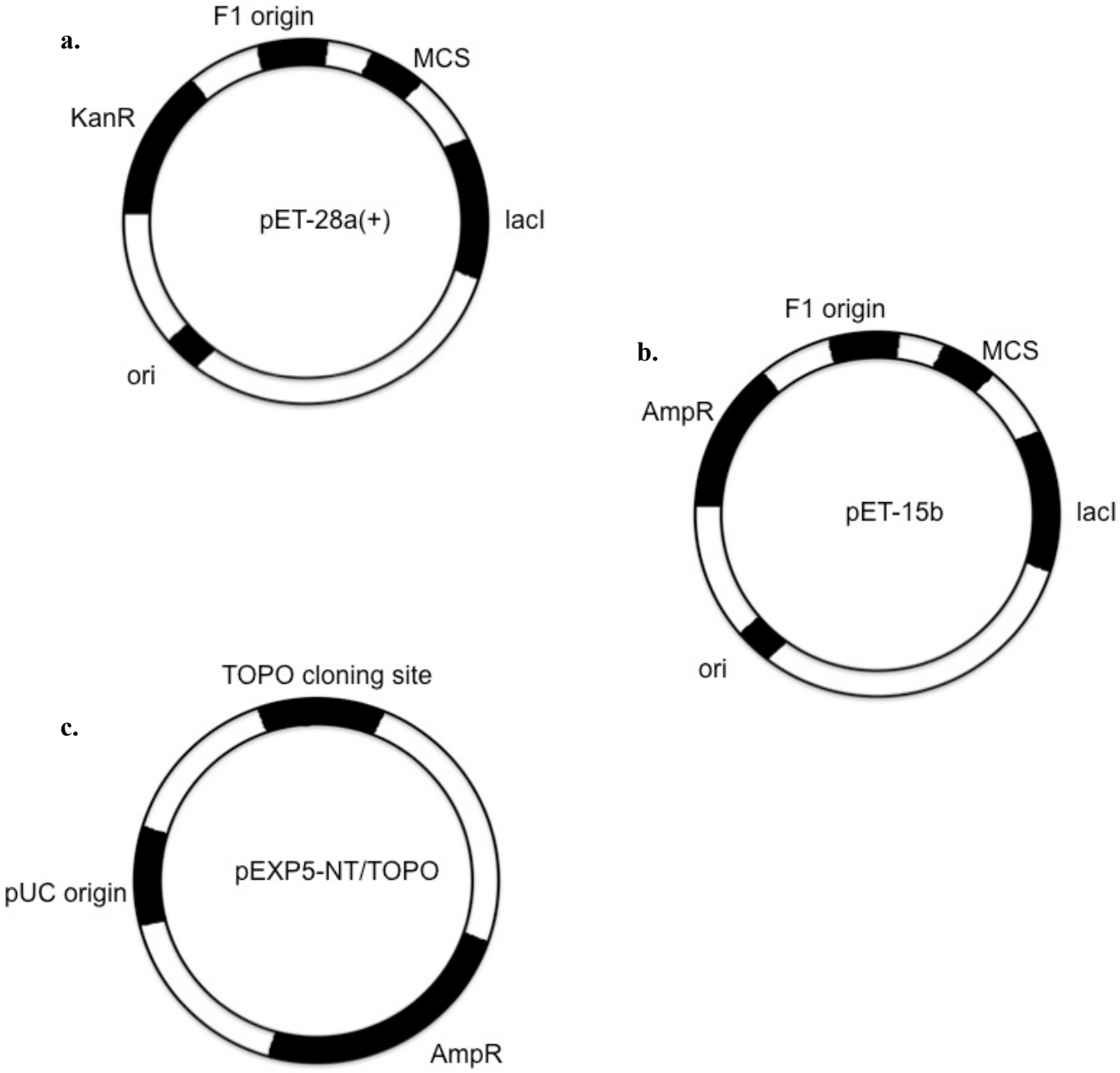

Figure 2.1 Empty Plasmid Vectors used in this study

Plasmid pET-28a(+)-OQLOLCN containing a truncated form of the LolC gene (BPSL_2277) from *B. pseudomallei* K96243 was obtained as a gift from Dr. Omar Qazi (UT Austin). This construct, is in the pET-28a(+) plasmid with the DNA sequence corresponding to residues 44-266 of the protein inserted between the *NdeI* and *BamHI* sites in the multiple cloning region of the plasmid, adding an N-terminal polyhistidine tag (Figure 2.2c).

The helper phage M13K07 was obtained from NEB (Ipswich, MA). This phage is a derivative of M13 filamentous phage that has a mutation at the origin of replication to add a kanamycin resistance gene and a P15A origin of replication from *E. coli*. This helper phage is often used for phage display to select antibody fragments (fABs) against molecular targets. In this project, however, it was used for PCR and cloning without purifying the genomic DNA.

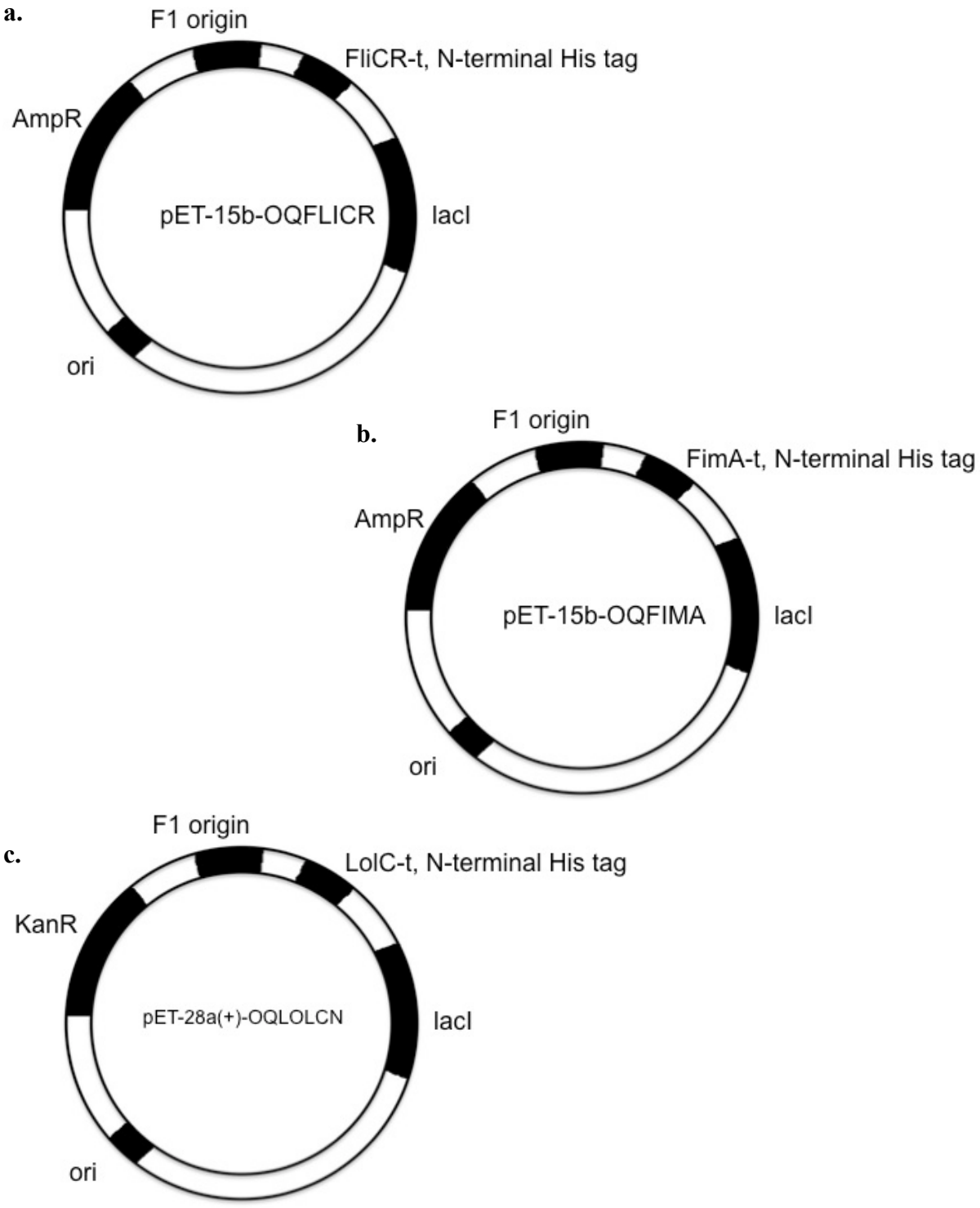

Figure 2.2 Plasmid expression vectors used in this study

SECTION 2.5 COMPETENT CELLS

5 mL of LB broth were inoculated from a glycerol stock of the relevant strain of *E. coli* and grown overnight at 37 ˚C with 250 rpm shaking. 20 mL of LB broth were then inoculated with 500 µL (1:50 dilution) of the overnight culture and grown at 37 ˚C with 250 rpm shaking until the Optical Density at 600 nm (OD_{600}) reached 0.6. Cells were centrifuged at 3,000 x *g* for 5 min and resuspended in 30 mL cold, sterile 10% (v/v) glycerol. Cells were pelleted again at 3,000 x *g* for 10 min and the supernatant removed and replaced with 30 mL fresh cold, sterile 10% glycerol. This wash was performed twice more for a total of three washes. The resulting cell pellet was resuspended in 500 µL of cold, sterile 10% glycerol, divided into 85 µL aliquots in 1.5-mL microfuge tubes, and stored at -80 ˚C. Competent cells were thawed on ice as needed.

SECTION 2.6 TRANSFORMATION

100 ng of purified plasmid or 30 µL of cleaned ligation product (Section 2.13) were added to 85 µL of competent cells (Section 2.5) and transferred to an electroporation cuvette (BioRad, Hercules, CA). The mixture of cells and DNA was pulse electroporated at 1800 V and transferred to 1.5 mL of LB broth and grown at 37 ˚C with shaking at 250 rpm for one h. Cells were centrifuged for 2 m at 240 x *g* and the supernatant discarded. Cell pellets were resupended in 110 µL LB broth. 100 µL of this suspension was spread neat onto L-agar plates containing the relevant antibiotic. The remaining 10 µL was diluted by the addition of 90 µL of LB broth and spread on L-agar plates, with the relevant antibiotic, as a 10^{-1} dilution. Agar plates were grown at 37 ˚C

overnight and visually scanned for transformed colonies. Bacteria that had incorporated the plasmid carried the antibiotic resistance gene and could grow on the antibiotic-containing media, whereas non-transformed colonies did not have the antibiotic resistance gene and would not survive on the antibiotic-containing media.

SECTION 2.7 GROWTH OF CULTURES

All cultures were supplemented with antibiotics as required. L-agar plates were streaked with cultures and incubated at 37 ˚C overnight. Liquid cultures were grown in standard glass or plastic baffled flasks with shaking at 250 rpm at 37 ˚C or 18 ˚C. Glycerol stocks were prepared by inoculating 5 mL of LB broth with a single colony and growing overnight 37 ˚C with shaking. 420 µL of sterile 50% (v/v) glycerol were added to 1 mL of overnight culture, vortexed to mix, and frozen at -80 ˚C for long-term storage.

SECTION 2.8 PRIMER DESIGN

Targets were chosen using proteomics, bioinformatics, comparative genomics and data from previously published work. Specific gene sequences for *Burkholderia* genes were obtained from CMR (Peterson et al. 2001), burkholderia.com, (Winsor et al. 2008), and Kyoto Encyclopedia of Genes and Genomes (KEGG) (Kanehisa 2000). These sequences were analyzed using the programs Signal P 3.0 (Bendtsen et al. 2004), TMHMM 2.0 (Krogh et al. 2001), and PHYRE or PHYRE 2 (Kelley and Sternberg 2009) to assess their suitability and to aid with construct design. DNA sequence of the targets

was analyzed for restriction sites using NEBcutter 2.0 (Vincze et al. 2003) or by using a built-in application in the Geneious Pro program (Drummond et al. 2011). Primers for pET-28a and pET15-b constructs consisted of 18-25 nucleotides corresponding to the beginning or the end of the sequence to be amplified along with insertions for the indicated restriction sites and, if not supplied by the plasmid, the insertion of a stop codon at the terminus of the sequence. Primers were flanked by random nucleotide sequences 4-5 nucleotides long to protect the restriction site from degradation. Primers for cloning in the TOPO system typically contained 18-25 nucleotides corresponding to the sequence of the gene, and the insertion of a termination codon at the end of the reverse primer. Primers were analyzed for melting temperature using OligoAnalyzer 3.1 on the IDT website, www.idtdna.com (Owczarzy 2005). Primer sequences were adjusted in length so that the forward and reverse primer melting temperatures were within 4 ˚C of one another and preferably in the range of 60-65 ˚C (Table 2.2).

Target	Primer	F/R	Tm	Vector	Sequence 5'-3'	aa cloned	DNA bp	kDa protein	His Tag	Restriction sites
BMA_A0810	KJ1	F	63.7	TOPO	TCCACGTCGACCTCGACCGG	21-386	1095	35.2	N-terminal	n/a
BMA_A0810	KJ2	R	63.9		TTACGTATCGGTCTGCTGCAGCGCTT					n/a
BPSL_1705	KJ3	F	63.8	TOPO	ATAGGCGGCGGGGGCTCAATACC	26-1200	3525	108.3	N-terminal	n/a
BPSL_1705	KJ4	R	64.1		TTACGTGCCCAACGCGATCGAGC					n/a
BTH_II0878	KJ5	F	60.4	TOPO	GGGGAAACAACCGATATCGGGC	34-424	1173	40.8	N-terminal	n/a
BTH_II0878	KJ6	R	59.7		TTAGAGCTGATTCCTGTTTACCGCATCC					n/a
BPSL_0782	KJ9	F	61.5	TOPO	GATTATCTCGCGCGCAGCCG	31-172	426	16.5	N-terminal	n/a
BPSL_0782	KJ11	R	62.2		TCACGCGCGGCACTCG					n/a
M13K07 pIII	KCM17	F	60.9	pET15b	GATGCACATATGGCTGAAACTGTTGAAAGTTGTTTAG	19-217	651	25.7	N-terminal	NdeI
M13K07 pIII	KCM18	R	62.6		TTACGACTCGAGTCAAGCATTGACAGGAGG					XhoI
BPSL_3319	OQ41	F	70.9	pET28a	ATATATACCATGGCGGCGAAGATCGGCGGCGGCAT	166-292	423	13.9	C-terminal	NcoI
BPSL_3319	OQ42	R	64.5		TATATATGCGGCCGCGATGTCGAGGTTCGAGACCGTTTGCGG					NotI
BMA_0713	OQ59	F	65.6	pET28a	ATATATACCATGGCCAACACGAAAAACGCGCCGACGCG	35-179	477	16.2	C-terminal	NcoI
BMA_0713	OQ60	R	68.8		TATATATGCGGCCGCTTGCCGCACGACGCCGCACG					NotI

Table 2.2 Oligonucleotide primers used in this study

SECTION 2.9 AGAROSE GEL ELECTROPHORESIS

Agarose gels, 0.8 and 1.0% (w/v), were made by melting molecular grade agarose

powder in 1x TAE buffer (40 mM Tris-acetate, 1 mM EDTA) in a microwave. Gels contained 0.5 µg/mL ethidium bromide and were cast horizontally for either the Hoefer HE 33 Mini Horizontal Submarine Unit (40 mL) or the Owl Separation Systems D3 (100 mL). Gels were run in a tank containing 1x TAE buffer. DNA samples were mixed 1 in 6 with loading buffer (0.25% (w/v) bromophenol blue, 0.25% (w/v) xylene cyanol FF, 30% (v/v) glycerol in water) and loaded into the gels wells. Electrophoresis was typically performed at 100 V for 1 h.

SECTION 2.10 PURIFICATION OF DNA

DNA purification was performed in two ways.

DNA to be purified by Gel Extraction was electrophoresed in a 0.8% (w/v) agarose gel (Section 2.9). The gel band containing DNA of the correct size, as determined by visual examination next to a known molecular weight ladder, was excised with a sterile blade, placed in a microfuge tube and weighed to determine how much reagent to add to dissolve the agarose. The DNA was purified from the gel band using the QIAquick Gel Extraction Kit (Qiagen, Maryland) according to the manufacturer's instructions and eluted in 30-50 µL sterile water (Qiagen, Maryland).

DNA was also purified with the QIAquick PCR Purification Kit (Qiagen, Maryland) according to the manufacturer's instructions and eluted in 30-50 µL sterile water.

SECTION 2.11 PREPARATION OF PLASMID DNA

Plasmid DNA was purified from 5-10 mL bacterial cultures grown in LB broth using the QIAprep Spin Miniprep Kit (Qiagen, Maryland) according to the manufacturer's instructions. Plasmid DNA was eluted in 30-50 µL sterile water for short term-storage or in elution buffer provided for long-term storage.

SECTION 2.12 DNA DIGESTION WITH RESTRICTION ENZYMES

1 µg of DNA was digested in a final volume of 40-60 µL. The DNA, 10x enzyme buffer (supplied with the enzyme by NEB, Ipswich, MA), restriction enzymes, and water were gently mixed together and incubated at 37 ˚C in a water bath. The duration of incubation depended on the enzymes used, and varied from 2 h to overnight.

SECTION 2.13 DNA LIGATION

Ligations were generally performed in volumes of 30-50 µL with buffer supplied the enzyme (NEB, Ipswich, MA). The weight ratio of vector to insert was 1 to 3, and a minimum of 100 ng of vector was used. After the ligation, the ligation mixture was subjected to a PCR purification (Section 2.10) and eluted from the spin column in 30 µL sterile water.

SECTION 2.14 TOPO CLONING

Cloning into the TOPO vector was performed according to the manufacturer's

instructions in 6 µL using 3 µL of cleaned PCR product (Section 2.10), 1 µL provided salt solution, 1.5 µL sterile water, and 0.5 µL of the TOPO vector. Plasmid was then transformed into provided One Shot chemically competent *E. coli* cells by heat shock, grown in provided S.O.C. medium at 37 ˚C with shaking for 1 h, and spread on L-agar plates with carbenicillin for overnight selective growth.

SECTION 2.15 DNA CONCENTRATION

DNA concentration was determined using a Nanodrop 2000 Spectrophotometer (Thermo Fisher, Wilmington, DE). 2 µL of DNA were loaded onto the instrument and the absorbance was measured at a wavelength of 260 nm. Software included with the machine calculates the analyte concentration using a modified version of Beer's Law, c = (A * e)/b Where c is the nucleic acid concentration in ng/µL, A is the absorbance in AU, e is the extinction coefficient in ng-cm/µL and b is the path length in cm. The generally accepted extinction coefficient for double stranded DNA is 50 ng-cm/µl and for single stranded RNA is 40 ng-cm/µl. This calculation gives the concentration output in ng/µL.

SECTION 2. 16 POLYMERASE CHAIN REACTION

DNA sequences were amplified using the polymerase chain reaction (PCR). Templates were typically genomic DNA from *B. pseudomallei* K96243*, B. mallei* 23344*,* and *B. thailandensis* E264 (Section 2.3), but also included M13K07 filamentous phage (Section 2.4) and transformed bacterial colonies. PCR was performed using basic Taq

polymerase or Expand Long Template High Fidelity Taq/Tgo polymerase mixture (Section 2.1).

Amplification with either polymerase type was performed in volumes ranging from 10 µL to 100 µL. The PCR reactions generally contained 10% (v/v) of the provided 10x PCR buffer, 20% (v/v) of the Q buffer, if necessary (Qiagen, Maryland), 200 µM dNTP mixture, about 1 U of Taq/10µL of reaction, and approximately 1.5 ng of genomic DNA per 10 uL reaction. Amplification thermalcycler programs varied by the length of DNA to be replicated and the melting temperature of the specific primers used (Table 2.2). The general outline of the thermalcycler program was:

1. 94 ˚C for 5:00
2. 94 ˚C for 0:30
3. Annealing temperature and time varied by construct
4. 72 ˚C, time varied by construct
5. Repeat steps 2-4 29 times for a total of 30 cycles.
6. 72 ˚C for 10:00
7. 4 ˚C indefinitely

Agarose gel electrophoresis (Section 2.9) was used to verify amplification for a small scale PCR before moving on to larger volumes.

SECTION 2.17 DNA SEQUENCING

Recombinant plasmids grown in *E. coli* DH5α were purified as described above (Section 2.11). Purified plasmids were sent to the DNA Sequencing Facility in the Institute for Cellular and Molecular Biology at the University of Texas at Austin. Sequencing was performed using capillary-based electrophoresis on an AB 3730 series

machine with T7 sequencing and terminating primers (Table 2.3), added by the staff in the facility as indicated upon sample submission.

Primer name	Sequence
T7 Sequencing Primer	5'-TAATACGACTCACTATAGGG-3'
T7 Terminator Primer	5'-GCTAGTTATTGCTCAGCGGT-3'

Table 2.3 Sequencing Primers used in this study

SECTION 2.18 DNA SEQUENCE ANALYSIS

DNA sequences obtained post-sequencing from the DNA Sequencing Facility were analyzed against available genomic data using the program Geneious Pro (83).

SECTION 2.19 PROTEIN EXPRESSION OPTIMIZATION

Plasmids confirmed to contain the correct insert from DNA sequencing were transformed into *E. coli* BL21 strains (Section 2.6) for expression studies. Colonies were picked and grown in 5 ml LB broth overnight with the indicated antibiotics at 37 ˚C with 250 rpm shaking. On the following day, 50 µL of each overnight culture were added to 5 mL of LB broth containing the appropriate antibiotics and allowed to grow at 37 ˚C with shaking until an OD_{600} of 0.6 was reached. Cultures were then induced with either 1.0 or 0.1 M IPTG and grown with shaking at either 37 ˚C or 18 ˚C. Time points of 500 µL

were collected at 2 h, 4 h, 6 h and overnight for the 37 ˚C cultures, and at 6 h and overnight for the 18 ˚C cultures. Samples were spun down at 20,800 x *g* for 5 min, pellets were lysed by boiling with loading buffer, and were then run on SDS PAGE gels and visually analyzed for large overexpressed protein bands near the predicted protein size. Promising conditions were then scaled up to 100-mL cultures to test of solubility of the protein. 100 mL of LB broth plus antibiotic were inoculated with 1 mL overnight culture and grown under previously specified conditions. After growth cultures were spun down at 2,000 x *g* for 20 min, pellets were resuspended in 5 mL of lysis buffer. Cells were lysed by sonication (Misonix sonicator 3000; power level 7, 30 s pulse, wait/delay 30 sec, total time 3 min with a microtip probe), and insoluble material was removed by centrifugation at 19,118 x *g* for 40 min. Supernatant containing soluble proteins was decanted from the pellet, and small amounts of pellets were resuspended in 1x PBS and run alongside supernatants on SDS-PAGE gels (Section 2.29). Western blots were also performed to verify the expressed protein was present in the soluble portion (Section 2.30).

When proteins failed to express in soluble form using LB medium and then inducing with IPTG, expression was tested in Overnight Express Instant TB media (OE). OE was inoculated from single colonies isolated from LB agar plates or from glycerol stocks and grown at 37 ˚C with shaking overnight. Cell pellets were resuspended in 1x PBS and boiled with gel loading dye to lyse and run on SDS-PAGE gels. Gels were analyzed as above. *E. coli* strains demonstrating expression of inserts as judged by the

presence of a band of the predicted molar mass were then tested for solubility as described in Section 2.19.

SECTION 2.20 PROTEIN EXPRESSION IN LB BROTH

For expression in LB broth, 25 mL overnight cultures per 1-L expression culture were set up a day prior to the expression in LB broth containing indicated antibiotics and grown with shaking at 37 ˚C overnight. The next morning 6-L flasks each containing 2 L of autoclaved sterilized LB broth were inoculated with 40 mL of the overnight culture and grown with appropriate antibiotics until an OD_{600} of 0.6 was reached, approximately 3 h. At this point cultures were induced with IPTG to a final concentration of either 1.0 mM or 0.1 mM, based on previous expression studies. Cultures were grown with shaking at the temperature and time previously determined and cells were then pelleted 2,600 x *g* for 30 m in a fixed-angle rotor. Supernatants were discarded and cell pellets were either used immediately for protein purification or frozen at -20 ˚C until purification could be performed.

SECTION 2.21 PROTEIN EXPRESSION IN OVERNIGHT EXPRESS MEDIA

For expression in OE, microwave sterilized OE was added to autoclaved plastic baffled flasks at $1/10^{th}$ of their volume for aeration. OE was then inoculated from glycerol stocks and grown overnight at 37 ˚C with shaking and cells were pelleted by centrifugation at 2,600 x *g* for 30 min in a fixed-angle rotor the next day. Supernatants

were discarded and cell pellets were either used immediately for protein purification or frozen at -20 ˚C until purification could be performed.

If 18 ˚C growth was desired, 5 mL overnight cultures were first grown in OE at 37 ˚C. Overnight cultures were then used to inoculate fresh OE as above. This culture was grown for 4 h at 37 ˚C, then moved to 18 ˚C for 24 h. Cells were pelleted as in the previous paragraph.

SECTION 2.22 BOILATE PREPARATION

Whole cell boilates were prepared from 500 µL - 1 mL samples taken from liquid bacterial cell culture. Samples were centrifuged at 2700 x *g* for 2 min to pellet cells. Cells were resuspended in 100 − 200 µL PBS, and 6x protein sample buffer [125 mM Tris-HCL pH 6.8, 2% (w/v) SDS, 10% (v/v) β-mercaptoethanol, 0.9% (w/v) bromophenol blue, 45% (v/v) glycerol] was added appropriately. Samples were heated in a 90 ˚C heat block for 5 min. Prior to gel loading, samples were centrifuged at 17, 900 x *g* for 5 min to pellet insoluble material.

SECTION 2.23 SMALL SCALE PROTEIN PURIFICATION

Cell pellets obtained from Sections 2.20 or 2.21 were resuspended in 25-50 mL imidazole lysis buffer (2.6 mM NaH_2PO_4, 47.3 mM Na_2HPO_4, 500 mM NaCl, 10 mM imidazole, pH 8.0) with Complete protease inhibitor (Roche). Cells were lysed by sonication (Misonix sonicator 3000; power level 7, 30 s pulse, wait/delay 30 s, total time

4 m with a microtip probe), and insoluble material was removed by centrifugation at 19,118 x *g* for 40 min. Supernatant containing soluble proteins was decanted from the pellets and added to 0.5-1 mL washed and equilibrated Ni^{2+}-NTA agarose beads and left to incubate for 1 h at 4 ˚C with agitation. After incubating, the Ni^{2+}-NTA was allowed to settle and the remaining lysate was pipetted off the resin. Ni^{2+}-NTA agarose was washed with several volumes of imidazole wash buffer (2.6 mM NaH_2PO_4, 47.3 mM Na_2HPO_4, 500 mM NaCl, 25 mM imidazole, pH 8.0). After the last of the wash buffer was added, resin was loaded onto a small disposable column (BioRad). After all remaining wash buffer had flown through the resin, protein was eluted off of the Ni^{2+}-NTA by adding 0.5-1.5 mL imidazole elution buffer (2.6 mM NaH_2PO_4, 47.3 mM Na_2HPO_4, 500 mM NaCl, 200mM imidazole, pH 8.0) and allowing it to flow through the resin and out of the column. The eluted material was then collected and allowed to pass through the resin an additional time in order to maximize protein recovery.

SECTION 2.24 LARGE SCALE PROTEIN PURIFICATION

Cell pellets obtained from Sections 2.20 or 2.21 were resuspended in 100-200 mL imidazole lysis buffer (2.6 mM NaH_2PO_4, 47.3 mM Na_2HPO_4, 500 mM NaCl, 10 mM imidazole, pH 8.0) with Complete protease inhibitor (Roche). Cells were lysed by sonication (Misonix sonicator 3000; power level 7, 30 s pulse, wait/delay 30 s, total time 8 min with a microtip probe), and insoluble material was removed by centrifugation at 19,118 x *g* for 40 min. Supernatant containing soluble proteins was decanted from the

pellets and added to 1-5 mL washed and equilibrated Ni^{2+}-NTA agarose beads and left to incubate for 1 h at 4 ˚C with agitation in a glass column approximately I m long and 4 cm in diameter. After incubating, the Ni^{2+}-NTA was allowed to settle and the remaining lysate was allowed to flow though the column. Ni^{2+}-NTA agarose was washed with several volumes of imidazole wash buffer (2.6 mM NaH_2PO_4, 47.3 mM Na_2HPO_4, 500 mM NaCl, 25 mM imidazole, pH 8.0). After the last of the wash buffer was drained, protein was eluted off of the Ni^{2+}-NTA by adding 5 mL imidazole elution buffer (2.6 mM NaH_2PO_4, 47.3 mM Na_2HPO_4, 500 mM NaCl, 200mM imidazole, pH 8.0) and allowing it to flow through the resin and out of the column. A_{280} measurements were used to approximate eluted volume of protein by using the assumption that 1 absorption unit equals 1 mg/mL of protein and additional 5 mL elutions were performed until the A_{280} readings dropped below 0.1. If eluted protein was to be further purified by FPLC it was concentrated in Amicon Ultra centrifugal filter tubes by centrifugation at 1,900 x *g* to a volume of 2 mL or less as required for application to the FPLC column.

SECTION 2.25 PROTEIN MINIPREP

Protein minipreps were performed according to verbal instructions from Dr. Omar Qazi, as described below.

Overnight Express containing appropriate antibiotics was inoculated with the strain of interest and grown overnight at 37 ˚C with 250 rpm shaking. Cells were harvested by centrifugation at 960 x *g* for 10 min and resuspended in 1 mL of lysis buffer with 10 µL

of 200 mM PMSF and 110 µL Cell Lytic reagent and left at room temperature to lyse for15-20 m with gentle rocking.

100 µL of Ni^{2+}-NTA agarose was prepared by washing with 1 mL lysis buffer. After addition of the lysis buffer the Ni^{2+}-NTA agarose was allowed to settle and the supernatant was carefully pipeted off.

The lysed cells were centrifuged at 20,800 x *g* for 10 min to pellet the insoluble material. The supernatant was pipeted off and added to the washed Ni^{2+}-NTA agarose and incubated for 30-45 min at 4 ˚C with oscillation. After incubation, the Ni^{2+}-NTA was allowed to settle and the supernatant was carefully pipeted off. Three washes with 1 mL imidazole wash buffer were then performed as in Section 2.23. After the last wash, bound species were eluted with 75 µL of imidazole elution buffer and the sample was centrifuged at 110 x *g* for 1 min to pellet the Ni^{2+}-NTA. The eluted protein in the supernatant was removed by pipeting and saved.

Protein minipreps were also done from 20 mL LB cultures induced with IPTG at an OD_{600} of 0.6 and grown for 2, 4, 6 h, or overnight post-induction.

SECTION 2.26 DIALYSIS

Dialysis was performed using dialysis tubing (Section 2.1) with a 3,500 Da molecular mass cutoff. Tubing was washed in deionized water to remove storage buffer and rinsed in 1xHBS. One end of the tubing was securely closed using a dialysis clamp, and pooled protein elution samples were loaded into the open end of the tubing, which

was then securely closed with a second dialysis clamp. Samples were put in a 3-L beaker containing 2 L of 1xHBS with magnetic stirring for 1 h at 4 ˚C. After 1 h, samples were moved to 2 L of fresh 1xHBS and were left overnight with stirring at 4 ˚C. The next day, samples were carefully removed from the dialysis tubing by pipetting and frozen for long-term storage at −80 ˚C in small aliquots of 50-200 µL.

SECTION 2.27 SIZE EXCLUSION CHROMATOGRAPHY PURIFICATION

All size exclusion chromatography (SEC) of recombinant proteins was carried out using a Hi-Load™ 16/60 Superdex™ 200 Prep Grade Column (GE Healthcare Bio-Sciences AB, Uppsala Sweden, 10 - 600 kDa separation range for globular proteins) connected to an ÄKTA fast protein liquid chromatography (FPLC) system with fraction collector (GE Healthcare). All solutions and samples were stored at 4 ˚C and the FPLC system and fraction collector are enclosed in a refrigerator, maintained at 4 ˚C. The running buffer used was HBS with 150 mM NaCl and the SEC column was first equilibrated with 1 column volume (CV) of buffer at a flow rate of 0.5 to 1.0 mL/min. Between 1-2 mL of purified protein was loaded into a 2 ml loop and injected onto the SEC column after a 0.2 CV equilibration. The protein was eluted over 2 CVs at a flow rate of 1 mL/min and the fraction collector was set to collect 1-2 mL fractions. Fractions were assessed by SDS-PAGE to determine which peaks contained the protein of interest. Fractions found to contain the protein of interest were pooled, concentrated, and stored at -80 ˚C.

SEC column calibration was carried out by Dr. Qazi using low and high molecular weight calibration kits from GE Healthcare. 1.2 ml of a 1.0 mg ml-1 solution of blue dextran was loaded onto the SEC column at a flow rate of 1 mL/min in order to determine the void volume (V0) of the column. For molecular weight calibration a standard containing thyroglobulin (669 kDa), ferritin (440 kDa), aldolase (158 kDa), conalbumin (75 kDa), ovalbumin (44 kDa), carbonic anhydrase (29 kDa), ribonuclease A (13.7 kDa), and aprotinin (6.5 kDa) was made up in 1.5 ml of HBS and loaded. The UV absorption traces of the two standard runs were overlaid and the peak elution volumes determined. A graph of Log molecular weight against K_{av} was plotted where $K_{av} = (V_E-V_0)/(V_T-V_0)$ and V_E is the elution volume, V_0 is the void volume and V_T is the total column volume. This graph was used to determine the molecular weights of the unknown samples from the calculated K_{av}.

SECTION 2.28 PROTEIN CONCENTRATION DETERMINATION

Protein concentration was determined by the BCA Protein Assay (Thermo Scientific Pierce, Rockford IL), according to the manufacturer's specifications and read at A_{562}. A standard curve was prepared using dilutions of Bovine Serum Albumin (BSA) included in the kit and a BSA standard curve with a linear regression was generated in Excel. Protein concentrations were calculated by inserting the A_{562} values for the protein into the linear regression equation from the BSA standard curve.

SECTION 2.29 SDS POLYACRYLAMIDE GEL ELECTROPHORESIS

Proteins were analyzed by SDS-PAGE using a Power Pac 300 (BioRad, Hercules, CA) and hand-poured gels.

85 mm x 75 mm x 1 mm protein gels were prepared by first polymerizing 5 mL of resolving gel [0.1% (w/v) sodium dodecyl sulfate (SDS), 12% (v/v) bis-acrylamide] in the presence of 0.06% (v/v) tetraethylmethyldiamide (TEMED) and 0.1% (w/v) ammonium persulfate (APS). A 2-mL stacking gel (0.1% (w/v) SDS, 5% (v/v) bis-acrylamide) was polymerized atop the resolving gel in the presence of 0.01% (v/v) TEMED and 0.1% (w/v) APS. Protein samples were mixed 1 to 6 in a 5x concentrated protein sample buffer [125 mM Tris-HCL pH 6.8, 2% (w/v) SDS, 10% (v/v) β-mercaptoethanol, 0.9% (w/v) bromophenol blue, 45% (v/v) glycerol] and boiled for 5 min prior to loading. Crude samples were also centrifuged at 17,900 x *g* for 5 min before loading to pellet cell particles. Gels were electrophoresed using the Mini- PROTEAN® System (BioRad, Hercules, CA) at 180 V for 45-60 min in a Tris-Glycine buffer [25 mM Tris pH , 192 mM glycine, 0.1% (w/v) SDS]. For visualization of protein bands, gels were stained in 50% (w/v) Coomassie Brilliant Blue, 10% (v/v) acetic acid, and 45% methanol, destained in 10% acetic acid and 45% (v/v) methanol, and hydrated in 10% (v/v) glycerol. Gels were imaged using a scanner (Epson).

SECTION 2.30 WESTERN BLOT

Western blots were routinely performed to verify that proteins carried a 6xHis tag. Two PAGE gels were loaded in duplicate and run as previously described (Section 2.29).

One of the two gels was stained in Coomassie as previously described (Section 2.29) and the other was prepared for Western blot by being soaked in transfer buffer (25 mM Tris pH, 192 mM glycine, 20% (v/v) methanol) along with pads and nitrocellulose membrane. Pads, membrane and gel were sandwiched inside a TransBlot SD Semi-Dry Transfer Cell (BioRad, Hercules, CA) and run at 13 V for 15 min. Transfer was monitored using a pre-stained molecular weight standard. The nitrocellulose membrane was blocked in 50 mL of 2% (w/v) skimmed milk in PBT [0.5% (v/v) Tween in PBS] for 30 min with agitation at room temperature. The membrane was then washed in PBT and incubated with a mouse anti-polyhistidine monoclonal antibody (Sigma) diluted 1:2500 in PBT for 45 min with agitation at room temperature. After incubation with the antibody, the membrane was washed again with PBT and developed in a solution made with one tablet of 4-chloro-1-naphthol dissolved in 10 mL of methanol and diluted to 50 mL in PBS with 0.06% (v/v) Hydrogen Peroxide. Positive samples appear purple after developing. Blots were visually compared to Coomassie stained gels.

SECTION 2.31 PIII-LOLC ELISA

Purified LolC-t protein was added to different lanes of Nunc Maxisorp plates in 100 µL volumes at variable concentrations. The plates were covered in plastic wrap and left overnight at 4 ˚C to allow binding. Plates were washed two times with PBS/0.05% Tween (PBS/T) and blocked by incubating plates at 25 ˚C for 1 h with 200 µL volumes of 3% skimmed milk in PBS. Plates were washed 3 times with PBS/T and biotinylated pIII-t

protein was diluted to 50 μg/mL and 10 further doubling dilutions were also carried out. Dilutions were made in 3% milk-PBS/T and 100 μL of each dilution was added to the appropriate well for binding. The final column of wells on the plate contained only PBS/T as a negative control/reference. The plates were incubated at 25 ˚C for one h and washed three times as before. Streptavidin-Peroxidase Polymer was diluted 1 in 1,000 in PBS/T and added to microtiter plates in volumes of 100 mL per well. The plates were washed four times as previously described and 100 μL of TMB-Ultra was added to each well. The reaction was stopped after sufficient color development by the addition of 100 μL of 2 M H_2SO_4 to each well.

Elisa plates were read at 450 nm on a Tecan Infinite M200 plate reader. Each data point represents the mean of replicate absorbance values after reference subtraction.

This assay was also done with plates coated with heat-killed *B. pseudomallei* strain Bp82 at 1 OD/mL and detected with biotinylated pIII in the same fashion as above. Heat-killed *Pseudomonas aeruginosa* strain PAO1 was used as a negative control for binding.

SECTION 2.32 MASS SPECTROMETRY

Mass spectrometry to determine molecular mass of purified proteins was performed in the ICMB Protein and Metabolite Analysis Facility at the University of Texas at Austin on a AB Sciex 4000 QTrap hybrid triple quadrupole-linear ion trap with Shimadzu Prominence analytical LC.

SECTION 2.33 FLIC CLONING, EXPRESSION, AND PURIFICATION

A genomic preparation of *B. pseudomallei* K96243 DNA (A gift from Dr. Alfredo Torres, UTMB, Galveston TX) was used as the template in the amplification of the nucleotides 495 − 876 of the *fliC* gene, BPSL_3319, (corresponding to amino acid residues 166 − 292 of the FliC protein) using two synthetic oligonucleotide primers. The primers OQ41 and OQ42 (A gift from Dr. Omar Qazi, UT Austin) were used (Table 2.2). The forward primer OQ41, incorporates a unique *NcoI* site, which results in the insertion of two additional amino acid residues, methionine and glycine, at the beginning of the truncated FliC-t protein. The reverse primer, OQ42, incorporates a unique *NotI* site after ATC, the last codon of the fliC-t intended sequence. PCR amplifications were performed using Roche High Fidelity Taq/Tgo polymerase with the addition of 20% Q-buffer at an annealing temperature of 62 ˚C and an extension time of 2.5 min (Sections 2.1, 2.16). The resulting PCR product, a 423 bp fragment, was separated by electrophoresis on a 0.8% agarose gel (Section 2.9) and purified by gel extraction (Section 2.10). This cleaned PCR product was then digested with *NcoI* and *NotI* (Section 2.12) and ligated (Section 2.13) into the *NcoI* and *NotI* sites of the IPTG-inducible expression vector pET-28a(+) to create plasmid pET-28a(+)-KCMFLIC (Figure 2.3).

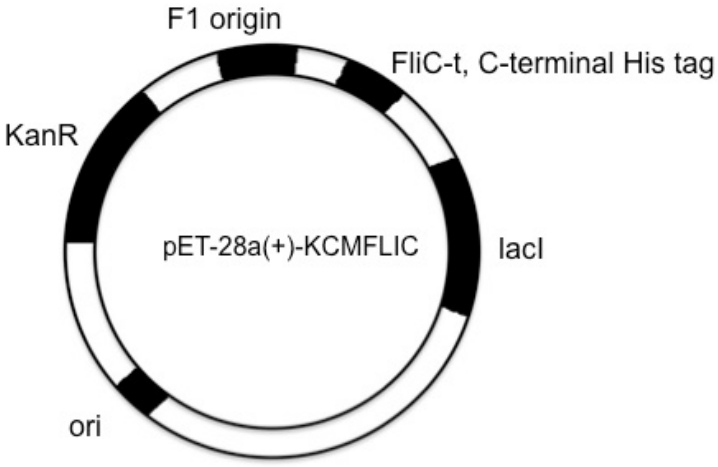

Figure 2.3 Construct pET-28a(+)-KCMFLIC

The ligation mixture was cleaned by PCR cleanup (Section 2.10) and transformed (Section 2.6) into electrocompetent *E. coli* DH5α cells (Section 2.3). Transformed cells were spread onto L-agar containing 50 µg/mL kanamycin and incubated at 37 ˚C. Single colonies were inoculated into 5 mL LB broth and grown overnight at 37 ˚C. Plasmids were then purified from the cells (Section 2.11) and submitted for sequencing (Section 2.17). Sequence data was analyzed (Section 2.18) and found to be free of mutations. Construct pET-28a(+)-KCMFLIC was then transformed (Section 2.6) into *E. coli* BL21_Rosetta (*DE3*) cells (Section 2.3) and spread onto L-agar plates containing 50 µg/mL kanamycin, creating strain KCM-Rosetta-FliC.

FliC-t protein was then expressed from strain KCM-Rosetta-FliC by growth in LB broth and induction with 1 mM IPTG at an OD_{600} of 0.6, followed by growth for 3.5 h at 37 ˚C (Section 2.20). Cells were centrifuged to pellet, and cell pellets were used to purify

FliC-t protein as described in Section 2.23. Purified protein was analyzed by SDS PAGE on Coomassie-stained acrylamide gels (Section 2.29) and subjected to dialysis for buffer exchange (Section 2.26).

SECTION 2.34 FLICR EXPRESSION AND PURIFICATION

Construct pET-15b-OQFLICR was obtained as a gift from Dr. Omar Qazi (UT Austin). This plasmid construct was transformed (Section 2.6) into *E. coli* strain BL21 (*DE3*) (Section 2.3) and spread onto L-agar plates containing 100 µg/mL carbenicillin, creating strain KCM-DE3-FliCR.

FliCR-t protein was then expressed from strain KCM-DE3-FliCR by growth in OE at 37 ˚C overnight (Section 2.21). After growth, cultures were centrifuged to pellet the cells, and this cell pellet was used to purify FliCR-t protein as described in Section 2.23. Eluted protein was further purified using size exclusion chromatography on the FPLC (Section 2.27), and FPLC calibration data was used to determine the size of the FliC-t protein. Purified protein was analyzed by SDS PAGE on Coomassie-stained acrylamide gels (Section 2.29) as well as by Western blot (Section 2.30) using a mouse anti-polyhistidine monoclonal antibody to recognize the polyhistidine tag on the FliCR-t protein.

SECTION 2.35 PILA-T CLONING, EXPRESSION, AND PURIFICATION

A genomic preparation of *B. pseudomallei* K96243 DNA (A gift from Dr. Alfredo

Torres, UTMB, Galveston TX) was used as the template in the amplification of the nucleotides 90-516 of the *pilA* gene, BPSL_0782, (corresponding to amino acid residues 31-172 of the PilA protein) using two synthetic oligonucleotide primers. The primers KJ9 and KJ11 were used (Table 2.2). Neither the forward primer, KJ9, nor the reverse primer, KJ11, incorporates extra DNA or amino acid residues to the construct, which ends with a TGA stop codon. PCR amplifications were performed using Roche High Fidelity Taq/Tgo polymerase with the addition of 20% Q-buffer and 5% DMSO at an annealing temperature of 59.4 ˚C and an extension time of 30 s (Sections 2.1, 2.16). The resulting PCR product, a 426 bp fragment, was separated by electrophoresis on a 0.8% agarose gel (Section 2.9) and purified by gel extraction (Section 2.10). This cleaned PCR product was ligated into the pEXP5-NT/TOPO vector (Section 2.14) to create plasmid pEXP5-NT/TOPO-KCMPILA (Figure 2.4), which was then transformed into One Shot chemically competent *E. coli* cells by heat shock (Section 2.14).

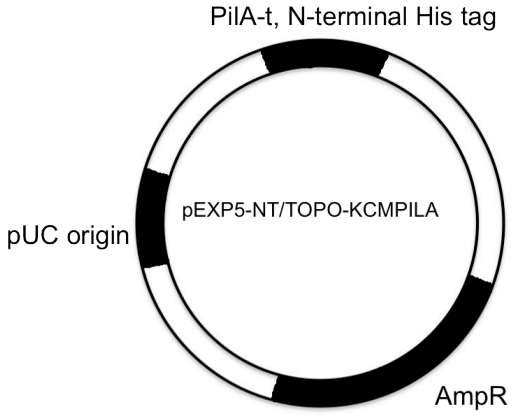

Figure 2.4 Construct pEXP5-NT/TOPO-KCMPILA

Transformed cells were spread onto L-agar containing 100 μg/mL ampicillin and incubated at 37 ˚C. Single colonies were inoculated into 5 mL LB broth and grown overnight at 37 ˚C. Plasmids were then purified from the cells (Section 2.11) and submitted for sequencing (Section 2.17). Sequence data was analyzed (Section 2.18) and found to be free of mutations. Construct pEXP5-NT/TOPO-KCMPILA was then transformed (Section 2.6) into *E. coli* BL21_Star™ (*DE3*) pLysS cells (Section 2.3) and spread onto L-agar containing 100 μg/mL ampicillin, creating strain KCM-pLysS-PilA.

PilA-t protein was then expressed from strain KCM-pLysS-PilA by growth in OE at 37 ˚C overnight (Section 2.21). After growth, cultures were centrifuged to pellet the cells, and this cell pellet was used to purify PilA-t protein as described in Section 2.23. Eluted protein was further purified using size exclusion chromatography on the FPLC (Section 2.27), and FPLC calibration data was used to determine the size of the PilA-t protein. Purified protein was analyzed by SDS PAGE on Coomassie-stained acrylamide gels (Section 2.29) as well as by Western blot (Section 2.30) using a mouse anti-polyhistidine monoclonal antibody to recognize the polyhistidine tag on the PilA-t protein.

SECTION 2.37 PIII-T CLONING, EXPRESSION, AND PURIFICATION

Phage M13K07 DNA, which contains the *g3p* gene, was used as the template in the amplification of the nucleotides 55-705 of the *g3p* gene (corresponding to the amino acid residues 166-292 of the pIII protein) using two synthetic oligonucleotide primers.

The primers, KCM17 and KCM18, were used (Table 2.2). The forward primer, KCM17, incorporates a unique *NdeI* site, which results in the insertion of 20 amino acid residues, including a 6x Histidine tag, at the beginning of the truncated pIII protein. The reverse primer, KCM18, adds a UGA stop codon and a unique *Xho*I site into the 3' end of the cloned DNA sequence. PCR amplifications were performed using NEB Taq polymerase with provided 10x buffer with an annealing temperature of 58 ˚C and an extension time of 1 min (Sections 2.1, 2.16). The resulting PCR product, a 678 bp fragment, was separated by electrophoresis on a 0.8% agarose gel (Section 2.9) and purified by gel extraction (Section 2.10). This cleaned PCR product was then digested with *NdeI* and *XhoI* (section 2.12) and ligated (Section 2.13) into the IPTG-inducible expression vector pET-15b to create plasmid pET-15b-KCMPIII (Figure 2.5).

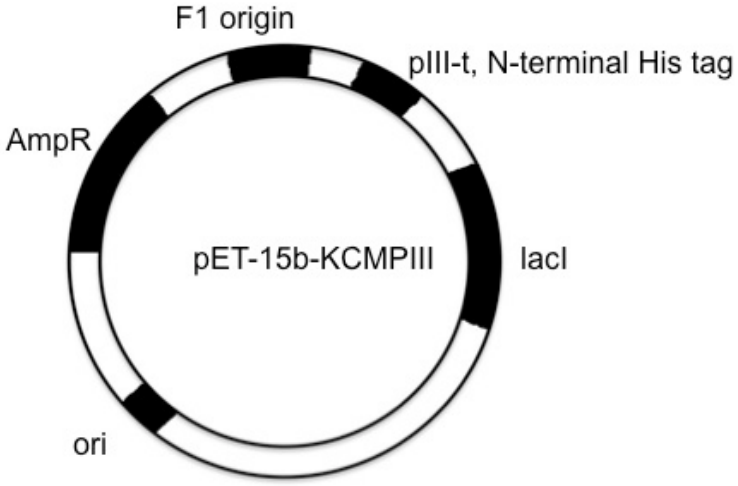

Figure 2.5 Construct pET-15b-KCMPIII

The ligation mixture was cleaned by PCR cleanup (Section 2.10) and transformed (Section 2.6) into electrocompetent *E. coli* DH5α cells (Section 2.3) and grown on L-agar plates containing 100 µg/mL of carbenicillin. Transformed cells were plated on L-agar containing 100 µg/mL carbenicillin and incubated at 37 ˚C. Single colonies were inoculated into 5 mL of LB broth and grown overnight at 37 ˚C. Plasmids were then purified from the cells (Section 2.11) and submitted for sequencing (Section 2.17). Sequence data was analyzed (Section 2.18) and found to be free of mutations. Construct pET-15b-KCMPIII was transformed (Section 2.6) into *E. coli* BL21_Rosetta (*DE3*) cells (Section 2.3) and spread onto L-agar plates containing 100 µg/mL carbenicillin, creating strain KCM-Rosetta-pIII.

pIII-t protein was then expressed from strain KCM-Rosetta-pIII by growth in LB broth and induction with 0.1 mM IPTG at an OD_{600} of 0.6, followed by growth for 4 h at 37 ˚C (Section 2.20). After growth, cultures were centrifuged to pellet the cells, and this cell pellet was used to purify pIII-t protein as described in Section 2.23. Eluted protein was further purified using size exclusion chromatography on the FPLC (Section 2.27), and FPLC calibration data was used to determine the size of the pIII-t protein. Purified protein was analyzed by SDS PAGE on Coomassie-stained acrylamide gels (Section 2.29) as well as by Western blot (Section 2.30) using a mouse anti-polyhistidine monoclonal antibody to recognize the polyhistidine tag on the pIII-t protein.

SECTION 2.37 FIMA-T CLONING, EXPRESSION, AND PURIFICATION

Construct pET-15b-OQFIMA was obtained as a gift from Dr. Omar Qazi (UT Austin). This plasmid construct was transformed (Section 2.6) into *E. coli* strain BL21_Star™ (*DE3*) (Section 2.3) and spread onto L-agar plates containing 100 µg/mL carbenicillin, creating strain KCM-Star-FimA.

FimA-t protein was then expressed from strain KCM-Star-FimA by growth in OE at 37 ˚C overnight (Section 2.21). After growth, cultures were centrifuged to pellet the cells, and this cell pellet was used to purify FimA-t protein as described in Section 2.23. Eluted protein was further purified using size exclusion chromatography on the FPLC (Section 2.27), and FPLC calibration data was used to determine the size of the FimA-t protein. Purified protein was analyzed by SDS PAGE on Coomassie-stained acrylamide gels (Section 2.29) as well as by Western blot (Section 2.30) using a mouse anti-polyhistidine monoclonal antibody to recognize the polyhistidine tag on the FimA-t protein.

SECTION 2.38 LOLC-T EXPRESSION AND PURIFICATION

Construct pET-28a(+)-OQLOLCN was obtained as a gift from Dr. Omar Qazi (UT Austin). This plasmid construct was transformed (Section 2.6) into *E. coli* strain BL21_Rosetta (*DE3*) (Section 2.3) and spread onto L-agar plates containing 50 µg/mL kanamycin, creating strain KCM-Rosetta-LolC.

LolC-t protein was then expressed from strain KCM-Star-FimA by growth in LB broth and induction with 1 mM IPTG at an OD_{600} of 0.6, followed by overnight growth at

18 ˚C (Section 2.20). After growth, cultures were centrifuged to pellet the cells, and this cell pellet was used to purify LolC-t protein as described in Section 2.24. Eluted protein was further purified using size exclusion chromatography on the FPLC (Section 2.27), and FPLC calibration data was used to determine the size of the LolC-t protein. Purified protein was analyzed by SDS PAGE on Coomassie-stained acrylamide gels (Section 2.29) as well as by Western blot (Section 2.30) using a mouse anti-polyhistidine monoclonal antibody to recognize the polyhistidine tag on the LolC-t protein.

SECTION 2.39 SODC-T CLONING, EXPRESSION, AND PURIFICATION

A genomic preparation of *B. mallei* 23344 DNA (A gift from Dr. Alfredo Torres, UTMB, Galveston TX) was used as the template in the amplification of the nucleotides 102-237 of the *sodC* gene, BMA_0713, (corresponding to amino acid residues 35-179 of the SodC protein) using two synthetic oligonucleotide primers. The primers, OQ59 and OQ60 (a gift from Dr. Omar Qazi, UT Austin) were used (Table 2.2). The forward primer, OQ59, incorporates a unique *NcoI* site, which results in the insertion of two additional amino acid residues, methionine and glycine, at the beginning of the truncated SodC-t protein. The reverse primer, OQ60, incorporates a unique *NotI* site after CAA, the last codon of the fliC-t intended sequence. PCR amplifications were performed using Roche High Fidelity Taq/Tgo polymerase with the addition of 20% Q-buffer at an annealing temperature of 62 ˚C and an extension time of 2.5 min (Sections 2.1, 2.16). The resulting PCR product, a 477 bp fragment, was separated by electrophoresis on a 0.8%

agarose gel (Section 2.9) and purified by gel extraction (Section 2.10). This cleaned PCR product was then digested with *NcoI* and *NotI* (Section 2.12) and ligated (Section 2.13) into the *NcoI* and *NotI* sites of the IPTG-inducible expression vector pET-28a(+) to create plasmid pET-28a(+)-KCMSODC (Figure 2.6).

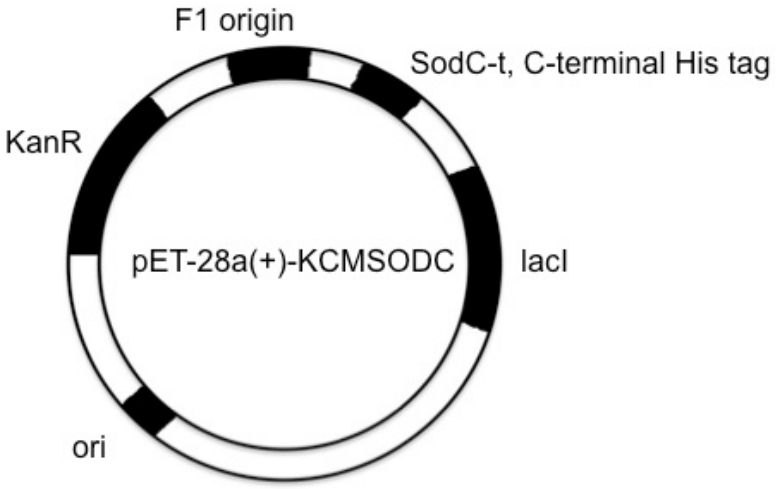

Figure 2.6 Construct pET-28a(+)-KCMSODC

The ligation mixture was cleaned by PCR cleanup (Section 2.10) and transformed (Section 2.6) into electrocompetent *E. coli* DH5α cells (Section 2.3). Transformed cells were spread onto L-agar containing 50 µg/mL kanamycin and incubated at 37 ˚C. Single colonies were inoculated into 5 mL LB broth and grown overnight at 37 ˚C. Plasmids were then purified from the cells (Section 2.11) and submitted for sequencing (Section 2.17). Sequence data was analyzed (Section 2.18) and found to be free of mutations. Construct pET-28a(+)-KCMSODC was then transformed (Section 2.6) into *E. coli*

BL21_Rosetta (*DE3*) cells (Section 2.3) and spread onto L-agar plates containing 50 µg/mL kanamycin, creating strain KCM-Rosetta-SodC.

SodC-t protein was then expressed from strain KCM-Rosetta-SodC by growth in LB broth and induction with 1 mM IPTG at an OD_{600} of 0.6, followed by growth for 3.5 h at 37 ˚C (Section 2.20). Cells were centrifuged to pellet, and cell pellets were used to purify SodC-t protein as described in Section 2.23. Purified protein was analyzed by SDS PAGE on Coomassie-stained acrylamide gels (Section 2.29) and subjected to buffer exchange by dialysis in 1x HBS (Section 2.26).

SECTION 2.40 BOPA-T EXPRESSION AND PURIFICATION

BopA-t protein was expressed from strain OQ-Rosetta-BopA114 (a gift from Dr. Omar Qazi, Section 2.3) by growth in LB broth and induction with 1 mM IPTG at an OD_{600} of 0.6, followed by overnight growth for at 37 ˚C (Section 2.20). Cells were centrifuged to pellet, and cell pellets were used to purify BopA-t protein as described in Section 2.24. Purified protein was subjected to dialysis and analyzed by SDS PAGE on Coomassie-stained acrylamide gels (Section 2.29) and Western blot (Section 2.30) using a mouse anti-polyhistidine monoclonal antibody to recognize the polyhistidine on the BopA-t protein.

SECTION 2.41 HEP-HAG PCR

Section 2.41a BMA_A0810

A genomic preparation of *B. mallei* 23344 DNA (A gift from Dr. Alfredo Torres, UTMB, Galveston TX) was used as the template in the amplification of the nucleotides 61-1158 of the BMA_A0810 gene (corresponding to amino acid residues 21-386 of the Hep Hag protein it encodes) using two synthetic oligonucleotide primers. The primers KJ1 and KJ2 were used (Table 2.2). The forward primer, KJ1, does not incorporate any additional nucleotides to the construct. The reverse primer, KJ2, incorporates a TAA stop codon after ACG, the last codon of the intended BMA_A0810 sequence. PCR amplifications were performed using Roche High Fidelity Taq/Tgo polymerase with the addition of 20% Q-buffer at an annealing temperature of 62 ˚C + 0.3 ˚C per cycle and an extension time of 2.5 min (Sections 2.1, 2.16). The resulting PCR product, a 1095 bp fragment, was separated by electrophoresis on a 0.8% agarose gel (Section 2.9) and purified by gel extraction (Section 2.10).

Section 2.41b BPSL_1705

A genomic preparation of *B. pseudomallei* K96243 DNA (A gift from Dr. Alfredo Torres, UTMB, Galveston TX) was used as the template in the amplification of the nucleotides 79-3603 of the BPSL_1705 gene (corresponding to amino acid residues 27-1201 of the Hep Hag autotransporter protein it encodes) using two synthetic oligonucleotide primers. The primers KJ3 and KJ4 were used (Table 2.2). The forward primer, KJ3, does not incorporate any additional nucleotides to the construct. The reverse

primer, KJ4, incorporates a TAA stop codon after ACG, the last codon of the intended BPSL_1705 sequence. PCR amplifications were performed using Roche High Fidelity Taq/Tgo polymerase with the addition of 20% Q-buffer at an annealing temperature of 64 ˚C and an extension time of 1.5 min (Sections 2.1, 2.16). The resulting PCR product, a 3525 bp fragment, was separated by electrophoresis on a 0.8% agarose gel (Section 2.9) and purified by gel extraction (Section 2.10).

Section 2.41c BTH_II0878

A genomic preparation of *B. thailandensis* E264 DNA (A gift from Dr. Annie Gnanam, UT Austin) was used as the template in the amplification of nucleotides 100-1272 of the BTH_II0878 gene (corresponding to amino acid residues 34-424 of the HepHag protein it encodes) using two synthetic oligonucleotide primers. The primers KJ5 and KJ6 were used (Table 2.2). The forward primer, KJ5, does not incorporate any additional nucleotides to the construct. The reverse primer, KJ6, incorporates a TAA stop codon after CTC, the last codon of the intended BTH_II0878 sequence. PCR amplifications were performed using Roche High Fidelity Taq/Tgo polymerase with the addition of 20% Q-buffer at an annealing temperature of 50.8 ˚C and an extension time of 1.5 min (Sections 2.1, 2.16). The resulting PCR product, a 1172 bp fragment, was separated by electrophoresis on a 0.8% agarose gel (Section 2.9) and purified by gel extraction (Section 2.10).

SECTION 2.42 TOLB PCR

A genomic preparation of *B. mallei* 23344 DNA (A gift from Dr. Alfredo Torres, UTMB, Galveston TX) was used as the template in the amplification of the nucleotides 70-1290 of the *tolB* gene, BMA_2081 (corresponding to amino acid residues 24-430 of the TolB protein) using two synthetic oligonucleotide primers. The primers OQ95 and OQ96 were used (Table 2.2). The forward primer, OQ95, incorporates a unique *NcoI* site, which results in the insertion of two additional amino acid residues, methionine and glycine, at the beginning of the truncated TolB-t protein. The reverse primer, OQ96, incorporates a unique *XhoI* site after the last codon of the tolB-t intended sequence. PCR amplifications were performed using Roche High Fidelity Taq/Tgo polymerase with the addition of 20% Q-buffer at an annealing temperature of 62 ˚C and an extension time of 2.5 min (Sections 2.1, 2.16). The resulting PCR product, a 1221 bp fragment, was separated by electrophoresis on a 0.8% agarose gel (Section 2.19) and purified by gel extraction (Section 2.10).

Chapter 3: Results

SECTION 3.1 CLONING, EXPRESSION AND PURIFICATION RESULTS

Section 3.1a FliC Cloning, Expression, and Purification Results

A truncated form of the *B. pseudomallei fliC* gene (*fliC*-t), BPSL_3319 (Section 2.33) was PCR-amplified (Figure 3.1), cloned into the *NcoI* and *NotI* sites of the pET-28a(+) vector, and transformed into *E. coli* DH5α cells. The resulting vector, pET-28a(+)-KCMFLIC (Figure 2.3), was verified by DNA sequencing.

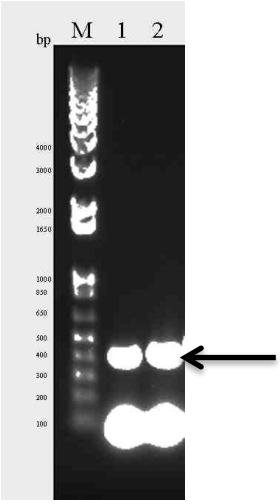

Figure 3.1 PCR Amplification of *fliC*-t.

Arrow at predicted size of DNA, 423 bp
1. PCR product of FliC-t.
2. PCR product of FliC-t with 0.5% DMSO added

The levels of IPTG-induced overproduction of a truncated recombinant *B.*

pseudomallei BPSL_3319, FliC (FliC-t) were initially analyzed from purification of overnight culture in *E. coli* strain BL21_Rosetta (*DE3*) transformed with construct pET-28a(+)-KCMFLIC grown in Overnight Express medium (OE) at either 37 ˚C or 18 ˚C. In this strategy, cells harvested were subjected to a protein miniprep (Section 2.25) and purified FliC-t protein was analyzed by SDS PAGE. The Coomassie-stained gel has strongly staining bands present in both the 37 ˚C and 18 ˚C samples at the predicted molecular mass of FliC-t, 13.9 kDa (Figure 3.2, at arrow). No Western blot was performed of this sample, so presence or absence of FliC-t in these samples is uncertain.

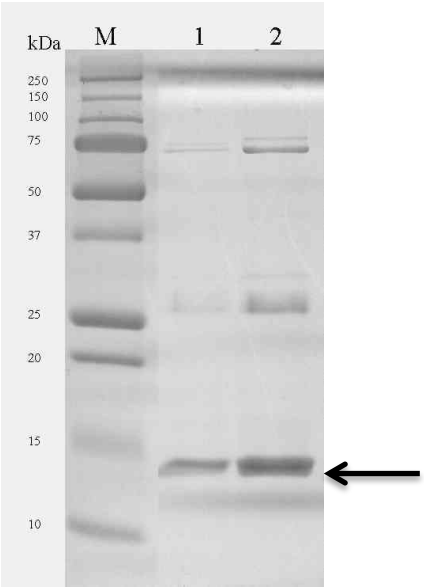

Figure 3.2: Protein Minipreps of FliC-t

Arrow at predicted molecular mass of FliC-t, 13.9 kDa
1. FliC-t grown in OE at 37 ˚C
2. FliC-t grown in OE at 18 ˚C

Section 3.1b FliCR-t Expression and Purification

The levels of IPTG-induced overproduction of a second truncated recombinant *B. pseudomallei* BPSL_3319, FliC (FliCR-t) were initially analyzed from overnight cultures of *E. coli* strains BL21 (*DE3*), BL21_Star™ (*DE3*), BL21_Rosetta (*DE3*), and BL21_Star™ (*DE3*) pLysS transformed with construct pET-15b-OQFLICR (Figure 2.2a), a gift from Dr. Omar Qazi) grown in OE. Cells were harvested and sonicated to obtain soluble and insoluble fractions, which were then analyzed by SDS PAGE. The Coomassie-stained acrylamide gel has a strongly staining band present in the soluble fraction at the predicted molecular mass of FliCR-t, 14.4 kDa in three of the four *E. coli* host strains: BL21 (*DE3*), BL21_Star™ (*DE3*), and BL21_Rosetta (*DE3*) (Figure 3.3, Lanes 1, 3, and 5, at the arrow).

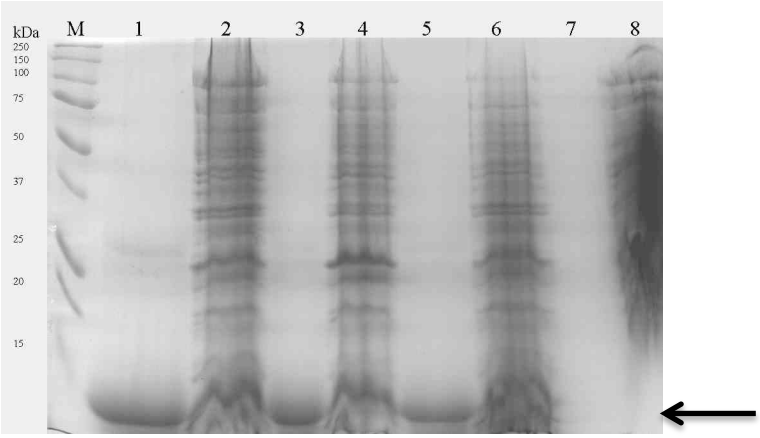

Figure 3.3: Initial Expression of FliCR-t in OE

Arrow at predicted molecular mass of FliCR-t, 14.4 kDa1. DE3 Soluble
2. DE3 Insoluble
3. *DE3 Soluble
4. *DE3 Insoluble
5. Rosetta Soluble
6. Rosetta Insoluble
7. pLysS Soluble
8. pLysS Insoluble

Strongly staining bands are also observed, likely at the predicted molecular mass of 14.4 kDa in the insoluble fraction of these strains, however overloading of these samples on the gel led to aberrant running of the samples (Figure 3.3, Lanes 2, 4, and 6). No band at 14.4 kDa was observed in the soluble fraction of the BL21_Star™ (*DE3*) pLysS strain (Figure 3.3, Lane 7). In addition, no band could be discerned in the insoluble fraction of this vector/host combination due to the presence of a large smear on the gel (Figure 3.3, Lane 8). No Western blot was performed of this expression gel (Figure 3.3), so the presence or absence of FliCR-t in these samples was not fully confirmed. Based on visual examination of the stained bands on the Coomassie-stained gel, the *E. coli* BL21 (*DE3*) host strain containing the pET-15b-OQFLICR construct, named KCM-DE3-FliCR, grown in OE was chosen for scaled up production of FliCR-t.

FliCR-t was purified in a two-step process: first by affinity chromatography using Ni^{2+}NTA agarose, and then by size-exclusion chromatography (sec) (Figure 3.4), and its size was determined by FPLC and mass-spectrometry (Appendix). The size of FliCR-t as determined by sec on the FPLC was calculated to be 22.1 kDa, which is quite a bit higher than the predicted molecular mass of FliCR-t, 14.4 kDa. This could be due to the shape of the protein. Calibration of the FPLC column was performed using globular proteins, and proteins that are not perfectly globular could run aberrantly in comparison. Mass spectrometry determined that the molecular mass of FliCR-t is 14.3 kDa, much closer to the predicted molecular mass of FliCR-t of 14.4 kDa. The small difference in molecular mass between predicted and actual could be due to the loss of the initial methionine of the

protein.

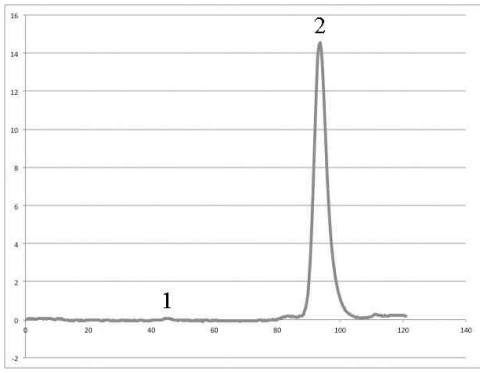

Figure 3.4: FPLC trace from FliCR-t Purification

Material from peak 2 was used.
1. 44.46 mL
2. 93.56 mL

Figure 3.5, a Coomassie-stained acrylamide gel, shows the optimized expression and purification of FliCR-t from strain KCM-DE3-FliCR. Production of FliCR-t is clearly induced using the OE (Figure 3.5, Lane 3, indicated by the arrow, compared to Lanes 1 and 2). Lysis of the resulting pellet by sonication yields a strongly staining band corresponding to FliCR-t in the both the soluble and insoluble fractions (Figure 3.5, Lanes 4 and 5). The accompanying Western blot (Figure 3.6), using a mouse anti-polyhistidine monoclonal antibody, again shows the presence of a strongly staining band near the 15-kDa molecular mass marker presumed to be FliCR-t. Purification of FliCR-t by affinity chromatography using NiNTA agarose removes all but a couple of the contaminating proteins from the suspension, leaving FliCR-t as the major species present (Figure 3.5, Lane 6). The Western blot confirms that these are contaminants, as the only band present on the blot corresponds to FliCR-t near the 15-kDa molecular mass marker

band (Figure 3.6, lane 6). Purification of FliCR-t by sec on the FPLC removes the remaining contaminants, leaving FliCR-t as the homogenous species in the solution (Figures 3.5 and 3.6, Lane 7).

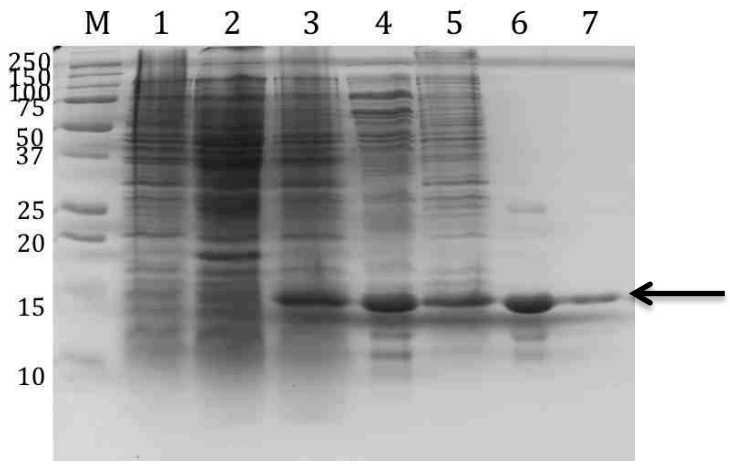

Figure 3.5: FliCR-t Expression and Purification Gel

Arrow at predicted molecular mass of FliCR, 14.4 kDa
1. BL21 (*DE3)* cell boilate, no vector
2. BL21 (*DE3)* with pET-15b boilate
3. KCM-DE3-FliCR boilate
4. Soluble fraction from FliCR-t purification
5. Insoluble fraction from FliCR-t purification
6. NiNTA purified FliCR-t
7. FPLC purified FliCR-t

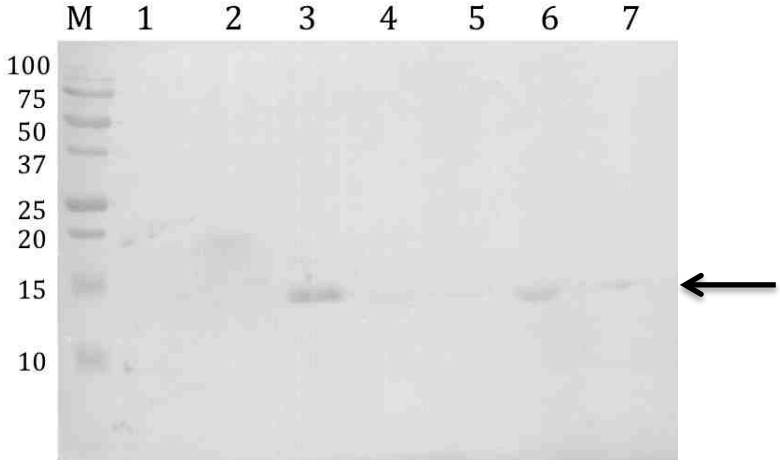

Figure 3.6: Western Blot of FliCR-t Expression and Purification

Arrow at predicted molecular mass of FliCR, 14.4 kDa
1. BL21 (*DE3)* cell boilate, no vector
2. BL21 (*DE3)* cells with pET-15b boilate
3. KCM-DE3-FliCR boilate
4. Soluble fraction from FliCR-t purification
5. Insoluble fraction from FliCR-t purification
6. NiNTA purified FliCR-t
7. FPLC purified FliCR-t

Section 3.1c PilA-t Cloning, Expression, and Purification Results

A truncated form of the *B. pseudomallei pilA* gene (*pilA*-t), BPSL_0782 (Section 2.35), was PCR-amplified, analyzed on an agarose gel (Figure 3.7), cloned into the pEXP5-NT/TOPO vector, and transformed into *E. coli* DH5α cells. The resulting vector, pEXP5-NT/TOPO-KCMPILA (Figure 2.4), was verified by DNA sequencing.

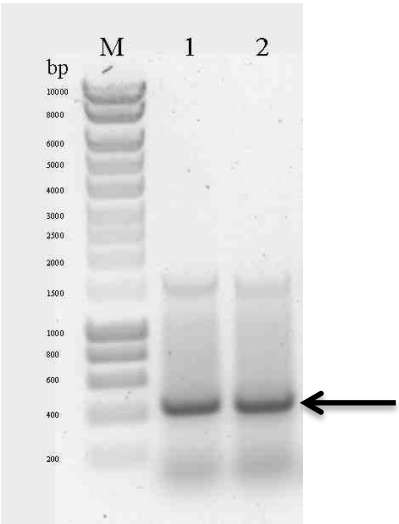

Figure 3.7: PCR of *pilA*-t

Arrow at predicted size of *pilA*-t, 426 bp
1. With 5% DMSO
2. With 10% DMSO

The levels of IPTG-induced overproduction of the recombinant *B. pseudomallei* BPSL_0782, PilA (PilA-t), were initially analyzed from an overnight culture of *E. coli* BL21_ Rosetta (*DE3*) cells transformed with pEXP5-NT/TOPO-KCMPILA (Figure 2.4) grown in OE media. After a protein miniprep (Section 2.25), crude cell boilates and purified protein were analyzed by SDS PAGE. No band corresponding to the predicted

molecular mass of 16.5 kDa of the expressed construct was visible in the purified sample on the Coomassie-stained gel (Figure 3.8, Lane 2). This may be due to under-loading of the gel lane, low protein concentrations, and/or absence of PilA-t after purification due to it not being eluted from the NiNTA agarose properly. The Coomassie-stained gel did have a band in the boilate sample, indicated by the arrow in Figure 3.8 estimated to near the 15 kDa molecular mass marker band, which could be PilA-t.

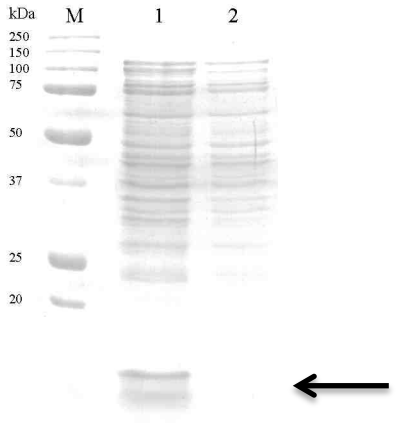

Figure 3.8: Expression and Purification in BL21_Rosetta (*DE3*)

Arrow at predicted molecular mass of PilA-t, 16.5 kDa
1. Crude cell boilate
2. Protein miniprep

The pEXP5-NT/TOPO-KCMPILA construct was then transformed into three additional *E. coli* expression strains, BL21 (*DE3*), BL21_Star™ (*DE3*), and BL21_Star™ (*DE3*) pLysS, and also re-transformed into BL21_Rosetta (*DE3*) competent cells. These four transformed strains were grown in either OE media or LB broth, the latter induced

with 1.0 mM IPTG at an OD_{600} of 0.6 in LB broth and then grown for 3.5 h at 37 ˚C. Whole cell boilates obtained from each of these expression conditions were analyzed by SDS PAGE, but interpretation of the Coomassie-stained gel was inconclusive due to over-loading (Figure 3.9).

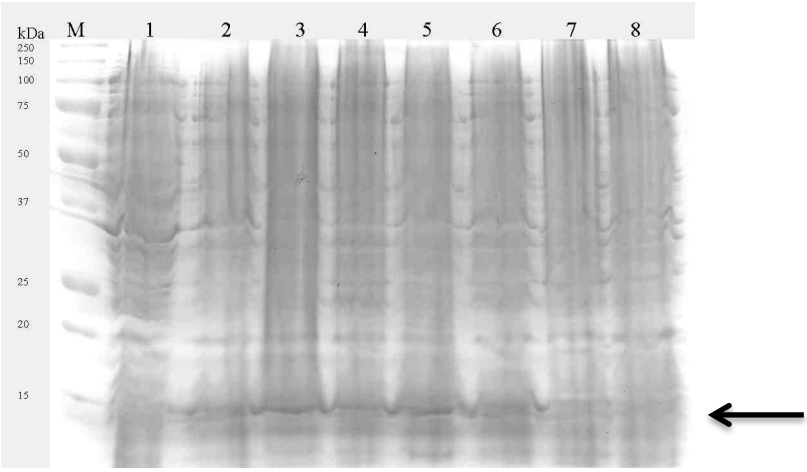

Figure 3.9: Expression in four *E. coli* strains in LB with 1 mM IPTG induction and OE. Crude cell boilates.

Arrow at predicted molecular mass of PilA-t, 16.5 kDa

1. BL21 (*DE3)*, LB
2. BL21 (*DE3)*, OE
3. BL21_Star™ (*DE3*) pLysS, LB
4. BL21_Star™ (*DE3*) pLysS, OE
5. BL21_Rosetta (*DE3*), LB
6. BL21_Rosetta (*DE3*), OE
7. BL21_Star™ (*DE3*), LB
8. BL21_Star™ (*DE3*), OE

Although the SDS PAGE analysis could have been repeated with reduced sample protein concentrations, expression was instead re-evaluated systematically in LB broth, inducing with 0.1 and 1.0 mM IPTG at an OD_{600} of 0.6. Whole cell boilates (Section 2.22) were made of samples taken post-induction at 2, 4, 6 h and overnight and analyzed by SDS PAGE using Coomassie-stained acrylamide gels (Figures 3.10, 3.11, 3.12, and 3.13). Strongly staining bands were observed migrating near the 15-kDa molecular mass

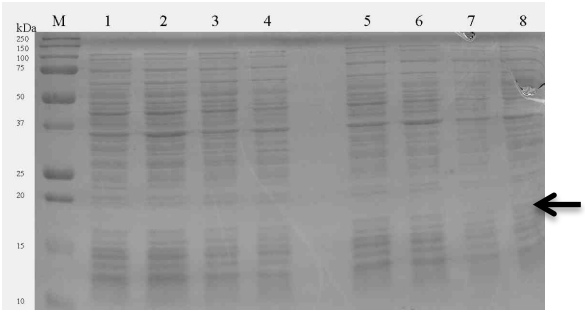

Figure 3.10: PilA-t Expression in BL21 (*DE3)*, LB broth.

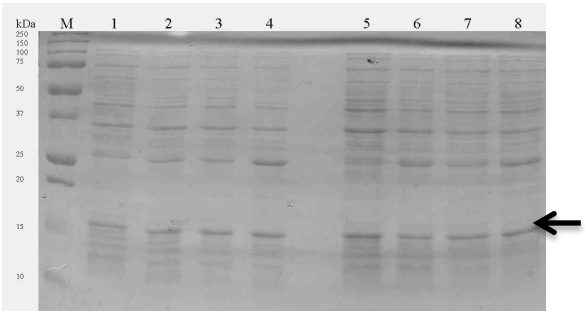

Figure 3.11: PilA-t expression in BL21_Star™ (*DE3*), LB broth.

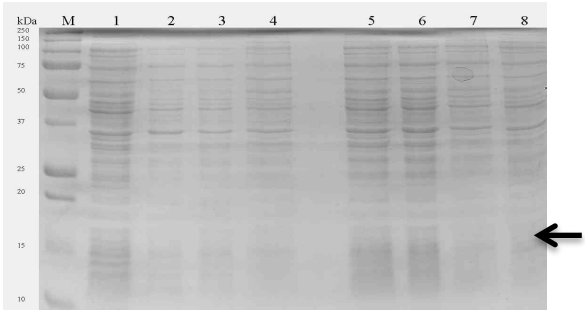

Figure 3.12: PilA-t expression in BL21_Rosetta (DE3), LB broth.

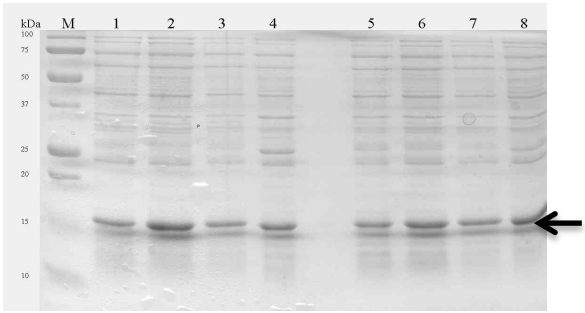

Figure 3.13: PilA-t expression in BL21_Star™ (*DE3*) pLysS, LB broth.

Lane key for Figures 3.10-3.13
Arrow at predicted molecular mass of PilA-t, 16.5 kDa
Crude cell boilates.
1. 0.1 mM IPTG induction, 2 h growth
2. 0.1 mM IPTG induction, 4 h growth
3. 0.1 mM IPTG induction, 6 h growth
4. 0.1 mM IPTG induction, overnight growth
5. 1.0 mM IPTG induction, 2 h growth
6. 1.0 mM IPTG induction, 4 h growth
7. 1.0 mM IPTG induction, 6 h growth
8. 1.0 mM IPTG induction, overnight growth

marker band, below the predicted 16.5-kDa molecular mass of PilA-t, using the *E. coli* expression host strains BL21_Star™ (*DE3*) (Figure 3.11) and BL21_Star™ (*DE3*) pLysS (Figure 3.13). Strongly staining bands were not seen near 15 or 16.5 kDa using the *E. coli* expression host strains BL21 (*DE3*) or BL21_Rosetta (*DE3*) (Figures 3.10 and 3.12). Western blots were not performed of these gels, so no definitive conclusions as to the presence or absence of PilA-t in these samples can be made. Based upon the SDS PAGE analysis above, however, PilA-t appeared to be present at substantial levels in the following three samples all transformed with pEXP5-NT/TOPO-KCMPILA: BL21_Star™ (*DE3*) induced with 1.0 mM IPTG at an OD_{600} of 0.6 and grown for 2 h post-induction, BL21_Star™ (*DE3*) pLysS induced with 0.1 mM IPTG at an OD_{600} of 0.6 and grown for 4 h post-induction, and BL21_Star™ (*DE3*) pLysS induced with 1.0 mM IPTG at an OD_{600} of 0.6 and grown for 4 h post-induction. These three boilates were analyzed by SDS PAGE (Figure 3.14) and Western blot (Figure 3.15) using an mouse anti-polyhistidine monoclonal antibody (Section 2.30). Moderately staining bands were seen on the gel for all three samples near the 15 kDa molecular mass marker band but below the predicted 16.5 kDa molecular mass of PilA-t (Figure 3.14). Weak bands on the nitrocellulose blot membrane (Figure 3.15) were also observed near the 15-kDa molecular mass marker band, suggesting these bands to be PilA-t.

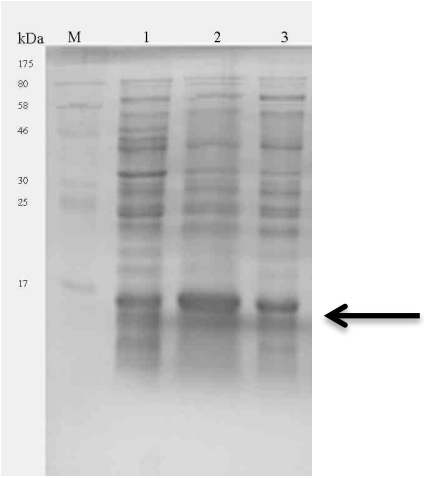

Figure 3.14: Gel of Promising Expression Conditions in LB broth. Crude cell boilates.

Arrow at predicted molecular mass of PilA-t, 16.5 kDa
1. BL21_Star™ (*DE3*) with 1.0 mM IPTG induction and 2 h growth
2. BL21_Star™ (*DE3*) pLysS with 0.1 mM IPTG induction and 4 h growth
3. BL21_Star™ (*DE3*) pLysS with 1.0 mM IPTG induction and 4 h growth

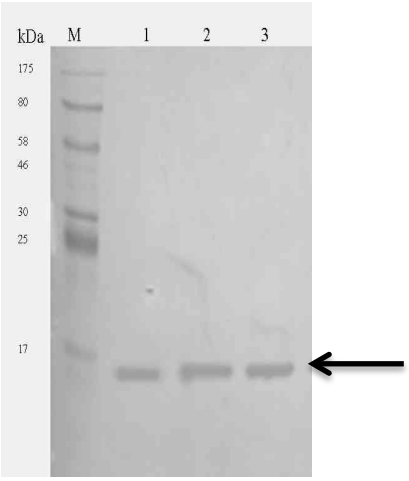

Figure 3.15: Western blot of Promising Expression Conditions in LB broth. Crude cell boilates.

Arrow at predicted molecular mass of PilA-t, 16.5 kDa
1. BL21_Star™ (*DE3*) with 1.0 mM IPTG induction and 2 h growth
2. BL21_Star™ (*DE3*) pLysS with 0.1 mM IPTG induction and 4 h growth
3. BL21_Star™ (*DE3*) pLysS with 1.0 mM IPTG induction and 4 h growth

The solubility of PilA-t was assessed using the three different expression conditions identified in the paragraph above. Cells were lysed by sonication (Section 2.24) and the soluble and insoluble fractions were analyzed by SDS PAGE using a Coomassie-stained acrylamide gel (Figure 3.16). Strongly staining bands migrating near the 15-kDa molecular mass marker indicated that large amounts of protein appeared to be in the insoluble fraction of the BL21_Star™ (*DE3*) strain expression (Figure 3.16, Lane 2). Weakly staining bands migrating near the 15-kDa molecular mass marker were present in the soluble fractions for all of the conditions analyzed on this gel (Figure 3.16, Lanes 1, 3, and 5).

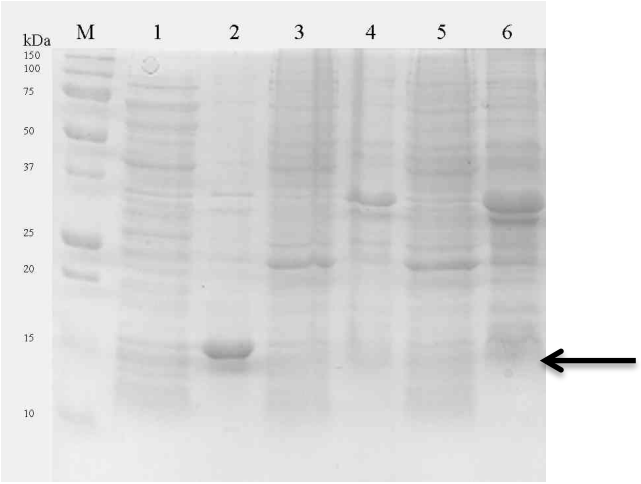

Figure 3.16: Solubility of promising PilA-t Expression Conditions in LB Broth

Arrow at predicted molecular mass of PilA-t, 16.5 kDa
1. BL21_Star™ (*DE3*) with 1.0 mM IPTG induction and 2 h growth, Soluble
2. BL21_Star™ (*DE3*) with 1.0 mM IPTG induction and 2 h growth, Insoluble
3. BL21_Star™ (*DE3*) pLysS with 0.1 mM IPTG induction and 4 h growth, Soluble
4. BL21_Star™ (*DE3*) pLysS with 0.1 mM IPTG induction and 4 h growth, Insoluble
5. BL21_Star™ (*DE3*) pLysS with 1.0 mM IPTG induction and 4 h growth, Soluble
6. BL21_Star™ (*DE3*) pLysS with 1.0 mM IPTG induction and 4 h growth, Insoluble

BL21_Star™ (*DE3*) and BL21_Star™ (*DE3*) pLysS transformed with pEXP5-NT/TOPO-KCMPILA were then grown in OE at 37 ˚C overnight in order to explore whether higher levels of soluble PilA-t could be obtained. These cells were lysed by sonication (Section 2.24) to separate soluble and insoluble components and analyzed by SDS PAGE on a Coomassie-stained acrylamide gel. Strongly staining bands were observed at near the 15-kDa molecular mass marker in the insoluble fractions of the sample from both bacterial strains (Figure 3.17, Lanes 2 and 4). A weakly staining band of soluble protein near the 15 kDa molecular mass marker was observed in the BL21_Star™ (*DE3*) pLysS sample (Figure 3.17, Lane 3) but not visibly observed in the BL21_Star™ (*DE3*) sample (Figure 3.17, Lane 1), possibly due to underloading of the acrylamide gel. No Western blot was done with this gel, so it is not possible to determine the presence or absence of soluble PilA-t in BL21_Star™ (*DE3*) cells. The *E. coli* BL21_Star™ (*DE3*) pLysS strain containing the pEXP5-NT/TOPO-KCMPILA construct, named KCM-pLysS-PilA, was chosen for scaled up production of PilA-t using OE.

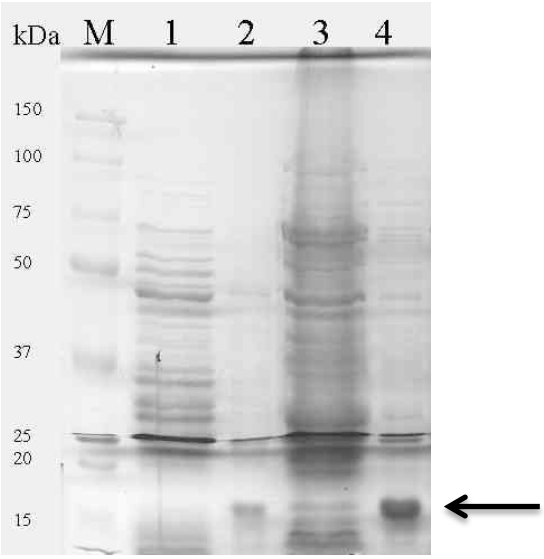

Figure 3.17: Solubility of PilA-t in OE

Arrow at predicted molecular mass of PilA-t, 16.5 kDa
1. BL21_Star™ (*DE3*), Soluble
2. BL21_Star™ (*DE3*), Insoluble
3. BL21_Star™ (*DE3*) pLysS, Soluble
4. BL21_Star™ (*DE3*) pLysS, Insoluble

PilA-t was purified in a two-step process: first by affinity chromatography using NiNTA agarose, and then by size-exclusion chromatography (sec) (Figure 3.18), and its size was calculated by FPLC and confirmed with mass spectrometry. The size of PilA-t as calculated by FPLC using a calibrated column is 22.2 kDa, which is quite a bit higher than the predicted molecular mass of PilA-t, 16.5 kDa. This could be due to the shape of the protein. Calibration of the FPLC column was performed using globular proteins, and proteins that are not perfectly globular could run aberrantly in comparison. Mass spectrometry determined the molecular mass of PilA-t to be 16.4 kDa, which is very close to the predicted molecular mass of 16.5 kDa (Appendix). The small difference in

molecular mass between predicted and actual could be due to the loss of the initial methionine of the protein.

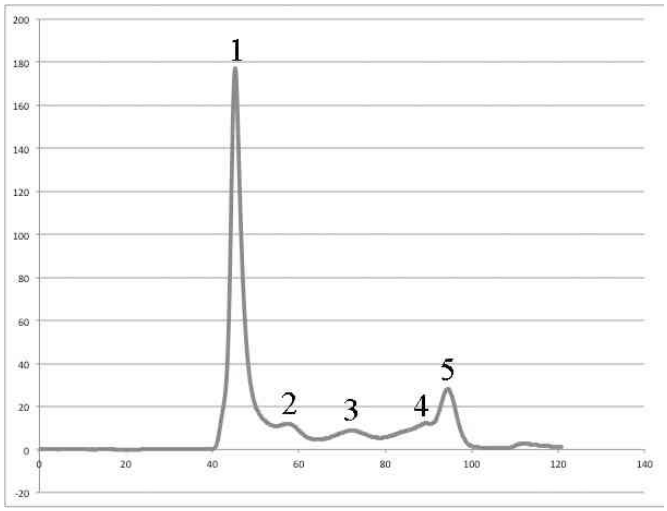

Figure 3.18: Representative FPLC trace from PilA-t purification

Material from peak 5 was collected.
1. 45.28 mL
2. 57.19 mL
3. 72.69 mL
4. 89.65 mL
5. 94.47 mL

Figure 3.19 shows the optimized expression and purification conditions used for the production of PilA-t from strain KCM-pLysS-PilA. Production of PilA-t is clearly induced using the OE (Figure 3.19, Lane 2, indicated by the arrow, compared to Lane 1). Lysis of the resulting cell pellet by sonication yields a weakly staining band corresponding to PilA-t (Figure 3.19, Lane 3) compared to the insoluble portion (Figure 3.19, Lane 4). The accompanying Western blot (Figure 3.20), using a mouse anti-polyhistidine monoclonal antibody, again shows the presence of a strongly staining band

near the 15 kDa molecular mass marker presumed to be PilA-t. The Western blot of the whole cell boilate and the insoluble pellet (Figure 3.20, Lanes 2 and 4) also shows the presence of some aggregates that are not present in the soluble fraction (Figure 3.20, Lane 3). Purification of PilA-t by affinity chromatography using NiNTA agarose removes all but a couple of the contaminating proteins from the suspension, leaving PilA-t as the major species present (Figure 3.19, Lane 5). The Western blot confirms that these are contaminants, as the only band present on the blot corresponds to PilA-t near the 15-kDa molecular mass marker band (Figure 3.20, lane 5). Purification of PilA-t by sec on the FPLC removes the remaining contaminants, leaving PilA-t as the homogenous species in the solution (Figures 3.19 and 3.20, Lane 6).

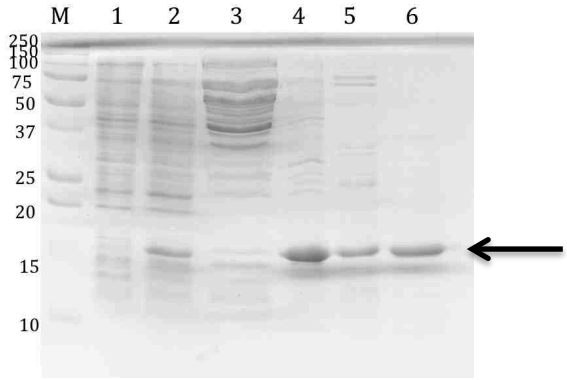

Figure 3.19: Gel of Expression and Purification in BL21_Star™ (*DE3*) pLysS in OE Broth

Arrow at predicted molecular mass of PilA-t, 16.5 kDa

1. BL21_Star™ (*DE3*) pLysS with no plasmid vector, Crude cell boilate
2. BL21_Star™ (*DE3*) pLysS expression cell pellet, crude cell boilate
3. Purification soluble fraction
4. Purification insoluble pellet
5. Ni^{2+}-NTA purified PilA-t
6. FPLC purified PilA-t

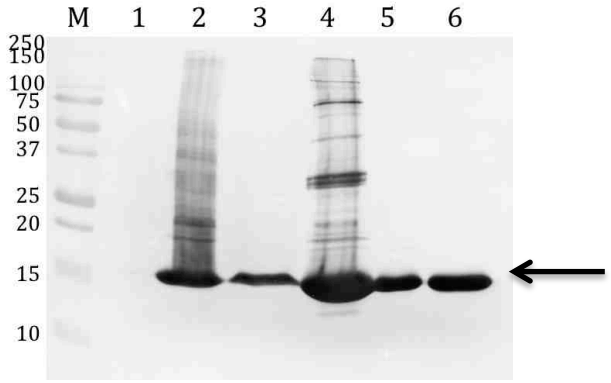

Figure 3.20: Western Blot of Expression and Purification in BL21_Star™ (*DE3*) pLysS in OE Broth

Arrow at predicted molecular mass of PilA-t, 16.5 kDa

1. BL21_Star™ (*DE3*) pLysS with no plasmid vector, Crude cell boilate
2. BL21_Star™ (*DE3*) pLysS expression cell pellet, crude cell boilate
3. Purification soluble fraction
4. Purification insoluble pellet
5. Ni^{2+}-NTA purified PilA-t
6. FPLC purified PilA-t

Section 3.1d pIII Cloning, Expression, and Purification Results

Previously, during rounds of phage panning in phage display against LolC-t protein, it was noticed that the M13K07 phage had a strong affinity for LolC-t protein (Dr. Mridula Rani, personal communication). It was believed that this interaction was between the pIII protein of the phage and the LolC-t protein (Dr. George Giorgiou, personal communication). If the pIII protein actually binds to LolC-t, this interaction could be exploited in our favor in order to use pIII protein as a detection reagent for pathogenic *Burkholderia* species. To this end, the pIII protein was cloned, expressed, and purified.

A truncated form of the phage M13K07 *g3p* gene (*g3p*-t) (Section 2.36), was PCR-

amplified and analyzed on an agarose gel (Figure 3.21), cloned into the pET-15b vector, and transformed into *E. coli* DH5α cells. The resulting vector, pET-15b-KCMPIII (Figure 2.5), was verified by DNA sequencing.

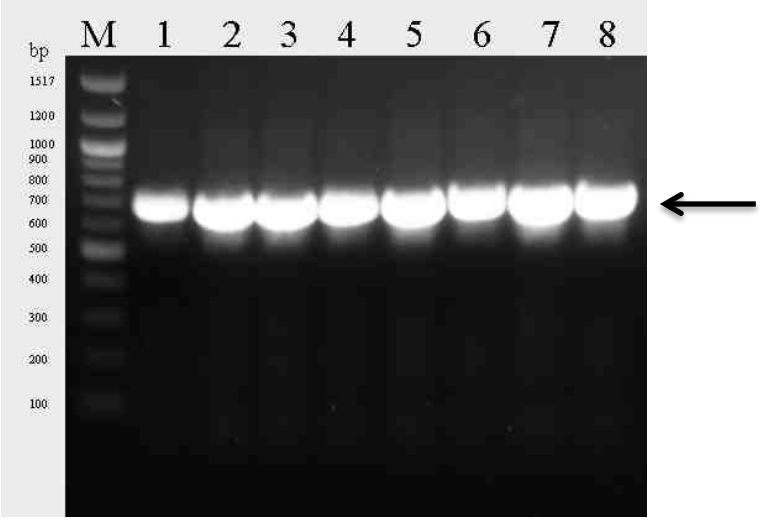

Figure 3.21: PCR of *g3p*-t DNA with different annealing temperatures

Arrow at predicted size of *g3p*-t DNA, 651 bp

1. 58.0 ˚C	3. 59.5 ˚C	5. 62.4 ˚C	7. 64.5 ˚C
2. 58.5 ˚C	4. 60.8 ˚C	6. 63.6 ˚C	8. 65.0 ˚

The levels of IPTG-induced overproduction of a truncated recombinant form of the phage M13K07 pIII protein (pIII-t) were initially analyzed using *E. coli* strains BL21 (*DE3)*, BL21_Star™ (*DE3*), BL21 Rosetta (*DE3*), and BL21_Star™ (*DE3*) pLysS transformed with construct pET-15b-KCMPIII (Figure 2.5). These transformed strains were grown in LB broth and induced with either 1.0 or 0.1 mM IPTG at an OD_{600} of 0.6. Samples were taken at 2, 4, 6 h, and overnight for cultures grown at 37 ˚C post-induction; and 6 h and overnight for cultures grown at 18 ˚C post-induction. Whole cell boilates

were analyzed by SDS PAGE using Coomassie-stained acrylamide gels. Weakly staining bands, consistent with the predicted molecular mass of 25.8 kDa, appear in all of the gels (Figures 3.22 through 3.29). In addition, all of the samples contained a strongly staining band at approximately 36 kDa (Figures 3.22 through 3.29, indicated by the arrow), which is considerably higher than the predicted molecular mass of the pIII-t protein. From these gels it appears that induction with 0.1 mM IPTG at an OD_{600} of 0.6 and protein expression for 4 h post-induction may be sufficient for overproduction of pIII-t in any of the four transformed strains studied.

Lane key for Figures 3.22-3.29
Arrow at presumptive pIII-t.
1. 37 ˚C, 2 h post-induction
2. 37 ˚C, 4 h post-induction
3. 37 ˚C, 6 h post-induction
4. 37 ˚C, overnight post-induction
5. 18 ˚C, 6 h post-induction
6. 18 ˚C, overnight post-induction

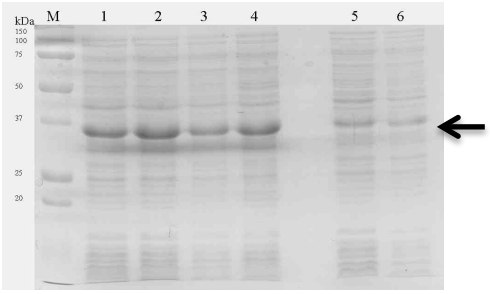

Figure 3.22: Expression of pIII-t in *E. coli* BL21 *(DE3)* with 0.1 mM IPTG induction

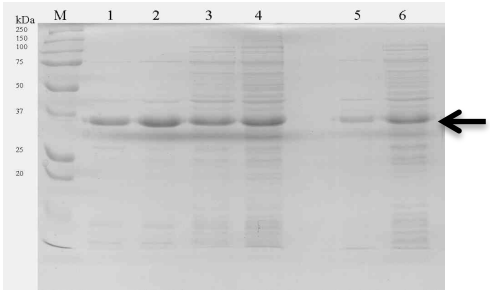

Figure 3.23: Expression of pIII-t in *E. coli* BL21 *(DE3)* with 1 mM IPTG induction

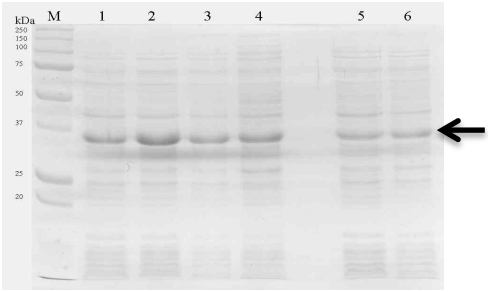

Figure 3.24: Expression of pIII-t in *E. coli* BL21_Star™ (*DE3*), 0.1 mM IPTG induction

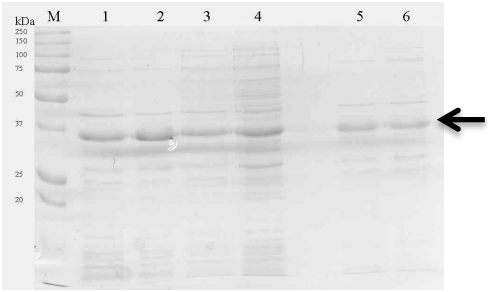

Figure 3.25: Expression of pIII-t in *E. coli* BL21_Star™ (*DE3*) with 1 mM IPTG induction

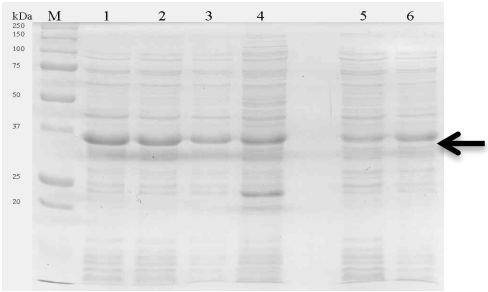

Figure 3.26: Expression of pIII-t in *E. coli* BL21_Rosetta (*DE3*), 0.1 mM IPTG induction

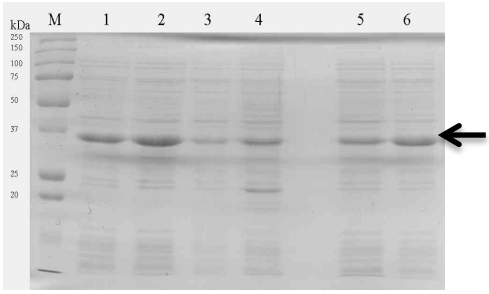

Figure 3.27: Expression of pIII-t in *E. coli* BL21_Rosetta (*DE3*) with 1 mM IPTG induction

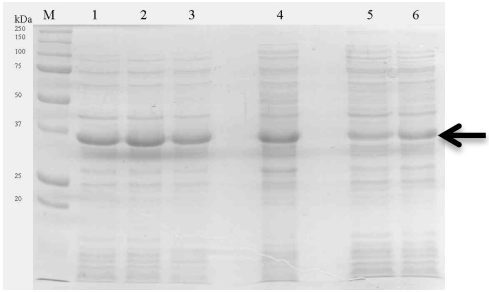

Figure 3.28: Expression of pIII-t in *E. coli* BL21_Star™ (*DE3*) pLysS, 0.1 mM IPTG

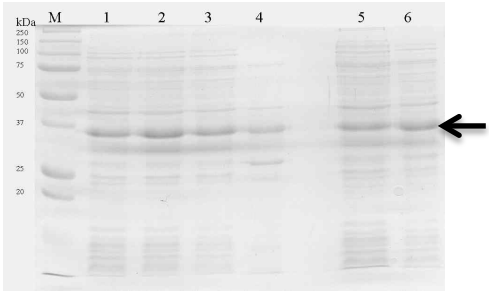

Figure 3.29: Expression of pIII-t in *E. coli* BL21_Star™ (*DE3*) pLysSwith 1 mM IPTG induction

The four transformed BL21 strains listed above were then assessed for their ability to express soluble pIII-t. Cells were grown in LB broth, induced with 0.1 mM IPTG at an OD_{600} of 0.6, and grown for 4 h post-induction. Harvested cell pellets were lysed by sonication to separate the soluble and insoluble cellular components. The soluble and insoluble fractions were then analyzed by SDS PAGE using Coomassie-stained acrylamide gels (Figure 3.30). A Western blot was also performed with a mouse anti-polyhistidine monoclonal antibody in order to determine the presence or absence of pIII-t (Figure 3.31). All four transformed cell types showed strongly staining bands in the insoluble portion of the sample migrating at approximately 36 kDa (Figure 3.31, indicated by arrow). Each strain also had a smaller band in the soluble fraction also migrating at approximately 36 kDa (Figure 3.30). The same 36-kDa bands stain strongly on the Western blot nitrocellulose membrane, indicative of the presence of pIII-t (Figure 3.31). The pIII-t truncated protein contains 3 disulfide bridges formed between 6 cysteines, and the aberrant migration of this protein at 36 kDa instead of 25.8 kDa could be due to disulfide bonds in the truncated protein that are either re-formed or not fully reduced before the sample is run on the gel.

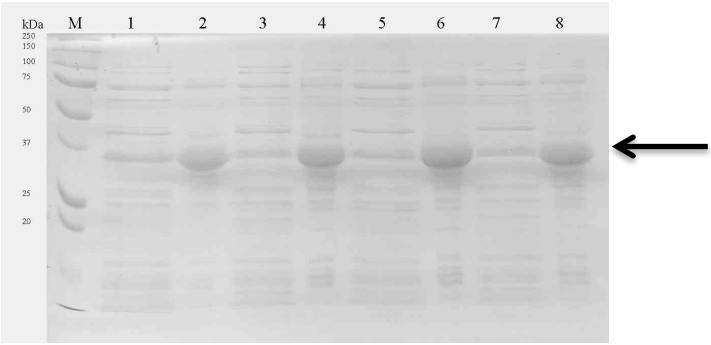

Figure 3.30: Soluble vs. Insoluble expression gel of pIII-t with 0.1 mM IPTG induction

Arrow at presumptive pIII-t

1. BL21 *(DE3)* soluble
2. BL21 *(DE3)* insoluble
3. BL21_Star™ (*DE3*) soluble
4. BL21_Star™ (*DE3*) insoluble
5. BL21_Rosetta (*DE3*) soluble
6. BL21_Rosetta (*DE3*) insoluble
7. BL21_Star™ (*DE3*) pLysS soluble
8. BL21_Star™ (*DE3*) pLysS insoluble

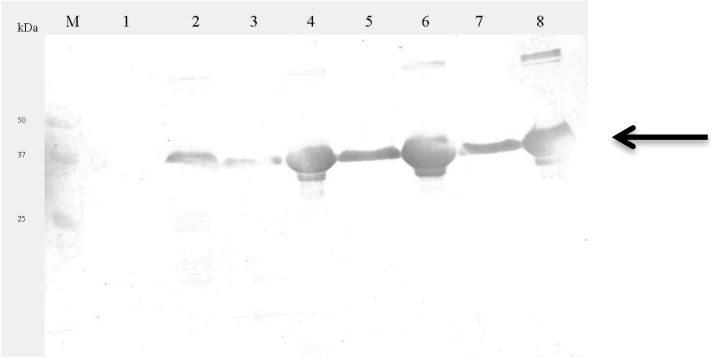

Figure 3.31: Soluble vs. Insoluble Western blot of pIII-t expression with 0.1 mM IPTG induction

Arrow at presumptive pIII-t.

1. BL21 *(DE3)* soluble
2. BL21 *(DE3)* insoluble
3. BL21_Star™ (*DE3*) soluble
4. BL21_Star™ (*DE3*) insoluble
5. BL21_Rosetta (*DE3*) soluble
6. BL21_Rosetta (*DE3*) insoluble
7. BL21_Star™ (*DE3*) pLysS soluble
8. BL21_Star™ (*DE3*) pLysS insoluble

Based upon the SDS PAGE and Western blot analyses, the *E. coli* BL21_Rosetta (*DE3*) host strain transformed with pET-15b-KCMPIII, named KCM-Rosetta-pIII, was used for scale-up of protein overproduction.

pIII-t was purified in a two-step process: first by affinity chromatography using NiNTA agarose, and then by size-exclusion chromatography (sec) (Figure 3.32), and its size was calculated by FPLC and confirmed with mass spectrometry (Appendix). The size of pIII-t as calculated by FPLC using a calibrated column is 31.2 kDa, which is quite a bit higher than the predicted molecular mass of pIII-t, 25.8 kDa. This could be due to the shape of the protein. Calibration of the FPLC column was performed using globular proteins, and proteins that are not perfectly globular could run aberrantly in comparison. Mass spectrometry determined the molecular mass of pIII-t to be 25.8 kDa, which is identical to the predicted molecular mass of 25.8 kDa.

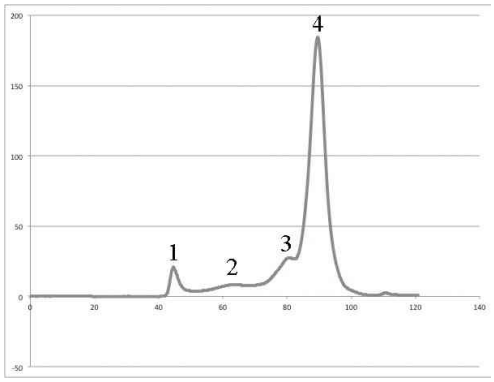

Figure 3.32: Representative FPLC trace from pIII-t purification

Material from peak 4 collected
1. 44.56 mL
2. 63.11 mL
3. 80.73 mL
4. 89.58 mL

Section 3.1e FimA-t Expression and Purification Results

The levels of IPTG-induced overproduction of a second truncated recombinant *B. pseudomallei* BPSL_1801, FimA (FimA-t) were initially analyzed from overnight cultures of *E. coli* strains BL21 (*DE3*), BL21_Star™ (*DE3*), BL21_Rosetta (*DE3*), and BL21_Star™ (*DE3*) pLysS transformed with construct pET-15b-OQFIMA (Figure 2.2b, a gift from Dr. Omar Qazi) grown in OE. Cells were harvested and sonicated to obtain soluble and insoluble fractions, which were then analyzed by SDS PAGE. The Coomassie-stained acrylamide gel showed strongly staining bands present in the soluble fractions approximately at the predicted molecular mass of FimA-t of 17.6 kDa, in all of the four *E. coli* host strains: BL21 (*DE3*), BL21_Star™ (*DE3*), BL21_Rosetta (*DE3*), and BL21_Star™ (*DE3*) pLysS (Figure 3.33, Lanes 1, 3, 5, and 7, indicated by the arrow).

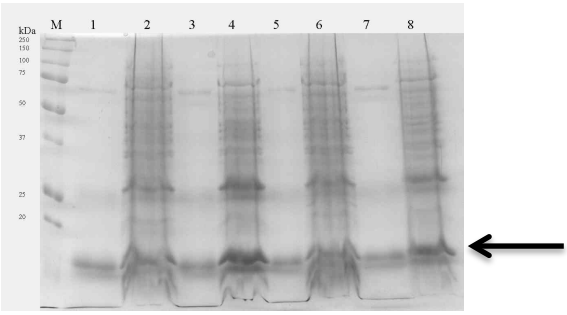

Figure 3.33: FimA Expression in OE Media Gel

Arrow at predicted FimA-t molecular mass, 17.6 kDa

1. DE3 Soluble
2. DE3 Insoluble
3. *DE3 Soluble
4. *DE3 Insoluble
5. Rosetta Soluble
6. Rosetta Insoluble
7. pLysS Soluble
8. pLysS Insoluble

Strongly staining bands are also observed migrating near the predicted molecular mass of

17.6 kDa in the insoluble fraction from these host strains, however overloading of these samples on the gel led to aberrant running of the samples (Figure 3.33, Lanes 2, 4, 6, and 8). No Western blot was performed of this expression gel, so the presence or absence of FimA-t in these samples was not fully confirmed. Based on visual examination of the stained bands on the Coomassie-stained gel, the *E. coli* BL21_Star™ (*DE3*) strain containing the pET-15b-OQFIMA construct, named KCM-Star-FimA, grown in OE was chosen for scaled up production of FimA-t.

FimA-t was purified in a two-step process: first by affinity chromatography using NiNTA agarose, and then by size-exclusion chromatography (sec) (Figure 3.34), and its size was calculated by FPLC. The size of FimA-t as calculated by FPLC using a calibrated column is 22.4 kDa, which is quite a bit higher than the predicted molecular mass of FimA-t, 17.6 kDa. This could be due to the shape of the protein. Calibration of the FPLC column was performed using globular proteins, and proteins that are not perfectly globular could run aberrantly in comparison.

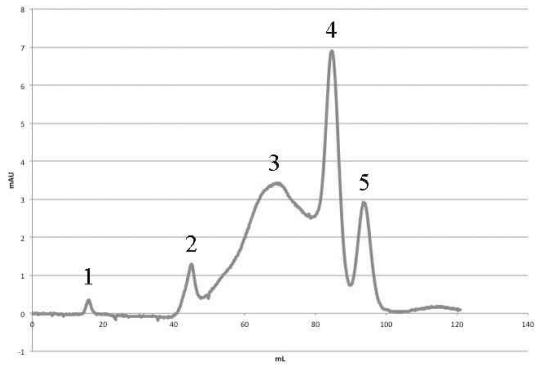

Figure 3.34: FPLC trace from FimA-t Purification

Material collected from peak 5 was used.

1. 15.93 mL	3. 67.45 mL	5. 93.88 mL
2. 44.91 mL	4. 84.71 mL	

Figure 3.35 shows the optimized expression and purification conditions used for the production of FimA-t from strain KCM-Star-FimA. Production of FimA-t is clearly induced using OE (Figure 3.35, Lane 3, indicated by the arrow, compared to Lanes 1 and 2). Lysis of the resulting cell pellet by sonication yields a strongly staining band corresponding to FimA-t (Figure 3.35, Lane 4) is present in both the soluble and insoluble fractions. The accompanying Western blot (Figure 3.36), using a mouse anti-polyhistidine monoclonal antibody, again shows the presence of a strongly staining band in each sample near the 15-kDa molecular mass marker presumed to be FimA-t. The Western blot of the whole cell boilate and the insoluble pellet (Figure 3.36, Lanes 3 and 5) also shows the presence of some aggregates that are not present in the soluble fraction (Figure 3.20, Lane 3). Purification of FimA-t by affinity chromatography removes all but a couple of the contaminating proteins, leaving FimA-t as the major species present

(Figure 3.35, Lane 6). The Western blot confirms most of these other bands to be contaminants, but there is some degradation of the FimA-t protein, likely at the C-terminus, that shows up as a couple of bands smaller than the main, strongly staining band of FimA-t near 15-kDa. Purification of FimA-t by sec on the FPLC removes some of the contaminants, but a high molecular mass contaminant near 75 kDa still remains in the sample (Figure 3.35, Lane 7). Absence of the 75-kDa band on the Western blot confirms this to be a contaminant and not a multimerized form of FimA-t (Figure 3.36, lane 7). It is unknown why this contaminant was not removed by sec.

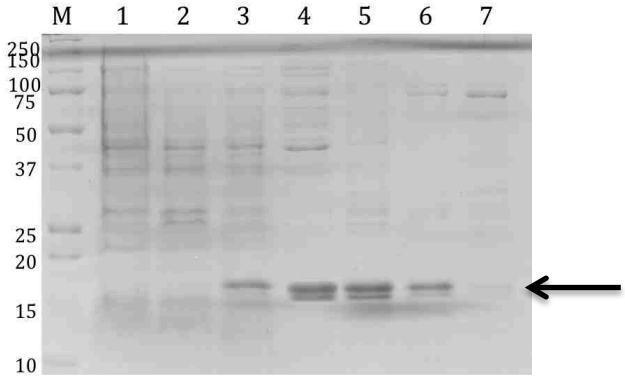

Figure 3.35: FimA Expression and Purification Gel

Arrow at predicted FimA-t molecular mass, 17.6 kDa
1. BL21_Star™ (*DE3*) boilate, no vector
2. BL21_Star™ (*DE3*), pET-15b boilate
3. KCM-Star-FimA boilate
4. Soluble fraction from FimA-t purification
5. Insoluble pellet from FimA-t purification
6. NiNTA purified FimA-t
7. FPLC purified FimA-t

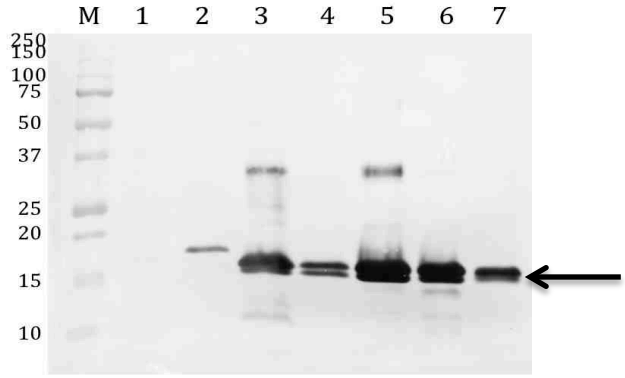

Figure 3.36: Western Blot of FimA Expression and Purification

Arrow at predicted FimA-t molecular mass, 17.6 kDa
1. BL21_Star™ (*DE3*) boilate, no vector
2. BL21_Star™ (*DE3*), pET-15b boilate
3. KCM-Star-FimA boilate
4. Soluble fraction from FimA-t purification
5. Insoluble pellet from FimA-t purification
6. NiNTA purified FimA-t
7. FPLC purified FimA-t

Section 3.1f LolC Expression and Purification

The levels of IPTG-induced overproduction of the recombinant predicted periplasmic domain of *B. pseudomallei* BPSL_2277, LolC (LolC-t) were initially analyzed in the *E. coli* BL21_Rosetta (*DE3*) strain transformed with pET-28a(+)-OQLOLCN (Figure 2.2c, a gift from Dr. Omar Qazi) using a purification-based analysis. This new strain, KCM-Rosetta-LolC, was grown in OE at 37 ˚C as previously reported (32). After a protein miniprep small-scale purification (Section 2.25), the purified soluble protein was analyzed by SDS PAGE using a Coomassie-stained acrylamide gel and a weakly staining band was observed near the LolC-t predicted molecular mass of 26.3 kDa (Figure 3.37, at the arrow) (Consistent with (Whitlock et al. 2010).

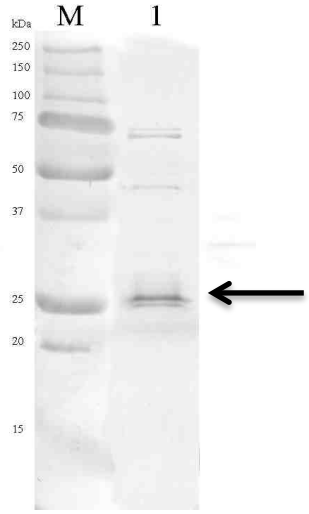

Figure 3.37: Purification of LolC-t in OE

Arrow at predicted molecular mass of LolC-t, 26.3 kDa
Lane 1: LolC-t protein miniprep from *E. coli* BL21_Rosetta (*DE3*)

To further optimize expression, *E. coli* BL21_Rosetta (*DE3*) cells transformed with

construct pET-28a(+)-OQLOLCN were then grown in OE at 18 ˚C (Section 2.21). After a protein miniprep (Section 2.25), the purified soluble protein was analyzed by SDS PAGE and Western blot with a mouse anti-polyhistidine monoclonal antibody alongside a sample grown in OE at 37 ˚C. A thick, strongly staining band was observed on the Coomassie-stained gel near 26.3 kDa, the predicted molecular mass of LolC-t, in the 18 ˚C sample, and a weakly staining band of the same size was observed in the 37 ˚C sample, as seen previously (Figure 3.38 at arrow). The Western blot suggests that the band near 26.3 kDa is LolC-t (Figure 3.39 at arrow). A second band also appears in the LolC-t sample grown at 18 ˚C in the Western blot, which appears to be a stable truncated species of LolC-t (Figure 3.39, Lane 2).

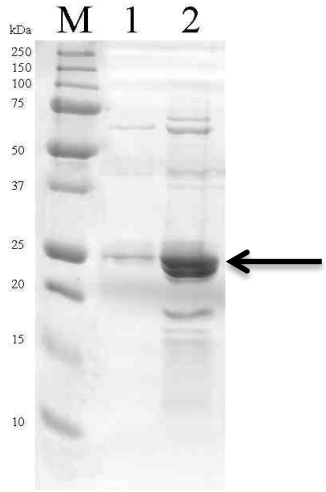

Figure 3.38: Gel comparison of LolC-t in 37 ˚C and 18 ˚C in BL21_Rosetta (*DE3*)

Arrow at predicted molecular mass of LolC-t, 26.3 kDa
1: LolC-t protein miniprep 37 ˚C
2: LolC-t protein miniprep 18 ˚C

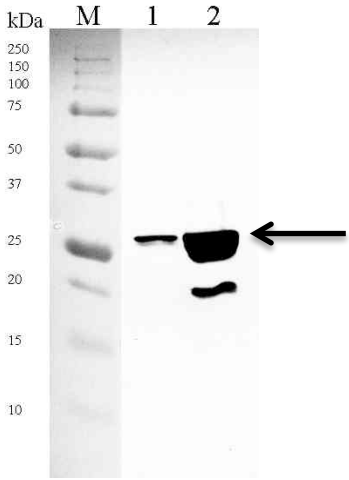

Figure 3.39: Western blot comparison of LolC-t in 37 ˚C and 18 ˚C in BL21_Rosetta (*DE3*)

Arrow at predicted molecular mass of LolC-t, 26.3 kDa
1: LolC-t protein miniprep 37 ˚C
2: LolC-t protein miniprep 18 ˚C

To further optimize expression via purification, LolC-t was then expressed in strain KCM-Rosetta-LolC using LB broth and 1.0 mM IPTG induction at an OD_{600} of 0.6. Cultures were moved to 18 ˚C post-induction and grown overnight for 16 h. Protein purification was performed, (Section 2.23) and the purified protein elution fractions were analyzed by SDS PAGE using a Coomassie-stained acrylamide gel. Strongly staining bands were seen in all of the eluted LolC-t fractions near 26.3 kDa (Figure 3.40, at the arrow), consistent with the previous Western blot for LolC-t. Scaled-up expression and purification of LolC-t was performed using the strain KCM-Rosetta-LolC grown in LB

broth with 1.0 mM IPTG induction at an OD_{600} of 0.6 and grown for 16 h post-induction at 18 ˚C.

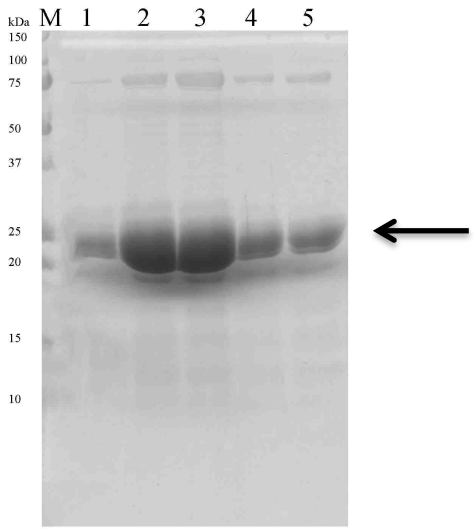

Figure 3.40: NiNTA-purified LolC-t eluted fractions from LB growth at 18 ˚C post-induction

Arrow at predicted molecular mass of LolC-t, 26.3 kDa
Lane 1-5: Eluted fractions 1-5

Purification of LolC-t was performed in a two-step process: first by affinity chromatography using NiNTA agarose, and then by size-exclusion chromatography (sec) (Figure 3.41), and its size was calculated by FPLC and measured by mass spectrometry (Appendix). The size of LolC-t as calculated by FPLC using a calibrated column is 34.6 kDa, which is quite a bit higher than the predicted molecular mass of LolC-t, 26.3 kDa. This could be due to the shape of the protein. Calibration of the FPLC column was performed using globular proteins, and proteins that are not perfectly globular could run

aberrantly in comparison. Mass spectrometry determined the mass of LolC-t to be 26.3 kDa, which is identical to the predicted molecular mass of 26.3 kDa.

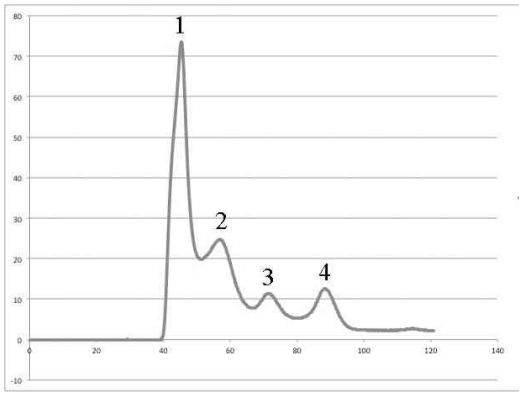

Figure 3.41: Representative FPLC trace from LolC-t Purification

Material from peak 4 was collected.
1. 45.39 mL
2. 56.88 mL
3. 71.74 mL
4. 88.15 mL

Section 3.1g BopA-t Expression and Purification Results

BopA-t was expressed and purified as described in Section 2.40 and the affinity-purified protein was analyzed by SDS PAGE (Figure 3.42) and Western blot (Figure 3.43) using a mouse anti-polyhistidine monoclonal antibody. As apparent in the gel and Western images, BopA is an incredibly labile protein, prone to degradation during purification. Most of the bands present on the gel (Figure 3.42), even those that are not found on the Western blot (Figure 3.43), are likely degraded products of BopA, and could have lost part or all of their polyhistidine tag. Full-length BopA-t, as indicated by the arrow in Figures 3.42 and 3.43, has not previously been present using different

expression and purification protocols (Dr. Omar Qazi, personal communication).

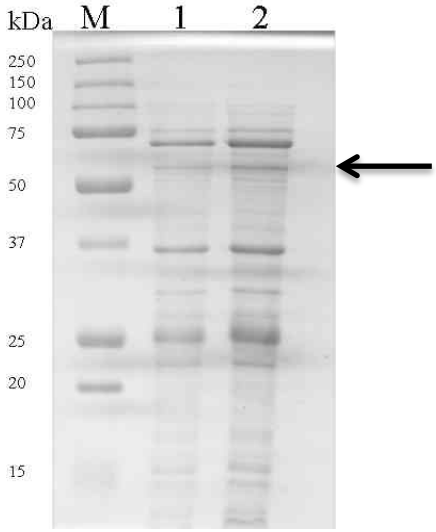

Figure 3.42: Gel of affinity purified BopA-t

Arrow at the predicted molecular mass of BopA-t, 54.7 kDa
1. 2.5 mg total protein loaded
2. 5 mg total protein loaded

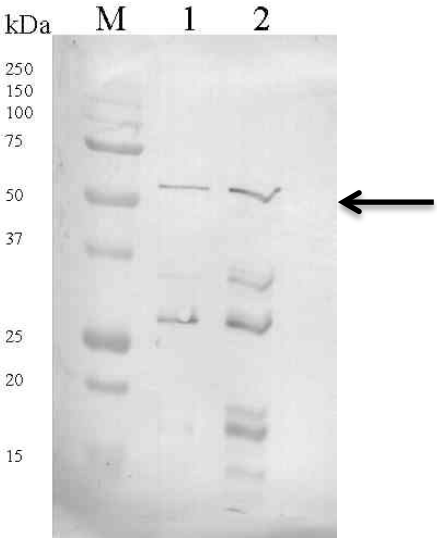

Figure 3.43: Western blot of affinity purified BopA-t

Arrow at the predicted molecular mass of BopA-t, 54.7 kDa
1. 2.5 mg total protein loaded
2. 5 mg total protein loaded

Section 3.1h SodC Cloning, Expression and Purification Results

A truncated form of *B. mallei sodC* gene (*sodC*-t), BMA_0713 (Section 2.39), was PCR-amplified (Figure 3.44), cloned into the *NcoI* and *NotI* sites of the pET-28a(+) vector, and transformed into *E. coli* DH5α cells. The resulting vector, pET-28a(+)-KCMSOD (Figure 2.6), was verified by DNA sequencing.

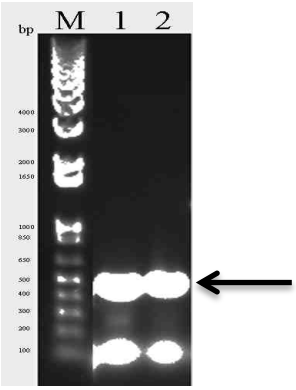

Figure 3.44: PCR of the *sodC*-t gene

Arrow at predicted size of *sodC*-t DNA, 477 bp
1. Regular PCR conditions
2. With added 0.5% DMSO

The levels of IPTG-induced overproduction of a truncated recombinant *B. mallei* BMA_0713, SodC (SodC-t) were initially analyzed from purification of overnight culture in *E. coli* strain BL21_Rosetta (*DE3*) transformed with construct pET-28a(+)-KCMSODC (new strain KCM-Rosetta-SodC) grown in OE media (OE) at 37 ˚C. In this strategy, cells harvested were subjected to a protein miniprep (Section 2.25) and purified SodC-t protein was analyzed by SDS PAGE. The Coomassie-stained gel has strongly staining bands present in the purified samples at the predicted molecular mass of SodC-t, 16.2 kDa (Figure 3.45, at arrow). No Western blot was performed of this sample, so presence or absence of FliC-t in these samples is uncertain.

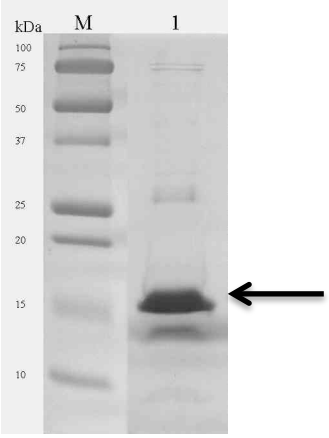

Figure 3.45: Purification of SodC-t from growth in OE at 37 ˚C

Arrow at predicted molecular mass of SodC-t, 16.2 kDa
1. Purified SodC-t

SodC-t was then purified by protein miniprep from KCM-Rosetta-SodC cells grown in OE at 18 ˚C, and this purified SodC-t was analyzed by SDS PAGE in comparison to SodC-t grown at 37 ˚C from the previous paragraph (Figure 3.46). Strongly staining bands were present in the samples from both expression conditions, with more protein apparently being produced at 18 ˚C than 37 ˚C, however, this may be to unequal loading of protein samples. A Western blot was prepared from these samples as well (Figure 3.47), which confirms the strongly staining bands at the arrow, just above the 15 kDa molecular mass marker, to be SodC-t.

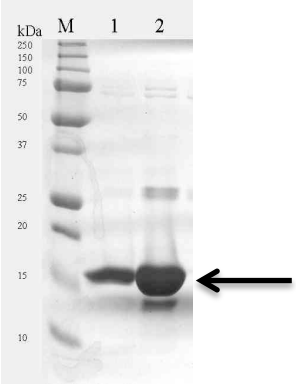

Figure 3.46: Purification gel of SodC-t in OE Broth

Arrow at predicted molecular mass of SodC-t, 16.2 kDa
1. Grown at 37 ˚C
2. Grown at 18 ˚C

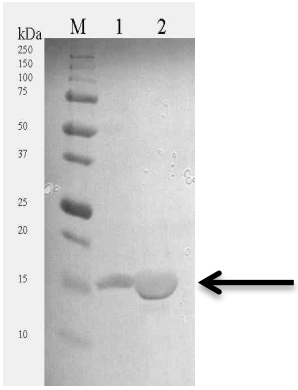

Figure 3.47: Purification Western blot of SodC-t in OE Broth

Arrow at predicted molecular mass of SodC-t, 16.2 kDa
1. Grown at 37 ˚C
2. Grown at 18 ˚C

SodC-t was then purified from strain KCM-Rosetta-SodC grown in LB broth induced with 1 mM IPTG at an OD_{600} of 0.6 and grown overnight at 18 ˚C post-induction. This sample was purified as described in Section 2.23 and eluted from the column in 5 fractions, which were analyzed by SDS PAGE using a Coomassie-stained acrylamide gel. Figure 3.48 has strongly staining bands at the predicted molecular mass of SodC-t in all of the 5 fractions. These conditions were chosen for scaled-up production of SodC-t.

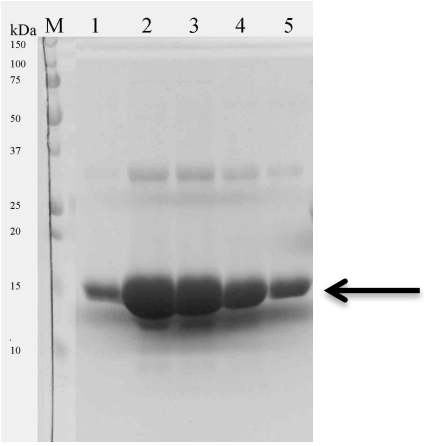

Figure 3.48: Purification of SodC-t from LB broth at 18 ˚C with 1 mM IPTG induction

Arrow at predicted molecular mass of SodC-t, 16.2 kDa
1-5: Eluted fractions of SodC-t

SECTION 3.2 ELISA RESULTS

Section 3.2a LolC-t and pIII-t ELISA

ELISA was performed with LolC-t and biotinylated pIII-t to determine if the two proteins would bind to each other in their purified forms. As seen in figure 3.49, they do indeed bind to each other in a concentration-dependent manner.

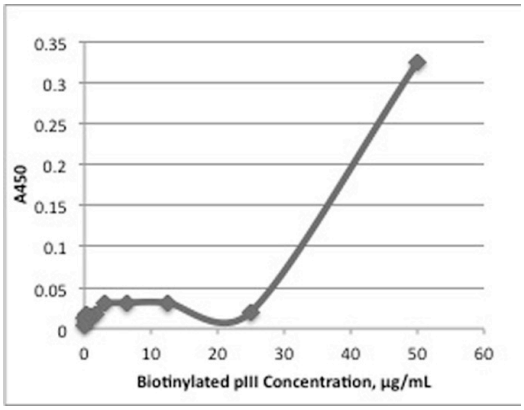

Figure 3.49: LolC-t and biotinylated pIII-t

Section 3.2b Heat-killed cells and biotinylated pIII-t ELISA

ELISA was performed with heat-killed (HK) *B. pseudomallei* strain Bp82 and biotinylated pIII-t protein to determine if the LolC epitope that binds to pIII-t would be available in the HK cells. *Pseudomonas aeruginosa* strain PAO1 was used as a negative control. As seen in Figure 3.50, biotinylated pIII-t binds with higher affinity to HK Bp82 cells than to HK PAO1 cells, although it is seen to bind to the HK PAO1 cells as well.

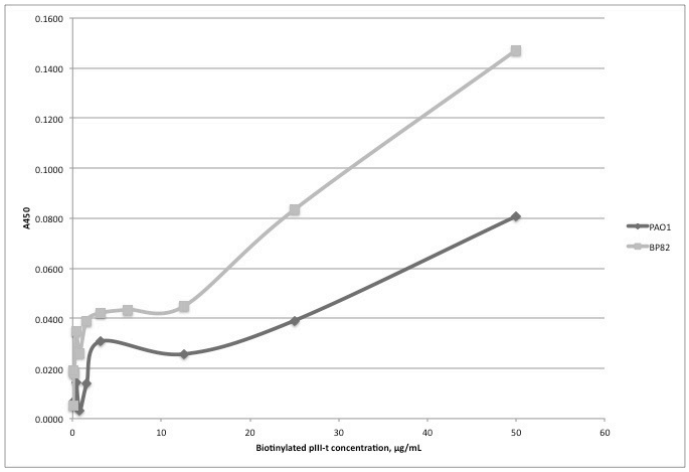

Figure 3.50: Heat-killed BP82 and PAO1 cells with biotinylated pIII-t

Chapter 4: Discussion

SECTION 4.1 PROJECT AIMS RECAP

The aims of this project were to generate highly purified surface located and immunogenic target proteins FliC, PilA, FimA, and LolC from *B. pseudomallei* and BopA and SodC from *B. mallei*. These protein targets will be used to generate high affinity diagnostic reagents including aptamers and antibodies that will be used in a diagnostic assay for melioidosis and glanders. In addition, the protein pIII was cloned, expressed, and purified as a diagnostic reagent to detect LolC protein.

SECTION 4.2 GENERAL DISCUSSION

There is an intuitive and pervasive assumption that surface-expressed proteins are most likely to evoke an antibody response in the host, due to their accessibility to the immune system. Many bacterial proteins that have been shown to be protective against disease have signal sequences that would locate them to the outside of the cell membrane (Davies et al. 2005). Because of this, proteins from *B. pseudomallei* and *B. mallei* that are expected to be extracellular were mainly chosen for this study, including FliC, PilA, and FimA. Other proteins in this study included those that have already been shown to be protective in models of glanders and melioidosis, LolC and BopA.

It has been hypothesized that high affinity reagents such as aptamers and antibodies that can bind to these purified outer-membrane associated proteins could also be used to detect them on the surface of the bacteria, and thus would be able to capture and detect whole cell organisms. This work has identified one such detection reagent, pIII protein from the phage M13K07, which may be able to specifically detect LolC protein. The development of other detection reagents is yet incomplete and ongoing.

SECTION 4.3 DISCUSSION OF FLIC

In this study, two recombinant forms of FliC were expressed and purified. One of these truncated proteins, FliCR-t, has been shown to be highly pure with no identified contaminants. The other truncated FliC, FliC-t, has not been extensively purified as of yet.

FliC remains an excellent diagnostic target. It is externally expressed on *B. pseudomallei* with many copies present in each bacterial flagellum. FliC has also been identified as a protein that is highly immunogenic during melioidosis infection (Felgner et al. 2009), confirming that it is accessible to the immune system during infection. Because *B. mallei* is non-flagellated, reagents that recognize FliC would be ideal in the differentiation between melioidosis and glanders infections. While this consideration is not integral to diagnosis in areas where melioidosis is endemic due to the low incidence of human glanders, it could be vital in the identification of a biological terrorism threat. The *fliC* gene is already being used in several PCR-based diagnostic assays in this role

(Suppiah et al. 2010) Currently RNA aptamers are being selected against FliCR-t.

FliC is also a potential vaccine candidate. It has been shown that a plasmid DNA vaccine encoding the fliC gene is protective against melioidosis (Chen et al. 2006). This plasmid vaccine expressed the FliC protein *in vivo*, suggesting that the FliC protein itself could be protective without the addition of O-polysaccharide (Brett and Woods 1996). In addition, flagellins from other bacterial species, such as closely related *Pseudomonas aeruginosa,* have been shown to be protective against bacterial challenge (Campodonico et al. 2010).

Future work with FliC-t needs to begin with size exclusion chromatography purification on the FPLC to remove any contaminating protein from the *E. coli* host strain. After this is done, it should be used in the generation of high-affinity aptamers, fragment antibodies (fABs), and commercially obtained mouse monoclonal antibodies.

Future work on FliCR-t includes the continuation of aptamer selections, as well as the beginning of fAB selections and commercial production of mouse monoclonal antibodies. These reagents would then be used in a novel Luminex assay for melioidosis as well as in diagnostic assays to suit the developing world, including rapid immunofluorescence (Wuthiekanun et al. 2002) and latex agglutination (Amornchai et al. 2007).

SECTION 4.4 DISCUSSION OF PILA-T AND FIMA-T

In this study, a recombinant truncated form of PilA from *B. pseudomallei* was

cloned, expressed, and purified. This protein, PilA-t, is incredibly pure with no identified contaminants. A truncated form of FimA from *B. Pseudomallei* was also expressed and purified. This protein, FimA-t, still contains some high molecular mass contaminating proteins.

PilA is an excellent diagnostic target. It has been demonstrated that highly immunogenic PilA expressed during experimental glanders infection, and that PilA elicits an IgG immune response in the host (Fernandes et al. 2007). Both PilA and FimA also appear to be up-regulated during infection in response to taurine found in animal cells (Nandi et al. 2010). PilA, although highly immunogenic, has been demonstrated to not be protective against experimental glanders. Currently, PilA-t is being used for the selection of diagnostic reagents including aptamers and fragment antibodies (fABs).

Future work with PilA-t would include using it as a target to obtain highly sensitive and selective diagnostic reagents. This includes continuing aptamer and fAB selections, as well as using PilA-t in the generation of commercially produced mouse monoclonal antibodies. It has already been shown that immunization with PilA leads to a high production of IgG antibodies, and it is therefore likely that high affinity antibodies would be obtained from the commercial mouse route.

Future work for FimA-t has to begin with better purification methods to remove the high molecular mass contaminants found in the current preparation. When suitably pure protein has been achieved, it can also be used for the generation of diagnostic reagents such as aptamers, fABs, and monoclonal antibodies.

SECTION 4.5 DISCUSSION OF LOLC-T AND PIII-T

In this study a recombinant truncated form of LolC from *B. pseudomallei* was expressed and purified. This protein, LolC-t, is highly purified with no identified contaminants. A second form of LolC-t has also been seen as a stably truncated species on Coomassie-stained acrylamide gel. In addition, a truncated form of the pIII gene from phage M13K07 was cloned, expressed, and purified to be used as a detection agent for LolC-t. This protein, pIII-t, is highly purified. Assays using pIII-t as a detection reagent for LolC-t and heat-killed *B. pseudomallei* Bp82 cells demonstrated it to bind with some specificity to both samples, but pIII also bound to the *P. aeruginosa* cells used as a negative control.

The cellular location of LolC remains unclear. It is reported to be located in the periplasmic space between the inner and outer membranes of the bacteria, and have no surface-expressed domains (reviewed in Narita 2011), but its role as a protective antigen in melioidosis and glanders infections calls this into question. Because the only assay performed in this study was against heat-killed cells that had been broken open, no determination can be made about the location of this protein. However, it is apparent that the levels of LolC expression in *B. pseudomallei* are high enough to detect by interaction with pIII-t *in vitro*.

Future work with these proteins will be necessary to characterize the nature of the binding between LolC and pIII, as well as between pIII and whole cell bacteria including

live *B. pseudomallei, B. mallei,* and *B. thailandensis*. If it is binding with high affinity to live cells, it could be used as a capture agent on a Luminex assay to detect *Burkholderia* species from infected samples.

Additional work should also be done on the second LolC-t band as seen in Figures 3.38 and 3.39. This second band represents a stable degraded form of LolC-t that could be selected, used for vaccination studies, and possibly patented. To do this, the sample would have to be FPLC purified and fractions corresponding to the smaller band would be collected. This purified protein could be directly used for vaccination studies, but ideally it would be used to determine where the protein is being cleaved in order to reliably express this truncated protein as a single species. To do this, mass spectrometry would be performed on the purified sample to obtain the size of the peptide. This would be compared to the size of the LolC-t protein, 26.3 kDa. Because the polyhistidine tag on the N-terminus of the protein, we know that the degradation is occurring at the C-terminal end of the protein. The number of additional amino acid residues that would need to be removed from the construct could then be calculated based on the difference between the molecular mass of the current construct and the molecular mass of the degraded sample. Then the further truncated LolC-t2 construct could be designed from this data, cloned, expressed, and purified, and this purified protein could be used in vaccine trials. If this LolC-t2 is protective, it would also narrow down the protective epitope of the LolC.

And finally, LolC-t should be tested in the marmoset model of infection to

determine if it is protective in non-human primates (Nelson et al. 2011).

SECTION 4.6 DISCUSSION OF BOPA-T

In this study, BopA-t was expressed and purified in a different way than previously published (Whitlock et al. 2010). This resulted in a different pattern of the purified protein, including a full-length sample that had not been present in the previous preparation. This sample has been tested in mice and was shown to not be protective (data not shown), whereas the previous preparation of BopA-t was highly protective. This may be due to aggregates that formed in the previous preparation that are not present in the current preparation as described here. Future work with this preparation of BopA-t could include a second vaccine trial, perhaps with a different adjuvant, to attempt to recreate the protection as seen in Dr. Qazi's preparation of the material. Additionally, further work should be done to optimize the expression and purification schema of BopA-t in order to prevent the degradation of the protein and provide a homogenous species of BopA-t that is easily reproducible.

SECTION 4.7 FINAL SUMMARY

This study resulted in the production of several highly purified truncated protein targets from *B. pseudomallei* and *B. mallei*, FliC, PilA, FimA, LolC, and BopA, as well as the potential diagnostic reagent protein pIII from filamentous phage M13K07. Development of additional high affinity diagnostic reagents, including aptamers, fABs,

and monoclonal antibodies, against protein targets produced in this study is ongoing. When these reagents become available they could be used to develop a highly specific and sensitive diagnostic assay that could be used globally to diagnose melioidosis and glanders.

Appendix: Mass Spectrometry Data

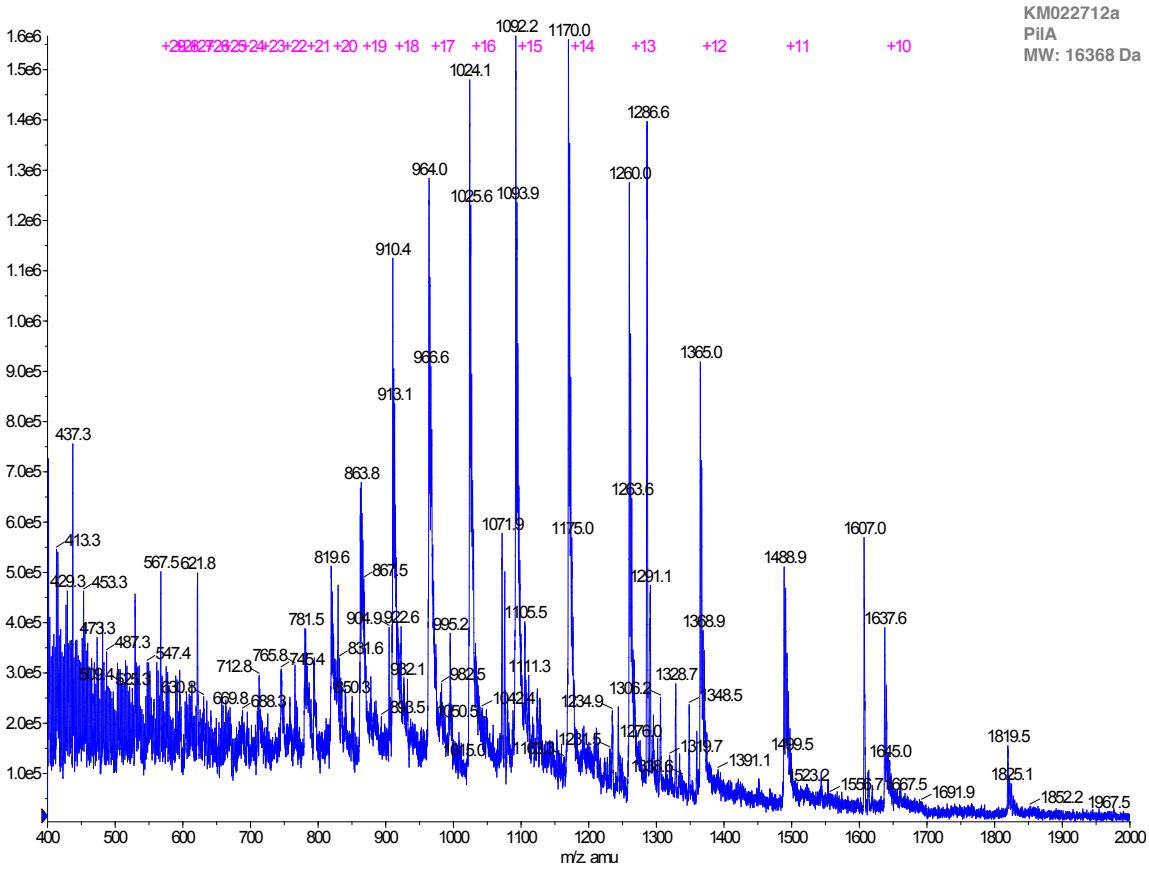

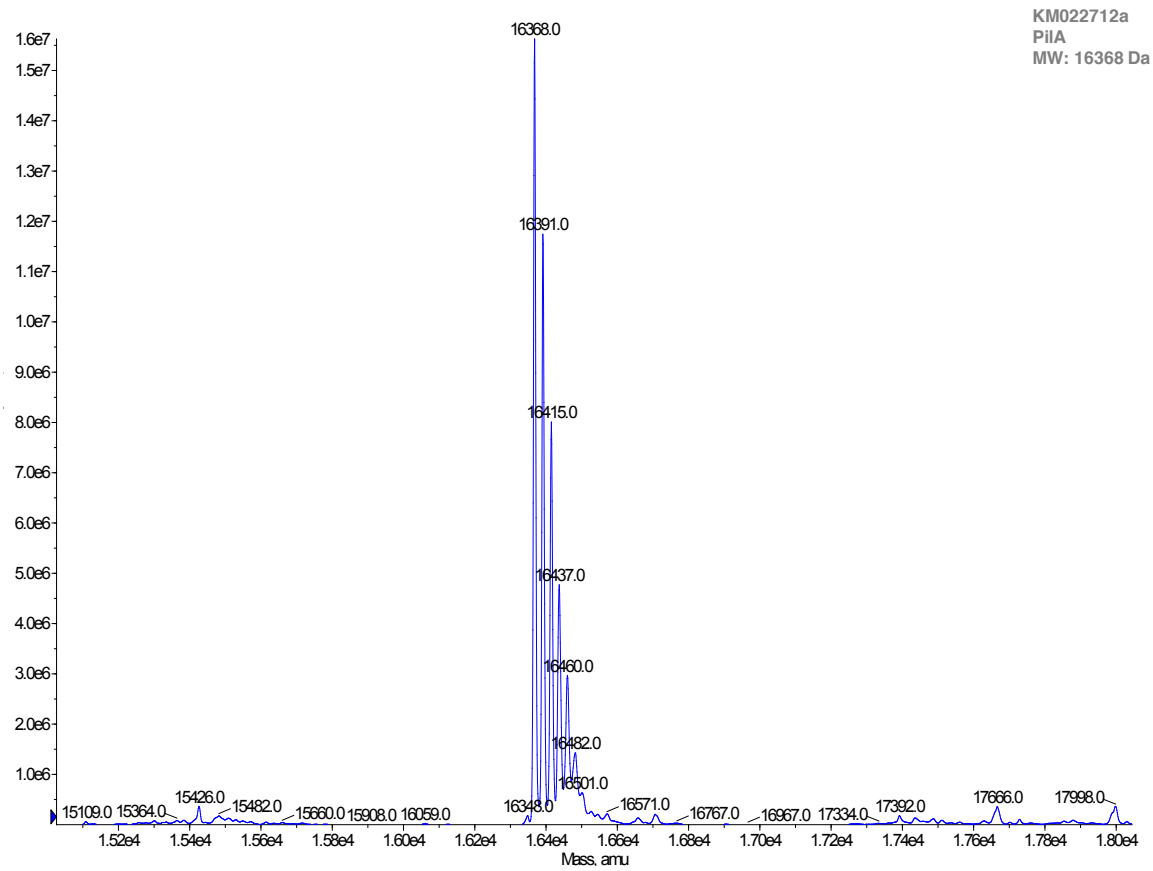
KM022712a
PilA
MW: 16368 Da
16368.0
16391.0
16415.0
16437.0
16460.0
16482.0
16501.0
15109.0
15364.0
15426.0
15482.0
15660.0
15908.0
16059.0
16348.0
16571.0
16767.0
16967.0
17334.0
17392.0
17666.0
17998.0
1.6e7
1.5e7
1.4e7
1.3e7
1.2e7
1.1e7
1.0e7
9.0e6
8.0e6
7.0e6
6.0e6
5.0e6
4.0e6
3.0e6
2.0e6
1.0e6
1.52e4
1.54e4
1.56e4
1.58e4
1.60e4
1.62e4
1.64e4
1.66e4
1.68e4
1.70e4
1.72e4
1.74e4
1.76e4
1.78e4
1.80e4
Mass, amu

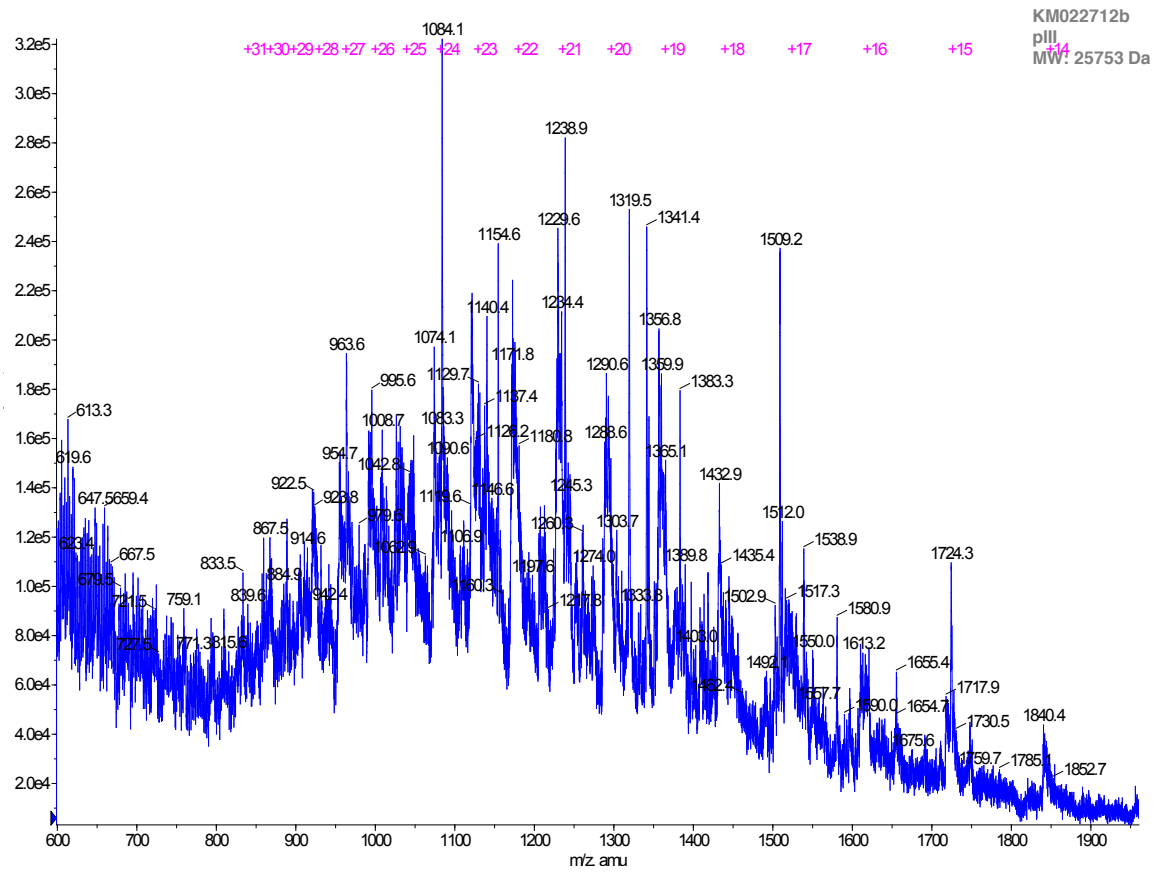
KM022712b
pIII
MW: 25753 Da
+31 +30 +29 +28 +27 +26 +25 +24 +23 +22 +21 +20 +19 +18 +17 +16 +15 +14
m/z amu

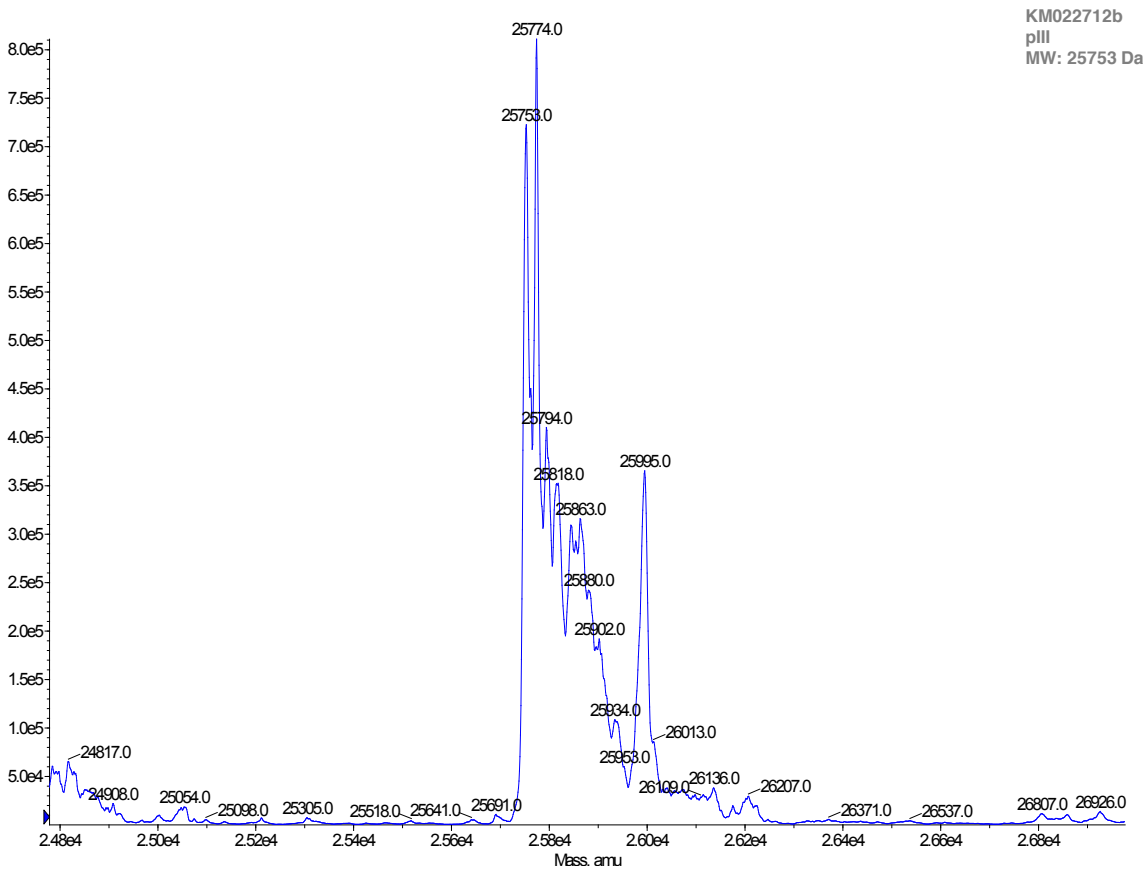
KM022712b
pIII
MW: 25753 Da
25774.0
25753.0
25794.0
25995.0
25818.0
25863.0
25880.0
25902.0
25934.0
26013.0
25953.0
26109.0
26136.0
26207.0
24817.0
24908.0
25054.0
25098.0
25305.0
25518.0
25641.0
25691.0
26371.0
26537.0
26807.0
26926.0
8.0e5
7.5e5
7.0e5
6.5e5
6.0e5
5.5e5
5.0e5
4.5e5
4.0e5
3.5e5
3.0e5
2.5e5
2.0e5
1.5e5
1.0e5
5.0e4
2.48e4
2.50e4
2.52e4
2.54e4
2.56e4
2.58e4
2.60e4
2.62e4
2.64e4
2.66e4
2.68e4
Mass, amu

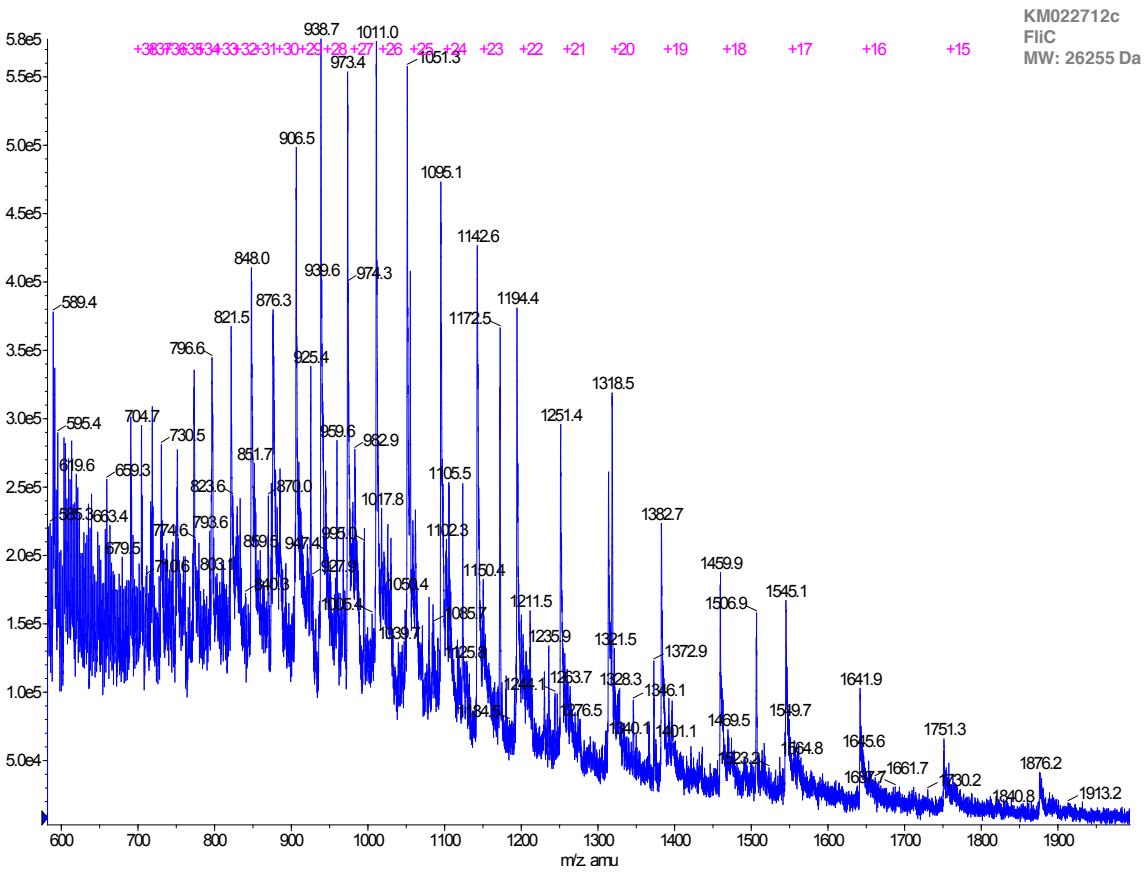
KM022712c
FliC
MW: 26255 Da
m/z amu

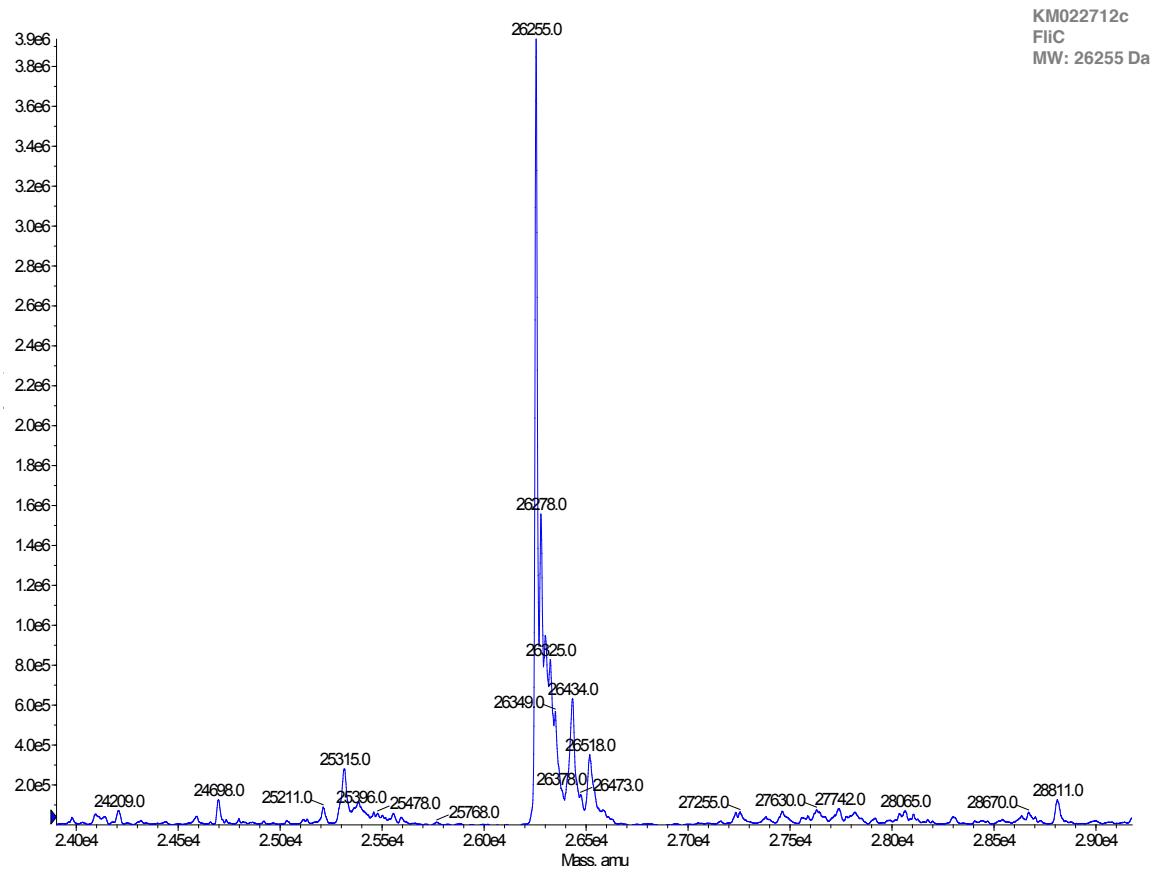
KM022712c
FliC
MW: 26255 Da
26255.0
26278.0
26325.0
26434.0
26349.0
26518.0
25315.0
26378.0
26473.0
24209.0
24698.0
25211.0
25396.0
25478.0
25768.0
27255.0
27630.0
27742.0
28065.0
28670.0
28811.0
Mass, amu

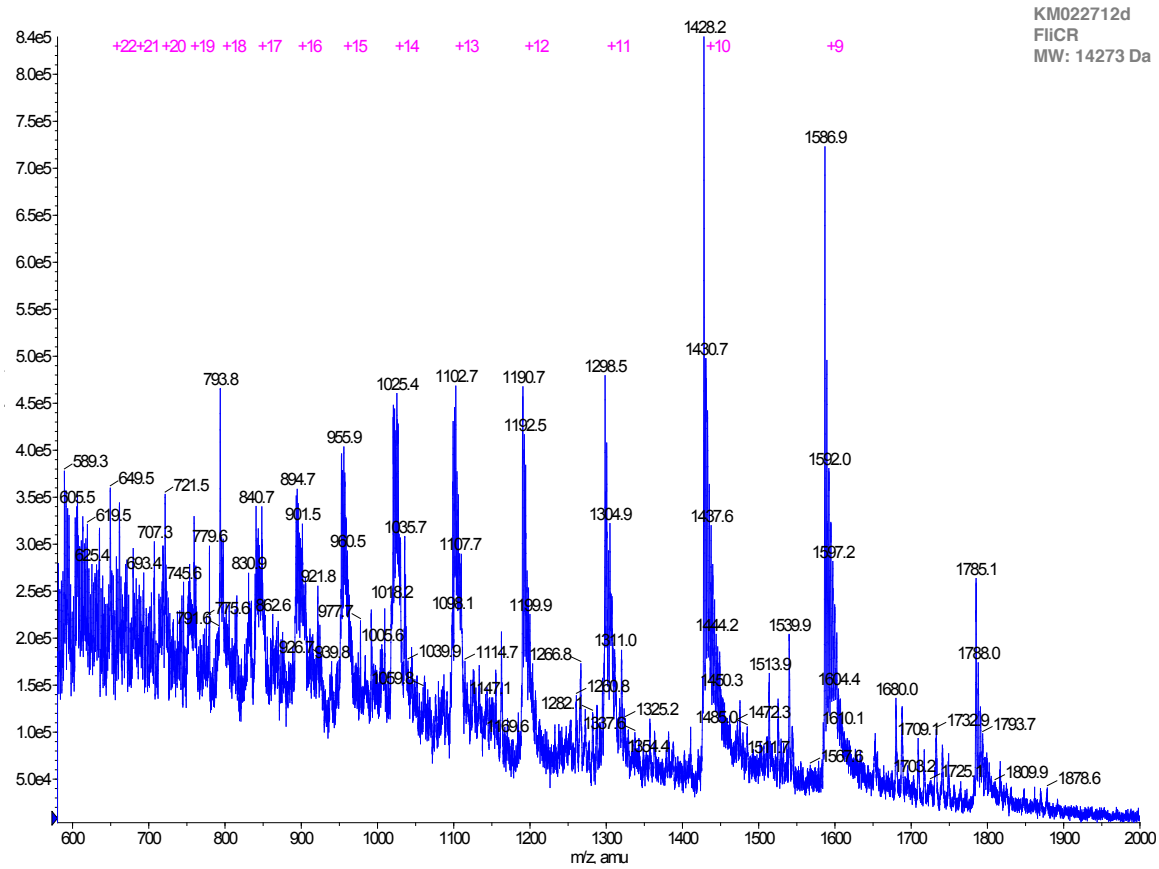
KM022712d
FliCR
MW: 14273 Da
+22 +21 +20 +19 +18 +17 +16 +15 +14 +13 +12 +11 +10 +9
m/z, amu

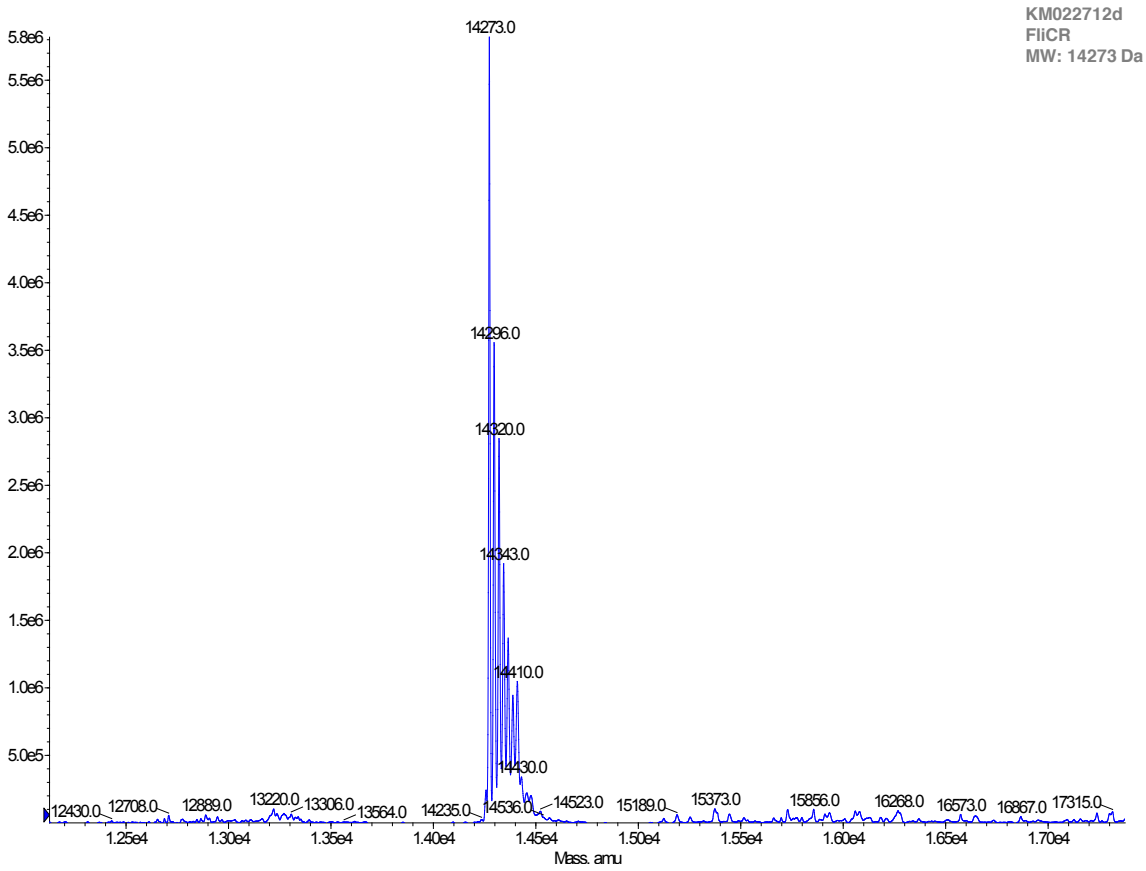
KM022712d
FliCR
MW: 14273 Da
14273.0
14296.0
14320.0
14343.0
14410.0
14430.0
12430.0
12708.0
12889.0
13220.0
13306.0
13564.0
14235.0
14536.0
14523.0
15189.0
15373.0
15856.0
16268.0
16573.0
16867.0
17315.0
5.8e6
5.5e6
5.0e6
4.5e6
4.0e6
3.5e6
3.0e6
2.5e6
2.0e6
1.5e6
1.0e6
5.0e5
1.25e4
1.30e4
1.35e4
1.40e4
1.45e4
1.50e4
1.55e4
1.60e4
1.65e4
1.70e4
Mass, amu

References

Alcantara, R. B., R. D. Read, M. W. Valderas, T. D. Brown and R. M. Roop, 2nd (2004). "Intact purine biosynthesis pathways are required for wild-type virulence of Brucella abortus 2308 in the BALB/c mouse model." Infect Immun **72**(8): 4911-4917.

Aldridge, P. and K. T. Hughes (2002). "Regulation of flagellar assembly." Curr Opin Microbiol **5**(2): 160-165.

Amornchai, P., W. Chierakul, V. Wuthiekanun, Y. Mahakhunkijcharoen, R. Phetsouvanh, B. J. Currie, P. N. Newton, N. van Vinh Chau, S. Wongratanacheewin, N. P. Day and S. J. Peacock (2007). "Accuracy of Burkholderia pseudomallei identification using the API 20NE system and a latex agglutination test." J Clin Microbiol **45**(11): 3774-3776.

Ashdown, L. R. (1979). "An improved screening technique for isolation of Pseudomonas pseudomallei from clinical specimens." Pathology **11**(2): 293-297.

Atkins, T., R. Prior, K. Mack, P. Russell, M. Nelson, J. Prior, J. Ellis, P. C. Oyston, G. Dougan and R. W. Titball (2002). "Characterisation of an acapsular mutant of Burkholderia pseudomallei identified by signature tagged mutagenesis." J Med Microbiol **51**(7): 539-547.

Bendtsen, J. D., H. Nielsen, G. von Heijne and S. Brunak (2004). "Improved prediction of signal peptides: SignalP 3.0." J. Mol. Biol. **340**: 783-795.

Boddey, J. A., C. P. Flegg, C. J. Day, I. R. Beacham and I. R. Peak (2006). "Temperature-regulated microcolony formation by Burkholderia pseudomallei requires pilA and enhances association with cultured human cells." Infect Immun **74**(9): 5374-5381.

Brett, P. J., D. Deshazer and D. E. Woods (1997). "Characterization of Burkholderia pseudomallei and Burkholderia pseudomallei-like strains." Epidemiol Infect **118**(2): 137-148.

Brett, P. J., D. DeShazer and D. E. Woods (1998). "Burkholderia thailandensis sp. nov., a Burkholderia pseudomallei-like species." Int J Syst Bacteriol **48 Pt 1**: 317-320.

Brett, P. J. and D. E. Woods (1996). "Structural and immunological characterization of Burkholderia pseudomallei O-polysaccharide-flagellin protein conjugates." Infect Immun **64**(7): 2824-2828.

Brinton, C. C., Jr. (1965). "The structure, function, synthesis and genetic control of bacterial pili and a molecular model for DNA and RNA transport in gram negative bacteria." Trans N Y Acad Sci **27**(8): 1003-1054.

Campodonico, V. L., N. J. Llosa, M. Grout, G. Doring, T. Maira-Litran and G. B. Pier (2010). "Evaluation of flagella and flagellin of Pseudomonas aeruginosa as vaccines." Infect Immun **78**(2): 746-755.

Cersini, A., M. C. Martino, I. Martini, G. Rossi and M. L. Bernardini (2003). "Analysis of virulence and inflammatory potential of Shigella flexneri purine biosynthesis mutants." Infect Immun **71**(12): 7002-7013.

Chen, Y. S., Y. S. Hsiao, H. H. Lin, Y. Liu and Y. L. Chen (2006). "CpG-modified plasmid DNA encoding flagellin improves immunogenicity and provides protection against Burkholderia pseudomallei infection in BALB/c mice." Infect Immun **74**(3): 1699-1705.

Chen, Y. S., D. Shiuan, S. C. Chen, S. M. Chye and Y. L. Chen (2003). "Recombinant truncated flagellin of Burkholderia pseudomallei as a molecular probe for diagnosis of melioidosis." Clin Diagn Lab Immunol **10**(3): 423-425.

Cheng, A. C. (2010). "Melioidosis: advances in diagnosis and treatment." Curr Opin Infect Dis **23**(6): 554-559.

Cheng, A. C. and B. J. Currie (2005). "Melioidosis: epidemiology, pathophysiology, and management." Clin Microbiol Rev **18**(2): 383-416.

Cheng, A. C., S. P. Jacups, L. Ward and B. J. Currie (2008). "Melioidosis and Aboriginal seasons in northern Australia." Trans R Soc Trop Med Hyg **102 Suppl 1**: S26-29.

Cheng, A. C., M. O'Brien, K. Freeman, G. Lum and B. J. Currie (2006). "Indirect hemagglutination assay in patients with melioidosis in northern Australia." Am J Trop Med Hyg **74**(2): 330-334.

Chierakul, W., A. Rajanuwong, V. Wuthiekanun, N. Teerawattanasook, M. Gasiprong, A. Simpson, W. Chaowagul and N. J. White (2004). "The changing pattern of bloodstream infections associated with the rise in HIV prevalence in northeastern Thailand." Trans R Soc Trop Med Hyg **98**(11): 678-686.

Chierakul, W., W. Winothai, C. Wattanawaitunechai, V. Wuthiekanun, T. Rugtaengan, J. Rattanalertnavee, P. Jitpratoom, W. Chaowagul, P. Singhasivanon, N. J. White, N. P. Day and S. J. Peacock (2005). "Melioidosis in 6 tsunami survivors in southern Thailand." Clin Infect Dis **41**(7): 982-990.

Chua, K. L., Y. Y. Chan and Y. H. Gan (2003). "Flagella are virulence determinants of Burkholderia pseudomallei." Infect Immun **71**(4): 1622-1629.

Chuaygud, T., S. Tungpradabkul, S. Sirisinha, K. L. Chua and P. Utaisincharoen (2008). "A role of Burkholderia pseudomallei flagella as a virulent factor." Trans R Soc Trop Med Hyg **102 Suppl 1**: S140-144.

Craig, L., M. E. Pique and J. A. Tainer (2004). "Type IV pilus structure and bacterial pathogenicity." Nat Rev Microbiol **2**(5): 363-378.

Currie, B. J., D. A. Fisher, D. M. Howard, J. N. Burrow, D. Lo, S. Selva-Nayagam, N. M. Anstey, S. E. Huffam, P. L. Snelling, P. J. Marks, D. P. Stephens, G. D. Lum, S. P. Jacups and V. L. Krause (2000). "Endemic melioidosis in tropical northern Australia: a 10-year prospective study and review of the literature." Clin Infect Dis **31**(4): 981-986.

Currie, B. J., D. A. Fisher, D. M. Howard, J. N. Burrow, S. Selvanayagam, P. L. Snelling, N. M. Anstey and M. J. Mayo (2000). "The epidemiology of melioidosis in Australia and Papua New Guinea." Acta Trop **74**(2-3): 121-127.

Dance, D. A. (1991). "Melioidosis: the tip of the iceberg?" Clin Microbiol Rev **4**(1): 52-60.

Dance, D. A. (2002). "Melioidosis." Curr Opin Infect Dis **15**(2): 127-132.

Dance, D. A. (2005). Melioidosis and Glanders as Possible Biological Weapons. Bioterrorism and Infectious Agents. F. a. Alibek. New York, Springer Science + Business Media, Inc.**:** 99-145.

Dance, D. A., V. Wuthiekanun, P. Naigowit and N. J. White (1989). "Identification of Pseudomonas pseudomallei in clinical practice: use of simple screening tests and API 20NE." J Clin Pathol **42**(6): 645-648.

Davies, D. H., X. Liang, J. E. Hernandez, A. Randall, S. Hirst, Y. Mu, K. M. Romero, T. T. Nguyen, M. Kalantari-Dehaghi, S. Crotty, P. Baldi, L. P. Villarreal and P. L. Felgner (2005). "Profiling the humoral immune response to infection by using proteome microarrays: high-throughput vaccine and diagnostic antigen discovery." Proc Natl Acad Sci U S A **102**(3): 547-552.

Derbyshire, J. B. (2002). "The eradication of glanders in Canada." Can Vet J **43**(9): 722-726.

DeShazer, D., D. M. Waag, D. L. Fritz and D. E. Woods (2001). "Identification of a Burkholderia mallei polysaccharide gene cluster by subtractive hybridization and demonstration that the encoded capsule is an essential virulence determinant." Microb Pathog **30**(5): 253-269.

Dodd, D. C., P. J. Bassford, Jr. and B. I. Eisenstein (1984). "Dependence of secretion and assembly of type 1 fimbrial subunits of Escherichia coli on normal protein export." J Bacteriol **159**(3): 1077-1079.

Drummond, A., B. Ashton, S. Buxton, M. Cheung, A. Cooper, C. Duran, M. Field, J. Heled, M. Kearse, S. Markowitz, R. Moir, S. Stones-Havas, S. Sturrock, T. Thierer and A. Wilson (2011). Geneious, KATE C MCCAUL THESIS.docx.

Elschner, M. C., H. C. Scholz, F. Melzer, M. Saqib, P. Marten, A. Rassbach, M. Dietzsch, G. Schmoock, V. L. de Assis Santana, M. M. de Souza, R. Wernery, U. Wernery and H. Neubauer (2011). "Use of a Western blot technique for the serodiagnosis of glanders." BMC Vet Res **7**: 4.

Endsley, J. J., A. G. Torres, C. M. Gonzales, V. G. Kosykh, V. L. Motin, J. W. Peterson, D. M. Estes and G. R. Klimpel (2009). "Comparative Antimicrobial Activity of Granulysin against Bacterial Biothreat Agents." Open Microbiol J **3**: 92-96.

Essex-Lopresti, A. E., J. A. Boddey, R. Thomas, M. P. Smith, M. G. Hartley, T. Atkins, N. F. Brown, C. H. Tsang, I. R. Peak, J. Hill, I. R. Beacham and R. W. Titball (2005). "A type IV pilin, PilA, Contributes To Adherence of Burkholderia pseudomallei and virulence in vivo." Infect Immun **73**(2): 1260-1264.

Felgner, P. L., M. A. Kayala, A. Vigil, C. Burk, R. Nakajima-Sasaki, J. Pablo, D. M. Molina, S. Hirst, J. S. Chew, D. Wang, G. Tan, M. Duffield, R. Yang, J. Neel, N. Chantratita, G. Bancroft, G. Lertmemongkolchai, D. H. Davies, P. Baldi, S. Peacock and R. W. Titball (2009). "A Burkholderia pseudomallei protein

microarray reveals serodiagnostic and cross-reactive antigens." Proc Natl Acad Sci U S A **106**(32): 13499-13504.

Fernandes, P. J., Q. Guo, D. M. Waag and M. S. Donnenberg (2007). "The type IV pilin of Burkholderia mallei is highly immunogenic but fails to protect against lethal aerosol challenge in a murine model." Infect Immun **75**(6): 3027-3032.

Galyov, E. E., P. J. Brett and D. DeShazer (2010). "Molecular insights into Burkholderia pseudomallei and Burkholderia mallei pathogenesis." Annu Rev Microbiol **64**: 495-517.

Glass, M. B., J. E. Gee, A. G. Steigerwalt, D. Cavuoti, T. Barton, R. D. Hardy, D. Godoy, B. G. Spratt, T. A. Clark and P. P. Wilkins (2006). "Pneumonia and septicemia caused by Burkholderia thailandensis in the United States." J Clin Microbiol **44**(12): 4601-4604.

Godoy, D., G. Randle, A. J. Simpson, D. M. Aanensen, T. L. Pitt, R. Kinoshita and B. G. Spratt (2003). "Multilocus sequence typing and evolutionary relationships among the causative agents of melioidosis and glanders, Burkholderia pseudomallei and Burkholderia mallei." J Clin Microbiol **41**(5): 2068-2079.

Goodyear, A., L. Kellihan, H. Bielefeldt-Ohmann, R. Troyer, K. Propst and S. Dow (2009). "Protection from pneumonic infection with burkholderia species by inhalational immunotherapy." Infect Immun **77**(4): 1579-1588.

Haraga, A., T. E. West, M. J. Brittnacher, S. J. Skerrett and S. I. Miller (2008). "Burkholderia thailandensis as a model system for the study of the virulence-associated type III secretion system of Burkholderia pseudomallei." Infect Immun **76**(11): 5402-5411.

Harland, D. N., K. Chu, A. Haque, M. Nelson, N. J. Walker, M. Sarkar-Tyson, T. P. Atkins, B. Moore, K. A. Brown, G. Bancroft, R. W. Titball and H. S. Atkins (2007). "Identification of a LolC homologue in Burkholderia pseudomallei, a novel protective antigen for melioidosis." Infect Immun **75**(8): 4173-4180.

Harley, V. S., D. A. Dance, B. S. Drasar and G. Tovey (1998). "Effects of Burkholderia pseudomallei and other Burkholderia species on eukaryotic cells in tissue culture." Microbios **96**(384): 71-93.

Holden, M. T., R. W. Titball, S. J. Peacock, A. M. Cerdeno-Tarraga, T. Atkins, L. C. Crossman, T. Pitt, C. Churcher, K. Mungall, S. D. Bentley, M. Sebaihia, N. R. Thomson, N. Bason, I. R. Beacham, K. Brooks, K. A. Brown, N. F. Brown, G. L. Challis, I. Cherevach, T. Chillingworth, A. Cronin, B. Crossett, P. Davis, D. DeShazer, T. Feltwell, A. Fraser, Z. Hance, H. Hauser, S. Holroyd, K. Jagels, K. E. Keith, M. Maddison, S. Moule, C. Price, M. A. Quail, E. Rabbinowitsch, K. Rutherford, M. Sanders, M. Simmonds, S. Songsivilai, K. Stevens, S. Tumapa, M. Vesaratchavest, S. Whitehead, C. Yeats, B. G. Barrell, P. C. Oyston and J. Parkhill (2004). "Genomic plasticity of the causative agent of melioidosis, Burkholderia pseudomallei." Proc Natl Acad Sci U S A **101**(39): 14240-14245.

Holliger, P., L. Riechmann and R. L. Williams (1999). "Crystal structure of the two N-terminal domains of g3p from filamentous phage fd at 1.9 A: evidence for conformational lability." J Mol Biol **288**(4): 649-657.

Horn, J. K. (2003). "Bacterial agents used for bioterrorism." Surg Infect (Larchmt) **4**(3): 281-287.

Howe, C. and W. R. Miller (1947). "Human glanders; report of six cases." Ann Intern Med **26**(1): 93-115.

Howe, C., A. Sampath and M. Spotnitz (1971). "The pseudomallei group: a review." J Infect Dis **124**(6): 598-606.

Jackson, M., F. X. Berthet, I. Otal, J. Rauzier, C. Martin, B. Gicquel and C. Guilhot (1996). "The Mycobacterium tuberculosis purine biosynthetic pathway: isolation and characterization of the purC and purL genes." Microbiology **142 (Pt 9)**: 2439-2447.

Judy, B. M., G. C. Whitlock, A. G. Torres and D. M. Estes (2009). "Comparison of the in vitro and in vivo susceptibilities of Burkholderia mallei to Ceftazidime and Levofloxacin." BMC Microbiol **9**: 88.

Kanehisa, M. (2000). Post-genome Informatics, Oxford University Press.

Kelley, L. A. and M. J. Sternberg (2009). "Protein structure prediction on the Web: a case study using the Phyre server." Nat Protoc **4**(3): 363-371.

Kenny, D. J., P. Russell, D. Rogers, S. M. Eley and R. W. Titball (1999). "In vitro susceptibilities of Burkholderia mallei in comparison to those of other pathogenic Burkholderia spp." Antimicrob Agents Chemother **43**(11): 2773-2775.

Krogh, A., B. Larsson, G. von Heijne and E. L. Sonnhammer (2001). "Predicting transmembrane protein topology with a hidden Markov model: application to complete genomes." J Mol Biol **305**(3): 567-580.

Lehavi, O., O. Aizenstien, L. H. Katz and A. Hourvitz (2002). "[Glanders--a potential disease for biological warfare in humans and animals]." Harefuah **141 Spec No**: 88-91, 119.

Lehoux, D. E., F. Sanschagrin and R. C. Levesque (2002). "Identification of in vivo essential genes from Pseudomonas aeruginosa by PCR-based signature-tagged mutagenesis." FEMS Microbiol Lett **210**(1): 73-80.

Lertpatanasuwan, N., K. Sermsri, A. Petkaseam, S. Trakulsomboon, V. Thamlikitkul and Y. Suputtamongkol (1999). "Arabinose-positive Burkholderia pseudomallei infection in humans: case report." Clin Infect Dis **28**(4): 927-928.

Limmathurotsakul, D. and S. J. Peacock (2011). "Melioidosis: a clinical overview." Br Med Bull **99**: 125-139.

Limmathurotsakul, D., S. Wongratanacheewin, N. Teerawattanasook, G. Wongsuvan, S. Chaisuksant, P. Chetchotisakd, W. Chaowagul, N. P. Day and S. J. Peacock (2010). "Increasing incidence of human melioidosis in Northeast Thailand." Am J Trop Med Hyg **82**(6): 1113-1117.

Lopez, J., J. Copps, C. Wilhelmsen, R. Moore, J. Kubay, M. St-Jacques, S. Halayko, C. Kranendonk, S. Toback, D. DeShazer, D. L. Fritz, M. Tom and D. E. Woods

(2003). "Characterization of experimental equine glanders." Microbes Infect **5**(12): 1125-1131.

Losada, L., C. M. Ronning, D. DeShazer, D. Woods, N. Fedorova, H. S. Kim, S. A. Shabalina, T. R. Pearson, L. Brinkac, P. Tan, T. Nandi, J. Crabtree, J. Badger, S. Beckstrom-Sternberg, M. Saqib, S. E. Schutzer, P. Keim and W. C. Nierman (2010). "Continuing evolution of Burkholderia mallei through genome reduction and large-scale rearrangements." Genome Biol Evol **2**: 102-116.

Nandi, T., C. Ong, A. P. Singh, J. Boddey, T. Atkins, M. Sarkar-Tyson, A. E. Essex-Lopresti, H. H. Chua, T. Pearson, J. F. Kreisberg, C. Nilsson, P. Ariyaratne, C. Ronning, L. Losada, Y. Ruan, W. K. Sung, D. Woods, R. W. Titball, I. Beacham, I. Peak, P. Keim, W. C. Nierman and P. Tan (2010). "A genomic survey of positive selection in Burkholderia pseudomallei provides insights into the evolution of accidental virulence." PLoS Pathog **6**(4): e1000845.

Narita, S. (2011). "ABC transporters involved in the biogenesis of the outer membrane in gram-negative bacteria." Biosci Biotechnol Biochem **75**(6): 1044-1054.

Nelson, M., R. E. Dean, F. J. Salguero, C. Taylor, P. C. Pearce, A. J. Simpson and M. S. Lever (2011). "Development of an acute model of inhalational melioidosis in the common marmoset (Callithrix jacchus)." Int J Exp Pathol **92**(6): 428-435.

Nelson, M., J. L. Prior, M. S. Lever, H. E. Jones, T. P. Atkins and R. W. Titball (2004). "Evaluation of lipopolysaccharide and capsular polysaccharide as subunit vaccines against experimental melioidosis." J Med Microbiol **53**(Pt 12): 1177-1182.

Neubauer, H., L. D. Sprague, R. Zacharia, H. Tomaso, S. Al Dahouk, R. Wernery, U. Wernery and H. C. Scholz (2005). "Serodiagnosis of Burkholderia mallei infections in horses: state-of-the-art and perspectives." J Vet Med B Infect Dis Vet Public Health **52**(5): 201-205.

Ngauy, V., Y. Lemeshev, L. Sadkowski and G. Crawford (2005). "Cutaneous melioidosis in a man who was taken as a prisoner of war by the Japanese during World War II." J Clin Microbiol **43**(2): 970-972.

Nierman, W. C., D. DeShazer, H. S. Kim, H. Tettelin, K. E. Nelson, T. Feldblyum, R. L. Ulrich, C. M. Ronning, L. M. Brinkac, S. C. Daugherty, T. D. Davidsen, R. T. Deboy, G. Dimitrov, R. J. Dodson, A. S. Durkin, M. L. Gwinn, D. H. Haft, H. Khouri, J. F. Kolonay, R. Madupu, Y. Mohammoud, W. C. Nelson, D. Radune, C. M. Romero, S. Sarria, J. Selengut, C. Shamblin, S. A. Sullivan, O. White, Y. Yu, N. Zafar, L. Zhou and C. M. Fraser (2004). "Structural flexibility in the Burkholderia mallei genome." Proc Natl Acad Sci U S A **101**(39): 14246-14251.

Nieves, W., S. Asakrah, O. Qazi, K. A. Brown, J. Kurtz, D. P. Aucoin, J. B. McLachlan, C. J. Roy and L. A. Morici (2011). "A naturally derived outer-membrane vesicle vaccine protects against lethal pulmonary Burkholderia pseudomallei infection." Vaccine **29**(46): 8381-8389.

Owczarzy, R. (2005). "Melting temperatures of nucleic acids: discrepancies in analysis." Biophys Chem **117**(3): 207-215.

Panzner, M. J., A. Deeraksa, A. Smith, B. D. Wright, K. M. Hindi, A. Kascatan-Nebioglu, A. G. Torres, B. M. Judy, C. E. Hovis, J. K. Hilliard, R. J. Mallett, E. Cope, D. M. Estes, C. L. Cannon, J. G. Leid and W. J. Youngs (2009). "Synthesis and in vitro Efficacy Studies of Silver Carbene Complexes on Biosafety Level 3 Bacteria." Eur J Inorg Chem **2009**(13): 1739-1745.

Patel, N., L. Conejero, M. De Reynal, A. Easton, G. J. Bancroft and R. W. Titball (2011). "Development of vaccines against burkholderia pseudomallei." Front Microbiol **2**: 198.

Peacock, S. J. (2006). "Melioidosis." Curr Opin Infect Dis **19**(5): 421-428.

Peacock, S. J., D. Limmathurotsakul, Y. Lubell, G. C. Koh, L. J. White, N. P. Day and R. W. Titball (2012). "Melioidosis vaccines: a systematic review and appraisal of the potential to exploit biodefense vaccines for public health purposes." PLoS Negl Trop Dis **6**(1): e1488.

Pechous, R. D., T. R. McCarthy, N. P. Mohapatra, S. Soni, R. M. Penoske, N. H. Salzman, D. W. Frank, J. S. Gunn and T. C. Zahrt (2008). "A Francisella tularensis Schu S4 purine auxotroph is highly attenuated in mice but offers limited protection against homologous intranasal challenge." PLoS One **3**(6): e2487.

Peterson, J. D., L. A. Umayam, T. M. Dickinson, E. K. Hickey and O. White (2001). "The Comprehensive Microbial Resource." Nucleic Acids Research **29**(1): 123-125.

Proft, T. and E. N. Baker (2009). "Pili in Gram-negative and Gram-positive bacteria - structure, assembly and their role in disease." Cell Mol Life Sci **66**(4): 613-635.

Propst, K. L., T. Mima, K. H. Choi, S. W. Dow and H. P. Schweizer (2010). "A Burkholderia pseudomallei deltapurM mutant is avirulent in immunocompetent and immunodeficient animals: candidate strain for exclusion from select-agent lists." Infect Immun **78**(7): 3136-3143.

Propst, K. L., R. M. Troyer, L. M. Kellihan, H. P. Schweizer and S. W. Dow (2010). "Immunotherapy markedly increases the effectiveness of antimicrobial therapy for treatment of Burkholderia pseudomallei infection." Antimicrob Agents Chemother **54**(5): 1785-1792.

Qazi, O., M. Rani, A. J. Gnanam, T. W. Cullen, C. M. Stead, H. Kensing, K. McCaul, S. Ngugi, J. L. Prior, A. Lipka, J. M. Nagy, C. W. Gregory, B. M. Judy, S. V. Harding, R. W. Titball, S. S. Sidhu, M. S. Trent, G. B. Kitto, A. Torres, D. M. Estes, B. Iverson, G. Georgiou and K. A. Brown (2011). "Development of reagents and assays for the detection of pathogenic Burkholderia species." Faraday Discuss **149**: 23-36; discussion 63-77.

Rotz, L. D., A. S. Khan, S. R. Lillibridge, S. M. Ostroff and J. M. Hughes (2002). "Public health assessment of potential biological terrorism agents." Emerg Infect Dis **8**(2): 225-230.

Sambrook, J., E. F. Fritsch and T. Maniatis (1989). Molecular Cloning: A Laboratory Manual, Cold Spring Harbor Laboratory.

Sanford, J. P. (1978). "Melioidosis: forgotten but not gone." Trans Am Clin Climatol Assoc **89**: 201-205.

Sarkar-Tyson, M., S. J. Smither, S. V. Harding, T. P. Atkins and R. W. Titball (2009). "Protective efficacy of heat-inactivated B. thailandensis, B. mallei or B. pseudomallei against experimental melioidosis and glanders." Vaccine **27**(33): 4447-4451.

Sarkar-Tyson, M. and R. W. Titball (2010). "Progress toward development of vaccines against melioidosis: A review." Clin Ther **32**(8): 1437-1445.

Schmitz, U., A. Versmold, P. Kaufmann and H. G. Frank (2000). "Phage display: a molecular tool for the generation of antibodies--a review." Placenta **21 Suppl A**: S106-112.

Sonthayanon, P., P. Krasao, V. Wuthiekanun, S. Panyim and S. Tungpradabkul (2002). "A simple method to detect and differentiate Burkholderia pseudomallei and Burkholderia thailandensis using specific flagellin gene primers." Mol Cell Probes **16**(3): 217-222.

Sprague, L. D., R. Zachariah, H. Neubauer, R. Wernery, M. Joseph, H. C. Scholz and U. Wernery (2009). "Prevalence-dependent use of serological tests for diagnosing glanders in horses." BMC Vet Res **5**: 32.

Srinivasan, A., C. N. Kraus, D. DeShazer, P. M. Becker, J. D. Dick, L. Spacek, J. G. Bartlett, W. R. Byrne and D. L. Thomas (2001). "Glanders in a military research microbiologist." N Engl J Med **345**(4): 256-258.

Stanton, A. and W. Fletcher (1932). Melioidosis: studies from the Institute of Medical Research, Federated Malay States. London, John Bale Sons & Danielson, Ltd. .

Suppiah, J., J. S. Thimma, S. H. Cheah and J. Vadivelu (2010). "Development and evaluation of polymerase chain reaction assay to detect Burkholderia genus and to differentiate the species in clinical specimens." FEMS Microbiol Lett **306**(1): 9-14.

Suputtamongkol, Y., W. Chaowagul, P. Chetchotisakd, N. Lertpatanasuwun, S. Intaranongpai, T. Ruchutrakool, D. Budhsarawong, P. Mootsikapun, V. Wuthiekanun, N. Teerawatasook and A. Lulitanond (1999). "Risk factors for melioidosis and bacteremic melioidosis." Clin Infect Dis **29**(2): 408-413.

Thibault, F. M., E. Hernandez, D. R. Vidal, M. Girardet and J. D. Cavallo (2004). "Antibiotic susceptibility of 65 isolates of Burkholderia pseudomallei and Burkholderia mallei to 35 antimicrobial agents." J Antimicrob Chemother **54**(6): 1134-1138.

Tippayawat, P., M. Pinsiri, D. Rinchai, D. Riyapa, A. Romphruk, Y. H. Gan, R. L. Houghton, P. L. Felgner, R. W. Titball, M. P. Stevens, E. E. Galyov, G. J. Bancroft and G. Lertmemongkolchai (2011). "Burkholderia pseudomallei proteins presented by monocyte-derived dendritic cells stimulate human memory T cells in vitro." Infect Immun **79**(1): 305-313.

Tippayawat, P., W. Saenwongsa, J. Mahawantung, D. Suwannasaen, P. Chetchotisakd, D. Limmathurotsakul, S. J. Peacock, P. L. Felgner, H. S. Atkins, R. W. Titball, G. J.

Bancroft and G. Lertmemongkolchai (2009). "Phenotypic and functional characterization of human memory T cell responses to Burkholderia pseudomallei." PLoS Negl Trop Dis **3**(4): e407.

Tomaso, H., T. L. Pitt, O. Landt, S. Al Dahouk, H. C. Scholz, E. C. Reisinger, L. D. Sprague, I. Rathmann and H. Neubauer (2005). "Rapid presumptive identification of Burkholderia pseudomallei with real-time PCR assays using fluorescent hybridization probes." Mol Cell Probes **19**(1): 9-20.

Tomaso, H., H. C. Scholz, S. Al Dahouk, T. L. Pitt, T. M. Treu and H. Neubauer (2004). "Development of 5' nuclease real-time PCR assays for the rapid identification of the burkholderia mallei//burkholderia pseudomallei complex." Diagn Mol Pathol **13**(4): 247-253.

Tong, S., S. Yang, Z. Lu and W. He (1996). "Laboratory investigation of ecological factors influencing the environmental presence of Burkholderia pseudomallei." Microbiol Immunol **40**(6): 451-453.

Ulrich, R. L. and D. DeShazer (2004). "Type III secretion: a virulence factor delivery system essential for the pathogenicity of Burkholderia mallei." Infect Immun **72**(2): 1150-1154.

Vanaporn, M., M. Wand, S. L. Michell, M. Sarkar-Tyson, P. Ireland, S. Goldman, C. Kewcharoenwong, D. Rinchai, G. Lertmemongkolchai and R. W. Titball (2011). "Superoxide dismutase C is required for intracellular survival and virulence of Burkholderia pseudomallei." Microbiology **157**(Pt 8): 2392-2400.

Vial, L., M. C. Groleau, V. Dekimpe and E. Deziel (2007). "Burkholderia diversity and versatility: an inventory of the extracellular products." J Microbiol Biotechnol **17**(9): 1407-1429.

Vincze, T., J. Posfai and R. J. Roberts (2003). "NEBcutter: A program to cleave DNA with restriction enzymes." Nucleic Acids Res **31**(13): 3688-3691.

Walsh, A. L. and V. Wuthiekanun (1996). "The laboratory diagnosis of melioidosis." Br J Biomed Sci **53**(4): 249-253.

Weber, D. R., L. E. Douglass, W. G. Brundage and T. C. Stallkamp (1969). "Acute varieties of melioidosis occurring in U. S. soldiers in Vietnam." Am J Med **46**(2): 234-244.

Wells, E. V., S. K. Cinti, T. A. Clark, J. T. Rudrik and M. L. Boulton (2011). "Melioidosis-Reactivation of Latent Disease: Case Presentation and Review." Infectious Diseases in Clinical Practice **19**(3): 161-166 110.1097/IPC.1090b1013e31820dc31858e.

Wernery, U., R. Wernery, M. Joseph, F. Al-Salloom, B. Johnson, J. Kinne, S. Jose, B. Tappendorf, H. Hornstra and H. C. Scholz (2011). "Natural Burkholderia mallei infection in Dromedary, Bahrain." Emerg Infect Dis **17**(7): 1277-1279.

West, T. E., C. W. Frevert, H. D. Liggitt and S. J. Skerrett (2008). "Inhalation of Burkholderia thailandensis results in lethal necrotizing pneumonia in mice: a surrogate model for pneumonic melioidosis." Trans R Soc Trop Med Hyg **102 Suppl 1**: S119-126.

White, N. J. (2003). "Melioidosis." Lancet **361**(9370): 1715-1722.
Whitlock, G. C., A. Deeraksa, O. Qazi, B. M. Judy, K. Taylor, K. L. Propst, A. J. Duffy, K. Johnson, G. B. Kitto, K. A. Brown, S. W. Dow, A. G. Torres and D. M. Estes (2010). "Protective response to subunit vaccination against intranasal Burkholderia mallei and B. pseudomallei challenge." Procedia in Vaccinology **2**(1): 73-77.
Whitlock, G. C., D. M. Estes and A. G. Torres (2007). "Glanders: off to the races with Burkholderia mallei." FEMS Microbiol Lett **277**(2): 115-122.
Whitlock, G. C., R. A. Lukaszewski, B. M. Judy, S. Paessler, A. G. Torres and D. M. Estes (2008). "Host immunity in the protective response to vaccination with heat-killed Burkholderia mallei." BMC Immunol **9**: 55.
Whitlock, G. C., G. A. Valbuena, V. L. Popov, B. M. Judy, D. M. Estes and A. G. Torres (2009). "Burkholderia mallei cellular interactions in a respiratory cell model." J Med Microbiol **58**(Pt 5): 554-562.
Whitmore, A. (1913). "An Account of a Glanders-like Disease occurring in Rangoon." J Hyg (Lond) **13**(1): 1-34 31.
Wiersinga, W. J., A. F. de Vos, R. de Beer, C. W. Wieland, J. J. Roelofs, D. E. Woods and T. van der Poll (2008). "Inflammation patterns induced by different Burkholderia species in mice." Cell Microbiol **10**(1): 81-87.
Wikraiphat, C., J. Charoensap, P. Utaisincharoen, S. Wongratanacheewin, S. Taweechaisupapong, D. E. Woods, J. G. Bolscher and S. Sirisinha (2009). "Comparative in vivo and in vitro analyses of putative virulence factors of Burkholderia pseudomallei using lipopolysaccharide, capsule and flagellin mutants." FEMS Immunol Med Microbiol **56**(3): 253-259.
Winsor, G. L., B. Khaira, T. Van Rossum, R. Lo, M. D. Whiteside and F. S. Brinkman (2008). "The Burkholderia Genome Database: facilitating flexible queries and comparative analyses." Bioinformatics **24**(23): 2803-2804.
Woods, D. E. (2002). "The use of animal infection models to study the pathogenesis of melioidosis and glanders." Trends Microbiol **10**(11): 483-484; discussion 484-485.
Woods, L. C. J. B. (2005). USAMRIID's Medical Management of Biological Casualties Handbook. Fort Detrick, MD, U.S. Army Medical Institute of Infectious Diseases.
Wuthiekanun, V., P. Amornchai, N. Saiprom, N. Chantratita, W. Chierakul, G. C. Koh, W. Chaowagul, N. P. Day, D. Limmathurotsakul and S. J. Peacock (2011). "Survey of antimicrobial resistance in clinical Burkholderia pseudomallei isolates over two decades in Northeast Thailand." Antimicrob Agents Chemother **55**(11): 5388-5391.
Wuthiekanun, V., N. Anuntagool, N. J. White and S. Sirisinha (2002). "Short report: a rapid method for the differentiation of Burkholderia pseudomallei and Burkholderia thailandensis." Am J Trop Med Hyg **66**(6): 759-761.
Wuthiekanun, V., W. Chierakul, S. Langa, W. Chaowagul, C. Panpitpat, P. Saipan, T. Thoujaikong, N. P. Day and S. J. Peacock (2006). "Development of antibodies to

Burkholderia pseudomallei during childhood in melioidosis-endemic northeast Thailand." Am J Trop Med Hyg **74**(6): 1074-1075.

Wuthiekanun, V., V. Desakorn, G. Wongsuvan, P. Amornchai, A. C. Cheng, B. Maharjan, D. Limmathurotsakul, W. Chierakul, N. J. White, N. P. Day and S. J. Peacock (2005). "Rapid immunofluorescence microscopy for diagnosis of melioidosis." Clin Diagn Lab Immunol **12**(4): 555-556.

Yu, Y., H. S. Kim, H. H. Chua, C. H. Lin, S. H. Sim, D. Lin, A. Derr, R. Engels, D. DeShazer, B. Birren, W. C. Nierman and P. Tan (2006). "Genomic patterns of pathogen evolution revealed by comparison of Burkholderia pseudomallei, the causative agent of melioidosis, to avirulent Burkholderia thailandensis." BMC Microbiol **6**: 46.